VYSOKÉ UČENÍ TECHNICKÉ V BRNĚ

BRNO UNIVERSITY OF TECHNOLOGY

FAKULTA STAVEBNÍ

FACULTY OF CIVIL ENGINEERING

ÚSTAV VODNÍCH STAVEB

INSTITUTE OF WATER STRUCTURES

NUMERICKÉ MODELOVÁNÍ UČINKŮ DO TĚSNĚNÍ SYPANÝCH HRÁZÍ A JEJICH PODLOŽÍ

Numerical modelling of resealing effects in earth dams

DIZERTAČNÍ PRÁCE

DOCTORAL THESIS

AUTOR PRÁCE   Ing. Somia Bredy
AUTHOR

VEDOUCÍ PRÁCE   Doc. Ing. Jan Jandora, CSc.
SUPERVISOR

BRNO 2020

ABSTRAKT

Tato studie se zaměřuje na nejdůležitější technologie těsnění; těsnící stěny a tryskové injektáže (jako hlavní spolehlivá možnost, při rekonstrukci inženýrských staveb). Tyto dva způsoby byly použity na přehradě Karolinka pro snížení průsaku tělesem hráze. Těsnící stěna zřízena centrální části v tělesa hráze. Byla na obou koncích prodloužena tryskovou injektáži. Studie se zabývá možností numerického modelování těchto dvou technologií. Zahrnut je způsob provádění opravy, interakce s přilehlou půdou, smrštění cementu, stabilita svahu, změna tlaku vody v pórech čase a účinky obou technologii na stabilitu svahu, průsaky a sedání hráze. Modelování bylo provedeno pomocí softwaru založeného na metodě konečných prvků Plaxis 3D.

KLÍČOVÁ SLOVA

Hráz; Vodního dílo Karolinka; Těsnění; Těsnící stěna; Trysková injektáž; Stabilita svahu; Metoda konečných prvků; 3D Analýza průsaků; Analýza posunutí; Smrštění cementu; Dynamická analýza; Citlivostní analýza.

ABSTRACT

This study focuses on the most important sealing technologies; Diaphragm walls and Jet grouting as a major most popular reliable option when it comes to engineering constructions rehabilitation. Those two methods have been used in Karolinka dam for reducing seepage through its body. Diaphragm walls were used along the dam, and jet grouting was used at both ends of the dam. The study deals with the possibility of numerical modelling of these two technologies. It is included how to carry out, interaction with adjacent soil, cement shrinkage, slope stability, changing of pore water pressure with the time, dynamic analysis of drilling rod and the effects of both technologies on slope stability, seepage and settlement of dam. This modelling was conducted with the finite element method based on software Plaxis 3D.

KEYWORDS

Earth dam; Karolinka dam; Sealing; Diaphragm wall; Jet grouting; Slope stability; Finite Element Method; 3D Seepage analysis; Displacement analysis; Cement Shrinkage; Dynamic Analysis; sensitivity analysis.

BIBLOGRAPHICAL CITATION

BREDY, SOMIA. *Numerical Modelling of Sealing Effects in Earth Dams*. Brno: University of Technology, Faculty of Civil Engineering, 2020. 100 page. Supervisor Eng. Jan Jandora, PhD.

STATUTORY DECLARATION

I declare that I have developed and written the enclosed thesis completely by myself, and have not used sources or means without declaration.

Brno   23 / 11/2020

…………………..

Eng. Somia Bredy

ACKNOWLEDGMENTS

CONTENTS

1 INTRODUCTION

1.1 General remarks

The earthen dams are one of the very ancient constructions, which have a great effect on human civilization. During the history, the earthen dams built to ward off the dangers of flooding, irrigating agricultural land, water storage, and generate electric power. Many earthen dams are vulnerable to failures due to (Jandora and Říha, 2007), (Ambikaipalan, 2011), (Fu et al, 2018):

❖ *Hydraulic failure:*

Hydraulic accounts for over 38.7 % of earthen dam failure and due to following reasons:

● Overtopping failure: It happens because of increasing the water level due to the uncontrolled flow of water over the dam. It occurs by excessive rainfall or by the failure of an upstream dam. During the overtopping, water begins to flow over the crest, and so the notch is created which increases with the time and leads to erosion.

●Wave move: The upstream face and shoulder can be prone to erosion by continuous-wave action unless it is adequately protected.

●Surface erosion: it may occur by heavy rainwater flowing down, which may lead to creating gullies and as a result, failure of the whole dam.

❖ *Seepage failure:*

Seepage accounts for 40.0% of earthen dam failure due to:

● Piping: It is the progressive internal erosion and removal of soil out of the dam causing seepage of water through a hole. Mostly, Internal erosion begins at the downstream toe and works back toward the reservoir, forming tunnels between the upstream and downstream of the dam.

● Sloughing: It occurs when the bottom of the outside of the dam becomes saturated because of the seepage, and therefore it creates sloughed surface.

● Dying tree roots: It is very important to remove the roots because it creates a large void, seepage paths and internal erosion problems.

● Loss of stability: In uncontrolled drawdown, water load disappears so that the development of pore pressures can affect the stability of the upstream and downstream slopes. The degree of stability is lowered by uncontrolled (discharge- charge).

❖ *Structural failure*

About 7.2% of failure is referred to structural failure, it takes on the form of a slide (rupture) of dam body or its foundation, bulges, cracks and displacement of material in either the downstream or upstream face. It is more prominent in large dams, and they are signs of serious instability of the dam.

❖ *Others*

About 2,6 % of failure may be due to:

● Vegetation: The trees and brush tend to facilitate surface erosion, create ideal habitats for burrowing animals and impedes visual and physical inspection. Large trees can overburden the dam with their weight and that it might cause the slope failures.

● Earthquake: Earthquake loading may lead to several damages on the dams. Dam body or foundation may lose shear strength because of earthquake shaking, that leads to slope failure and the rocks fall to reservoir displacing its water. And this results to the internal erosion and the expansion of the cracks until the failure of the whole dam.

The various causes leading to the failure of earthen dams are shown in Tab (1.1)

Table 1.1 Causes of earthen dam failure (Jandora and Říha, 2007)

Cause of failure	Hydraulic failure	Seepage failure	Structure failure	Other	Unknown
Percentage %	38.7	40.0	7.2	2.6	11.5

Figure (1.1) shows many different types of the failure of earthen dams
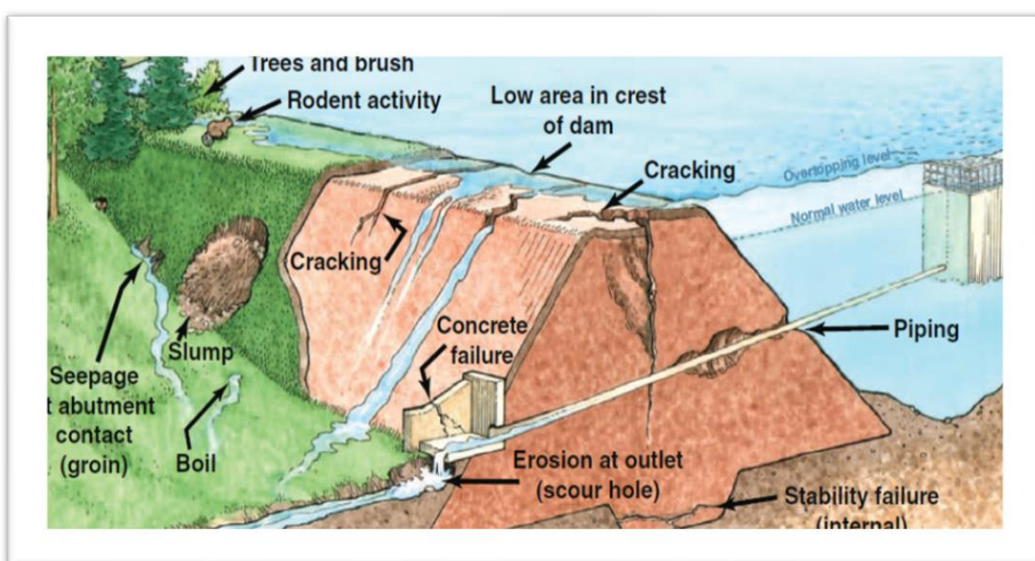
Fig. 1.1 Different types of potential dam failure modes (https://www.damsafety.org)

One of the main causes of the earthen dam failure is seepage problem because of running water slowly through body dam and its foundations, which directly effects on slope stability, and this will be a big problem if it causes weakening, piping or sloughing, so this problem has to be controlled, or will lead to rapid failure of dam. Sealing is used in the recent years as an integral process and an extremely effective treatment technology to control seepage in earthen dam, fill voids, strengthening and mitigate the flow of groundwater. Methods of sealing in dams have been developed in order to determine the pump pressure, mixture properties and stop time for accurate sealing. It is very important to achieve the required sealing while avoiding ground movement or any damage in structure due to applied pressure.

1.2 Aim of work

The specific objectives of this study are as follows:

➢ Studying sealing technique effect with respect to the settlement behaviour, stress, strain, displacement, water flow, pore water pressure and stiffness coefficients in the Karolinka dam.

➢ Numerical modelling of diaphragm walls and jet grouting processes to determine the state of the dam body and foundation; before, during and after sealing by using finite element method FEM which is performed by Plaxis 3D program in case study Karolinka dam.

➢ Studying the effect of sealing equipment loads and rotational motion of drilling rod on the stability of the Karolinka dam.

➢ Numerical modelling of the early age autogenous shrinkage of cement.

➢ Investigation of the failure state for grouting system in the connection zone.

➢ Dynamic analysis of the drilling rod.

➢ Comparing between computed result by Plaxis and actual result of the Karolinka dam to evaluate this research concerning its accuracy and appropriateness for reality.

1.3 Disposition

The different chapters of thesis contain the following:

Chapter 2

Contains an overview of the sealing, the theoretical knowledge about its history, literature review and its main methods.

Chapter 3

Contains a brief explanation of sealing method in the earthen dam, and detailed explanation about diaphragm wall and jet grouting.

Chapter 4

Contains comprehensive information about the dam and its soil. Reliability analysis of Karolinka dam, parameters of the soil, the numerical approach, and numerical solution in Plaxis 3D are explained.

Chapter 5

Contains the numerical modelling of diaphragm wall and jet grouting, parameters and other inputs are described in detail.

Chapter 6

Contains the results, discussion and conclusions.

Chapter 7

Contains the references, list of symbols, abbreviation, tables, figures, and appendices.

2 OVERVIEWS OF THE SEALING

2.1 Sealing technology

The sealing technology has been used for more than two centuries, as essential factor and an engineering method in order to avoid disastrous accidents and achieve the required advantages. Sealing is used for:

Permeability Reduction: The most widespread use of sealing is to reduce permeability of soil and rock, and therefore reducing seepage, hydrostatic forces acting on structures, and inhibiting internal erosion.

Filling purpose: The sealing is used to fill the holes, gaps, and existing cracks to decrease deformation and displacement of soil.

Strengthening –Stabilizing Purpose: The sealing improves mechanical properties and shear strength of the soil by increasing the cohesion, and bearing capacity. It eliminates the voids that affect either loading conditions or the response to loads. In other words, improvement in settlement.

2.2 Sealing history

Sealing has been used in the soil from the beginning of 1800s. Over the years, the sealing methods were developed, and the equipment was improved. The history of sealing technology can be summed up as:

- 1802: the first use of grouting was by Frenchman Charles Berigny for sealing the subsoil of the weir with mortar and spillway with clay suspension at Dieppe in France (Verfel, 1989).
- 1820: Mary grouted a lock on a canal of Saint Quentin by using mortar grout in France (Houlsby, 2008).
- 1864: Barlow was the first who used grouting in underground construction, he filled annular void left by the tail of the tunnel shield with grout (Verfel, 1989).
- 1876: the first use of grouting to fill fissures with cement in the rock under Tunstall dam in England (British Dam Society, 1994).
- 1893: the first use of grouting in dams in the USA for consolidation of the fissures rock mass beneath the New Croton dam, in New York (Henn, 1996).

- 1900: the grouting of dam construction spread to the Czech Republic (Verfel, 1989).

- 1912: the first major grouting at Tambach dam in Germany where a drilled hole was filled with cement which led to decrease in leakage about 58 % (Verfel, 1989).

- 1915: the first grouting at Janov concrete dam in Czech Republic to control the seepage from the left- hand downstream bank (Verfel, 1989).

- 1925: the first trial with chemical grouting was done by Joosten to improve the characteristics of soils in Germany and based on successive grouting of sodium silicate and calcium chloride (Kutzner, 1996).

- 1930: the grouting was carried out on 19 large dames in USA (Littlejohn, 2003).

- 1934: the first using of this technique in France for dam foundation to decrease permeability of Chavanon dam (Littlejohn, 2003).

- 1950: the first applied of diaphragm wall construction in California to protect an industrial area from flooding by A. d. Rhodes (Verfel, 1989).

- 1960: the first diaphragm wall was constructed in Slovakia at Teplice on Becva river (Verfel, 1989).

- 1965: the first applied of jet grouting to the soil by Yamakado brothers, under the name of the chemical churning pile (CCP) method (Xanthakos et al, 1994).

- 1968: providing Bystricka stone masonry dam with grout curtain in its foundation, Czech Republic (Dobes, 2002).

- 1969: the first using of pile foundation when corrective grouting was used to re-level a Rotterdam refinery in Netherlands (Henn, 1996).

- 1970: Japanese engineers Yahiro and Yoshida developed jet grout (JG) method (Xanthakos et al, 1994).

- 1974: first using of compensation grouting in tunnelling after the collapse of an old railway tunnel in England (Henn, 1996).

- 1977: the first using of compacting grouting to control ground movement during construction of the Bolton Hill tunnel (Henn, 1996).

- 1984: the diaphragm wall of concrete was built in Brombach dam over the full length of dam, Germany (Henn, 1996).

- 1987: the concrete diaphragm wall was constructed with a depth of (60 m) in Puclaro dam, Chile (Henn, 1996).

- 1997: the compensation grouting has been used to protect Big Ben in London (Haimoni and Wright, 1999).

- 2005: jet grouting has been used in Mostiště dam to control seepage in its cracked clay core, Czech Republic (Říha and Švancara, 2006).

- 2013: jet grouting and diaphragm wall were used in Karolinka dam to control the leakage on the downstream dam face, Czech Republic (Hodák, 2014).

- 2014: grouting has been used in Plumov dam to control the leakage from its body due to unstable foundation, Czech Republic (Povodí Moravy, 2020).

- 2015: grouting has been used in concrete Žermanice dam on the river Lučina to eliminate seepage along its expansion joints, Czech Republic (Darebník, 2017).

- 2017: grouting was used in Lichnov dam because of seepage through the right abutment, Czech Republic (Říha et al, 2020).

The diaphragm wall and jet grouting technology have been developed in concept of   design, equipment and material to be very suitable solution for many of engineering problems.

2.3 Literature review

The sealing technology was studied with many authors such as Chen and Zhang (1989) where they conducted a test on a section of an embankment dam in China, to monitor the relation between stress, and grouting pressure. Watanabe and Kanazawa (1995)   proposed a numerical method to evaluate static and dynamic behaviour of Tadami embankment dam with diaphragm wall constructed on riverbed sediment during earthquake. Morrmann (2004) presented an identification of relationships between wall and ground movement caused by excavation in the soft soil. Wisser, Augarde and Burd (2005) presented three-dimensional numerical modelling of grouting in clay to control ground movements caused by the construction of shallow tunnels. Piu (2005) presented some types of grouting with techniques, and compared between each method and its effect on displacement in soil through theoretical example by means software Plaxis 2D. Brzakala and Gorska (2007) simulated the ground movements during vertical wall installing process to determine the safety factor (SF) based on Flac 3D program. The numerical calculations reveal that SF of the wall decreases with its depth. Croce and Modoni (2007) presented the design of jet-grouting piles for various dam types, with particular attention to the discontinuities along the jet piles because of treatment axes deflection. Nikbakhtan, Aghababaei, and Pourrahimian (2007) investigated of the jet grouting effect on slope stability at Shahriar dam by using 3D analysis with Clara-W program. Dink and Wang (2008) presented 3D numerical model of mechanical response of ground, horizontal normal stress, shear stress, and ground displacement during construction of diaphragm wall. Janson (2008) studied radial ground improvement technology (RGIT) as a solver for the problem of excess pore pressure increasing during grouting

which leads to decrease in SF of saturated clay soil. Lagerlund (2009) presented remedial methods on dams damaged by internal erosion using different injection methods and compared between them. Fuchen, Xingqi, Wei and Aihua (2010) studied the grouting's influence on stress, strain and stability in earth-rock dam by using mud and materials with specific properties, based on FEM. Nikbakhtan and Ahangari (2010) introduced new relations between soilcrete diameter and its uniaxial compression strength with lifting and rotating speed, W/C ratio and grout pressure. Due to their experiments, the increasing in the grout pressure lead to increase both unconfined compressive strength UCS of soil and diameter of the soilcrete . On the other hand, the increasing in W/C ratio lead to increase both UCS and the diameter of the soilcrete. Conti, Sanctis and Viggiani (2012) studied the mechanisms of load transfer and the deformations of the ground during subsequent excavation and concreting in dry sand to evaluate the effects on wall deflections and the displacements of ground behind the wall by using FEM. Černý, Drochytka and Jandora (2012) studied the efficiency of using fly ash and clay as economical grout materials that increase homogeneity, and stability of the dam. Wang, Shen and Yang (2012) established a relationship among jet parameters, column diameter and soil properties which were applicable for most soil types. Hodak (2014) studied the effect of the weight of the machine on Karolinka dam displacement during construction diaphragm wall in its core. Chen, Wang, and Lei (2014) analysed the effect of installing diaphragm wall on adjacent soft clay. Masini, Rampello and Soga (2014) described an analytical model to evaluate the volume loss produced by pressure filtration of cement-bentonite grout as a function of soil, injection parameters, and difference of the jet-column's diameter. Michael, Thomash and Agnel (2015) presented a studied case of the jet grout columns construction to reduce seepage in the spillway and foundation of Morrison dam. Grambličková, Škvarka and Bednárová (2016) studied the remiditional actions of seepage in the Karolinka dam and simulated the leakage problem by FEM. Goh, Zhang, Zhang, Zhang and Liu (2017) studied the effect of soil parameters, wall diaphragm parameters and its depth on the maximum wall deflection by using FEM. Sivapriya, Gandhi and Sundaravadivelu (2018) studied in situ test the lateral movement during excavation in soft supported soil with diaphragm wall. Shu, Sun, Zhang and Wei (2019) investigated of the horizontal displacement, the maximum lateral deflection and lateral earth pressures on diaphragm wall during excavation in the clay zone in Jinan city, China. They found out that the deformation of surrounding building is adjacent to excavation 8 m away has three stages, including a uniform subsidence stage, an accelerated subsidence stage and a stable subsidence stage. Bayesteh and Sambermahani (2020) Studied the interaction between the low water clays and jet grout. They detected that there is a nonlinear

relationship between injection energy and the column diameter. They proposed the equation to estimate the diameter of the soilcrete column in low water content clays.

In my research, I modelled the processes of diaphragm wall and jet pile constructions in the Karolinka dam, in addition to studying their interaction with adjacent soil, shrinkage of cement and the effects of sealing as a solution for the seepage and displacement; to increase SF by Plaxis 3D.

2.4   Sealing techniques

2.4.1 Grout definition

Kutzner, (1996) gives a definition of grouting:

"The introduction with pressure of a material with the objective of waterproofing and consolidate in voids, cracks and porosity" (Benz, 2007).

 Volpi, (1998) gives another definition (Benz, 2007):

"the pumping of a stable fluid generally named "injection grout" into rock and soil to fill completely all cavities, voids and cracks, creating a solid sealed mass."

It divides into two main groups (Piu, 2005):

Suspension Grout: It is a mixture of one or many materials like cement, clay, lime, etc., which are suspended in a liquid medium.

Solution Grout: It consists of homogenous liquid mixture of two or more materials, and the most frequency products are sodium silicate and certain resins.

Figure (2.1) shows the application limits for grouting methods.
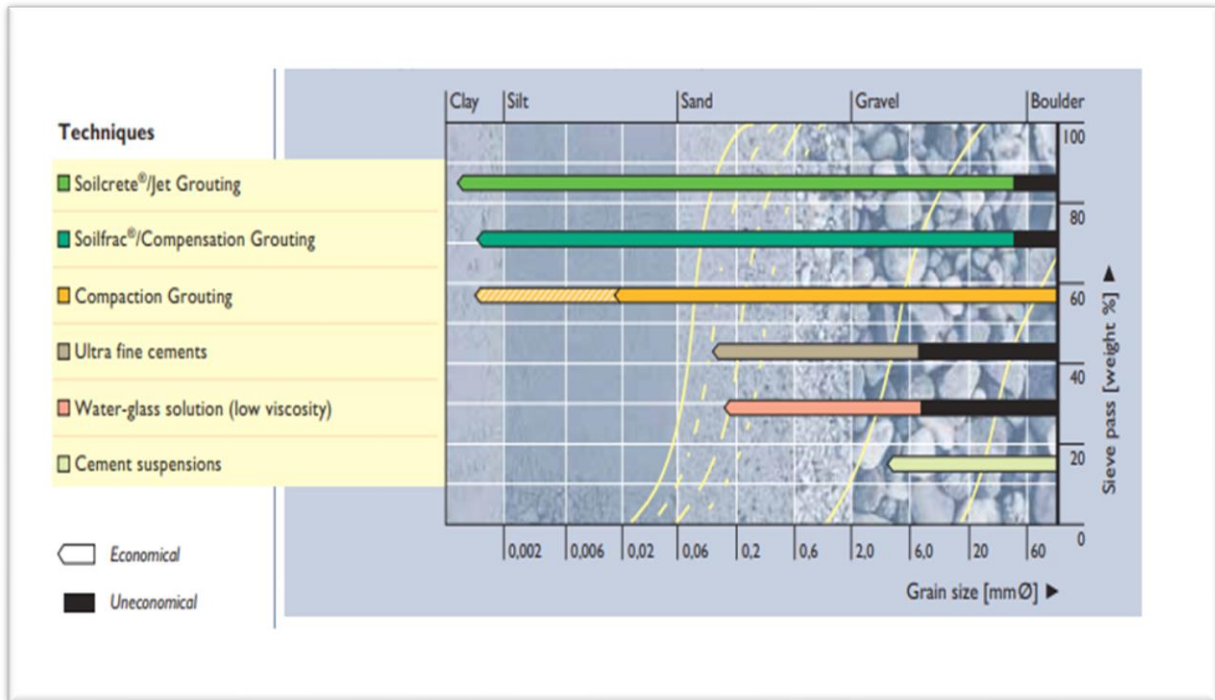
Fig. 2.1 Range of application for grouting techniques (Keller, 2005)

2.4.2 Main sealing methods

1. Permeation grouting

It is an injection of fluid grout with low pressure into the pores of soil without any change or displacement of surrounded soil by using cement or chemical materials to increase bearing capacity by filling all the voids and densifying the soil (Fig. 2. 2) (Keller, 2005).
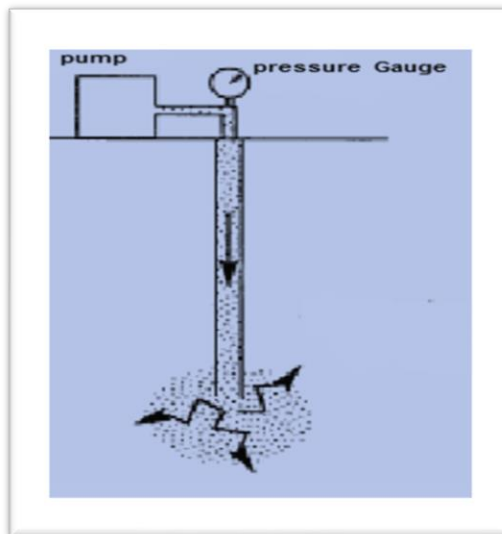
Fig. 2.2 Permeation grouting (Keogh, 2005)

13

2. Compaction grouting

This method of grouting is at a high-pressure level. It means displacing and compacting the adjacent compactable soil at the same time forming a bulb without fracturing the soil. Thus, mixture has to be with high viscosity to expand as a bulb without permeating (Fig. 2.3) (Xanthakos, Abramson and Bruce, 1994).
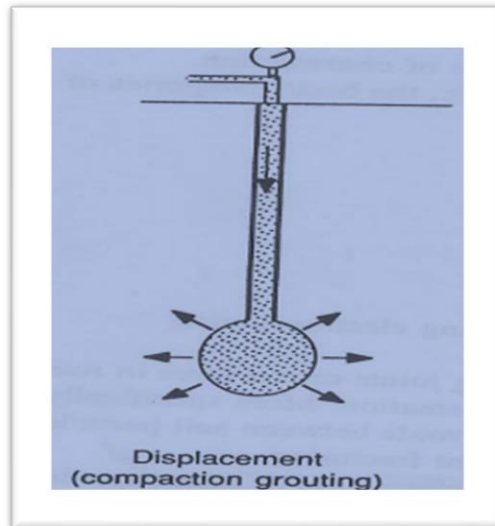
Fig. 2.3 Compaction grouting (Keogh, 2005)

3. Compensation grouting

It is a hydro fracture in the soil under high pressure by using low viscosity material and special pipes (tube-a-manchette TAM). The pressure from the grout causes cracks in the soil, and the fractures are filled with the mixture (Fig. 2.4) (Wisser, Augarde and Burd, 2005).
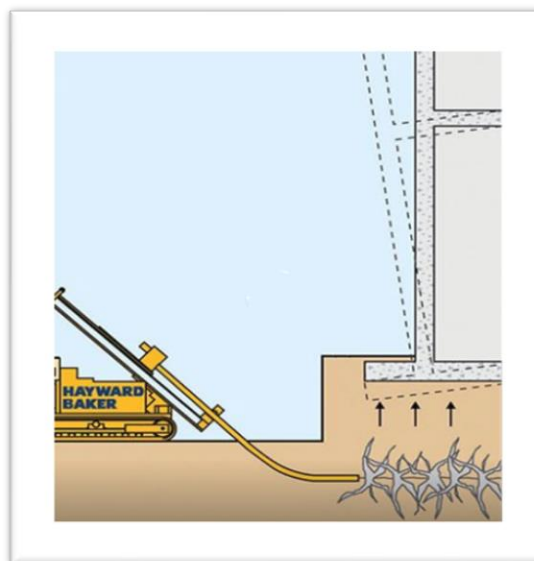
Fig. 2.4 Compensation grouting (Keller, 2005)

4.Vacuum grouting

It is a method of withdrawing air from the voids to create a vacuum, then using it to push grout in to fill the voids. The vacuum holds the structure together instead of adding the forces, such as the pressure injection, could be disruptive (Fig. 2. 5) (DSI, 2017).
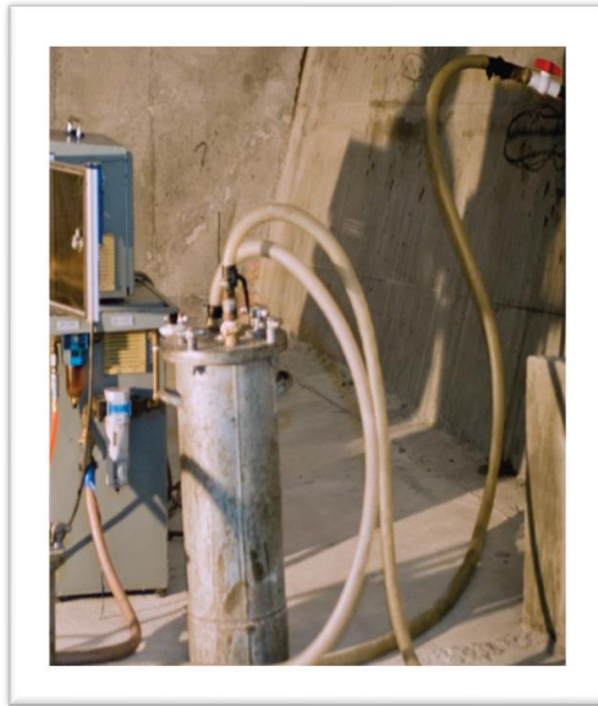
Fig. 2.5 Vacuum grouting (DSI, 2017)

5 Jet grouting

It is grouting with high pressure and velocity mixture that push through borehole to drill and mix with the soil at the same time to create soil of high strength and low permeability (Xanthakos, Abramson and Bruce, 1994).
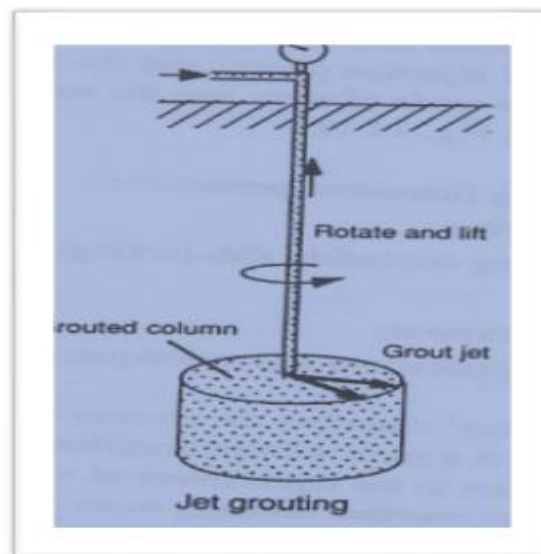
Fig. 2.6 Jet grouting (Keogh, 2005)

6 Diaphragm wall

A diaphragm wall is a supporting structural wall constructed in a deep excavated trench, to decrease water permeability as the most technical and economical solution.
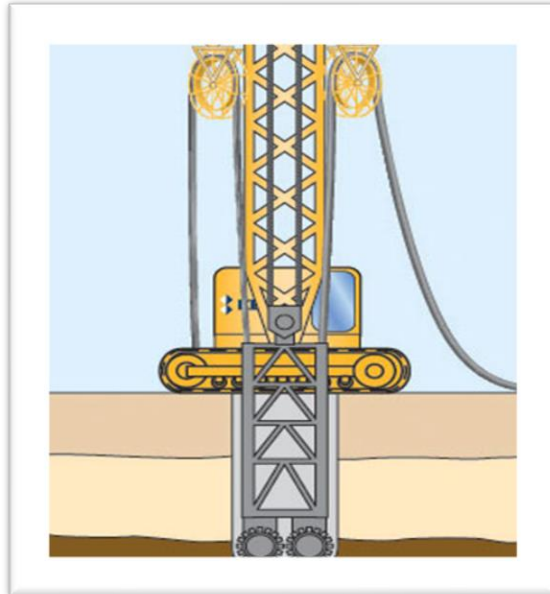
Fig. **2.7** Diaphragm wall (Keller, 2015)

2.4.3 Sealing materials

1. Cement: The most common type of cement is Portland cement which is mixed with water and sometimes sand.

2. **Bentonite:** It is a mixture of clay with additives that can create a permanent barrier to water flow.

3. Chemical mixture: The most common materials are sodium silicate, acrylate, lignin, urethane and resin grouts.

4. Resin material: The common types are tannin, phenol-formaldehyde and resorcinol formaldehyde.

5. Bituminous materials: There are many types of bitumen (asphalt), but the desirable type for sealing is an oxidized bitumen, because of its high solidification point.

3   SEALING IN THE EARTHEN DAM

   This technique has been used in remediation of the dams and their foundations (Bruce, 1990) as solver for many problem (seepage, settlement). When sealing is performed in a dam, caution must be taken in order not to cause damage to the core due to high pressures, and that is by the correct choice of the sealing method, pump pressures and appropriate procedure period. The main sealing methods used in the earthen dam are:

3.1 Diaphragm wall

  Although it is not grouting technique, diaphragm walls are often the best choice when the dam suffers big damage. This technique is widely used in construction work. It is used in the earthen dam over the last 40 years, and suited for clay-rich environments (Bolton and Stewart,1994).

3.1.1 Equipment

1. **Cutting drum:** They are equipped with tungsten carbide-tipped teeth that rotate in opposite directions to break up the soil.
2. **Guiding frame:** It is a heavy metal frame, serving as a guide.
3. **Tanks:** They are used for storing, and mixing bentonite slurry at site.
4. **Water pump:**   It keeps supplying the slurry tank with water.
5. **Slurry pump:** It is used for circulation of bentonite slurry at site.
6. **Tremie pipes:** They are connectable pipes made up off segments of 1 meter in length for concreting process.
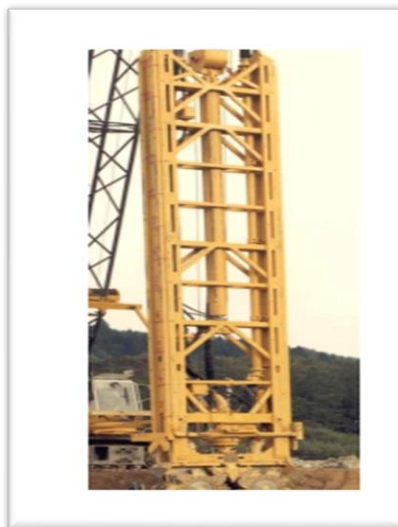
Fig 3.1 Guiding frame with cutting drum (Keller, 2005)

3.1.2 Construction process of diaphragm wall

1. Build guide wall: The guide wall is two parallel concrete beams constructed along the side of the wall as a guide to the clamshell, which excavates the trench and aids in the positioning of the final structure.

2. Build trench excavation: The vertical trench is dug using a clamshell or grab suspended by cables to a crane. The trench is filled with a slurry to produce a great lateral pressure sufficient enough to retain the vertical soil and prevent the sides of the trench from collapse.

3. Stope end installing: Two stop end plates will be placed at the ends of the excavated trench before concreting. The plates are withdrawn at the same time of concreting, so the continual diaphragm walls are constructed with tightly joined.

4. Concreting: Placing the concrete is done by using termite pipes to avoid the segregation of concrete. Once concrete being poured down, slurry will be displaced due to its lower density than concrete, then collected and refused.

Fig 3.2 Construction process of a diaphragm wall (Keller, 2005)

3.1.3 Diaphragm wall advantages

- It can be used at great depths up to (100 m).
- It works well with the high-cohesive soil.
- Diaphragm wall blocks excessive seepage along dam length
- The vibration because of diaphragm wall installation is less than other methods.
- It can be used as permanent structural wall to prevent water seepage and strengthen the structure.
- It can be used as a foundation element.
- High vertical and horizontal loads can be carried.
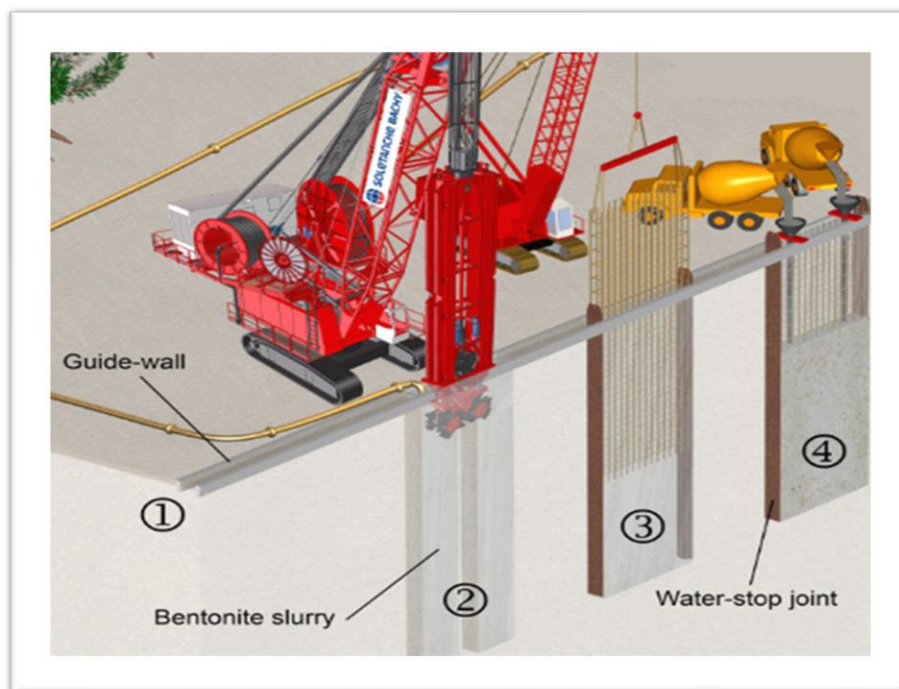- Low soil deformations just behind the wall as a result of the high bending stiffness of the wall.
- Execution is possible in case of hard layers in the soil.

3.1.4 Diaphragm wall disadvantages

- The final product is prone to shrinkage.
- It requires large-scale linings.
- It requires special equipment.
- Uneconomical in some cases (shallow basements).
- The risk of loss or spillage bentonite slurry.
- The high cost of cleaning and the disposable of slurry.
- The need to continue in the construction process starting from the excavation to the removal of the temporary end stop and concreting.

3.2 Jet grouting

Jet grouting is the most popular method for ground improvement. This technique is widely used over the world. Its application has been grown to a large variety of purposes as reducing structure displacements, increasing the bearing capacity and supporting open underground excavation. It is cutting and mixing the soil with grout material under high speed to form cylindrical columns (Fang et al, 1994). Jet grouting technique is used in earthen dam for reducing seepage through its body and foundation, without disturbing the nearby existing structures.

3.2.1 Equipment

1 **Drilling rig:** It is a steel machine that moves by a hydraulic motor; the rig consists of a mounted body on wheels or a track with a drill rod attached.

2 **Grout plant:** It includes cement silo with a suitable capacity, and grout mixer for colloidal mixing in batches. Also, it is provided with weighing measuring system for the materials that pass in each batch to feed the pump.

3 **Pumps:** It is very important to provide with pumps have capable of continuously delivering grout high pressure to work zone.

4 **Injection pipe:** It is a special kind of pipes known as Manchette tube, which is a PVC or metal, with the holes at equal spacing around its circumference, that are covered by a rubber sleeve to allow the grout to flow out and prevents it from going back (Choi, 2005).
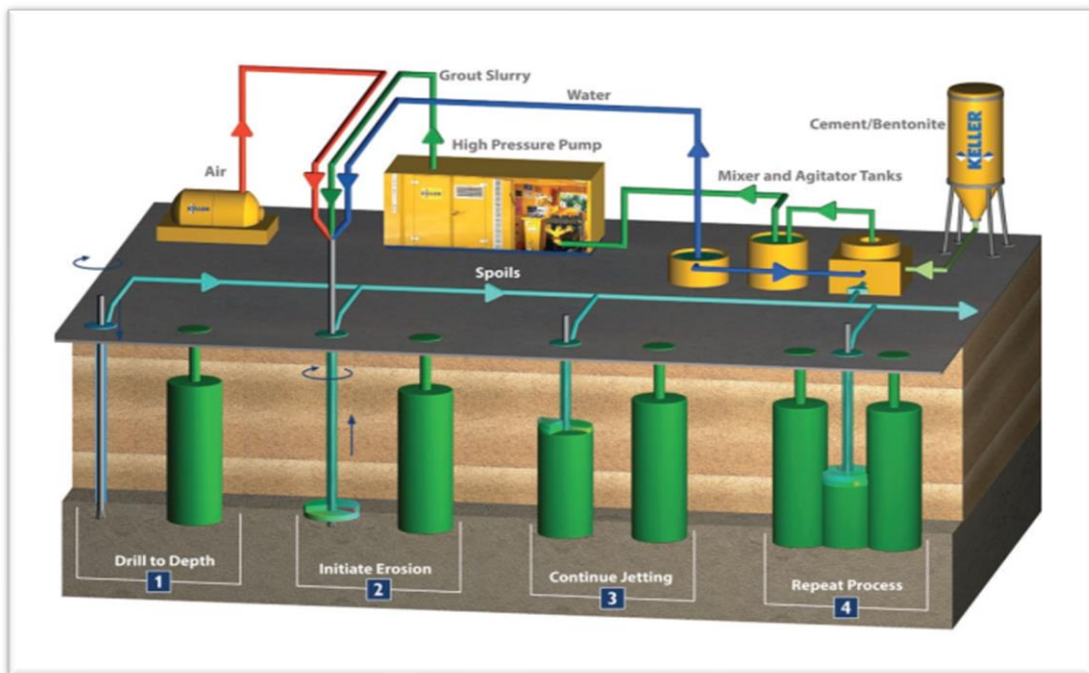
Fig. 3.3 Jet grouting equipment (Keller, 2005)

3.2.2 Jet grouting methods

The method of jet grouting varies based on what system of fluid is used in the grouting process, so they are grouped in three systems named (Choi, 2005) (Fig. 3.4):

A) Single jet system

In this case, the jetting fluid is injected into the ground through one or more nozzles with a high velocity of jet stream to cut, remove and mix in the soil. It is suitable for shallow depths and horizontal jet grout applications.

B) Double jet system

It is an injection with very high velocity jetting within a cone of air, where the excess soil is removed by the action of the airlift. It is suitable for more improvement and cohesive soils.

C)Triple jet system

In the triple jet system, soil loosening and removing happen by the effect of water and air shrouded with a high pressure and the space is filled with grout out of the lower nozzle. It is suitable for underpinning, slabs and cohesive soils.
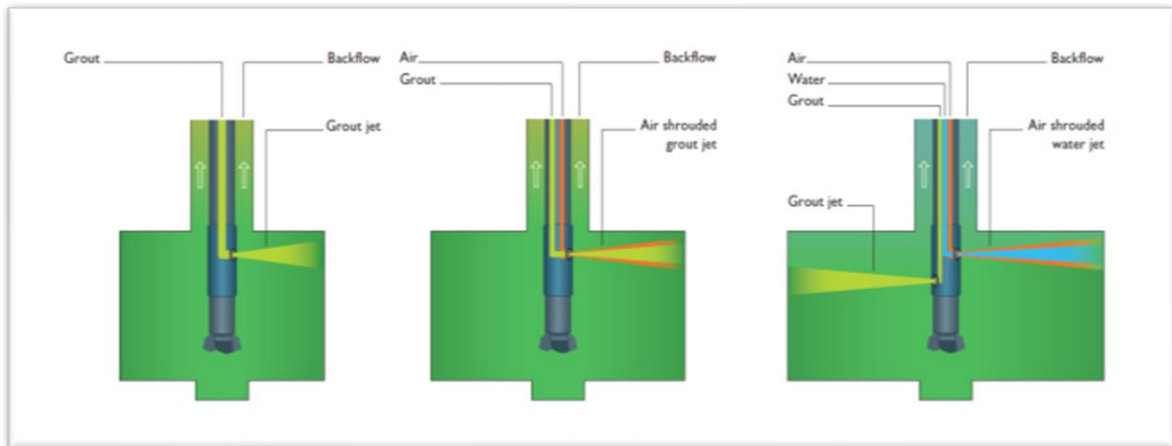
Fig. 3.4 Different injection techniques used in jet grouting (Keller, 2005)

3.2.3 Construction process of jet grouting

1. **Drilling:** The drill rod equipped with jet nozzle holder drills into the ground to the required depth.

2. **Jetting:** A jetting fluid is pumped through the jet nozzle at a high pressure. This erodes the soil from its natural position and mixes it with the jetting fluid.

3. **Grouting:** Jet rod rotates and simultaneously retracts then a grouting column forms in the soil (Choe, 2005).
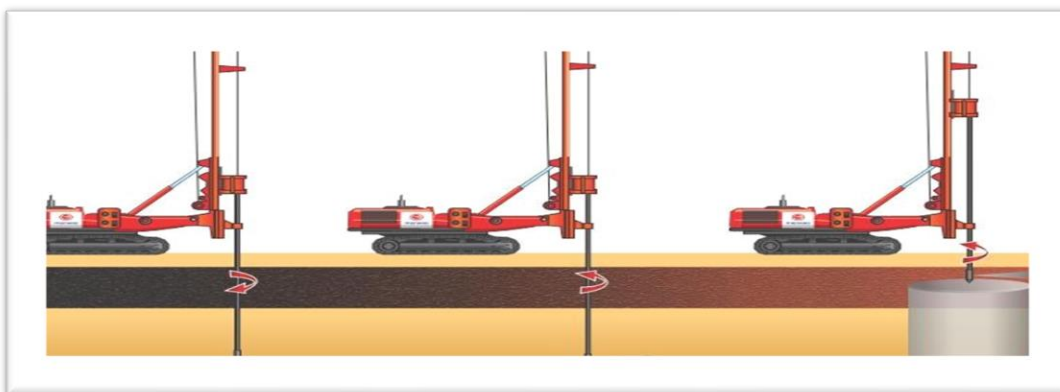
Fig. 3.5 Main steps of jet grouting (Keller, 2005)

21

3.2.4 Jet grouting advantages

- The final permeability is low.
- It is suitable for a wide range of soil types.
- The level of noise is lower than other systems.
- Large diameter columns can be formed up to 4 meters.
- It is able to operate in all conditions of engineering structures (confined, underground installations).
- Much faster than alternative methods.
- Jet grouting could be combined with other grouting methods as an integrated solution.

3.2.5 Jet grouting disadvantages

- The strength of the grouted pillar becomes too high.
- It might cause movement of ground and distresses to existing structures.
- The materials of chemical grouting have a negative impact on the soil groundwater.
- The required amount of grout is hard to estimate.
- It is very difficult to control heave in the cohesive soil.
- Spoil handling can be difficult.

4 MATHEMATICAL MODELLING OF SEALING IN KAROLINKA DAM

4.1 Information about dam

The Karolinka earth fill dam was constructed between 1977 and 1984, on the Stanovnice river above the town of Karolinka in the region of Vsetínsko, to supply the cities of Vsetínsko and Vlársko, with pure and wholesome water, protect from floods, and generate hydroelectric energy. The first filling of reservoir of Karolinka dam was in year of 1986. Karolinka dam is earth-fill dam consists of vertical clay gravelly core surrounded on both sides by filters of gravel extracted from the valley of the Stanovnice water stream. The face zones are formed by gravel sand from the Novy Hrozenkov and the upstream face is reinforced with macadam filled with bitumen. (Fig 4. 1) (Pařílková et al, 2016).
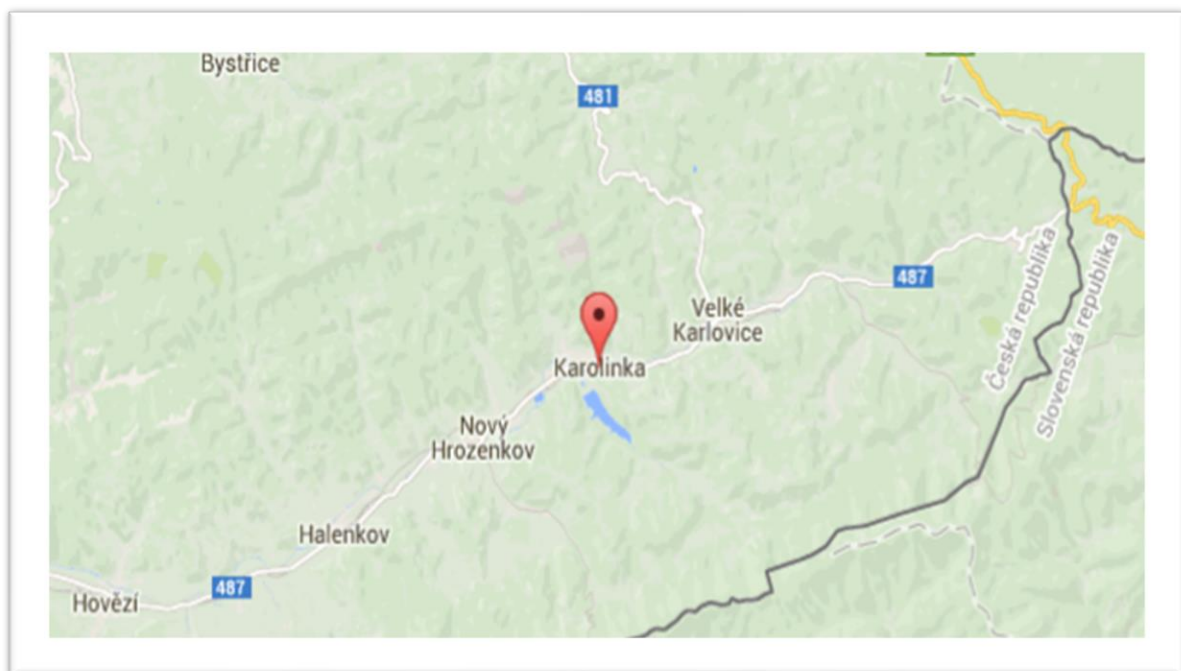
Fig. 4.1 Location of the Karolinka dam

Fig. 4.2 Karolinka aerial view (**http://www.pmo.cz**)

The Karolinka dam parameters used in modelling are shown in Tab. 4.1

Table 4.1 The Karolinka dam specifications

Reservoir

Inactive storage	929000 m^3
Active storage	5813000 m^3
Flood storage	653000 m^3
Reservoir volume	7521000 m^3
Reservoir area at max WL	489000 m^2
Reservoir area at permanent storage level	142000 m^2
Constant storage level	500.00 m a.s.l.
Maximum storage WL	520.00 m a.s.l.
Maximum flood level	521.80 m a.s.l.
Basin area	23100000 m^2

<u>Dam</u>

Category	II
Administration	Povodí Moravy
River	Stanovnice
Town	Karolinka
District	Vsetin
Length	392 m
Crest width	5 m
Height	39 m
Upstream slope	1: 3. 25
Downstream slope	1: 2.2 - 2.4

4.2 Climatic conditions

The case study area always undergoes strong precipitation in the months: (January, April, June, July, August, October and December). The rainiest month is June and the average amount of annual precipitation is 701.0 mm. The maximum annual temperature is 12.0° and the minimum is 3.0°. The coldest month is January and the warmest is August. The relative humidity ranges between 85 % in December and 70.0 % in April. The windiest month is January, with 4 m/s wind speed and the least windy month is August, with 2 m/s (world weather and climate information, 2016). The result of continuous monitoring of climate variables during the period (21-3-2011 to 26-7-2015) is illustrated in Fig (4.3).
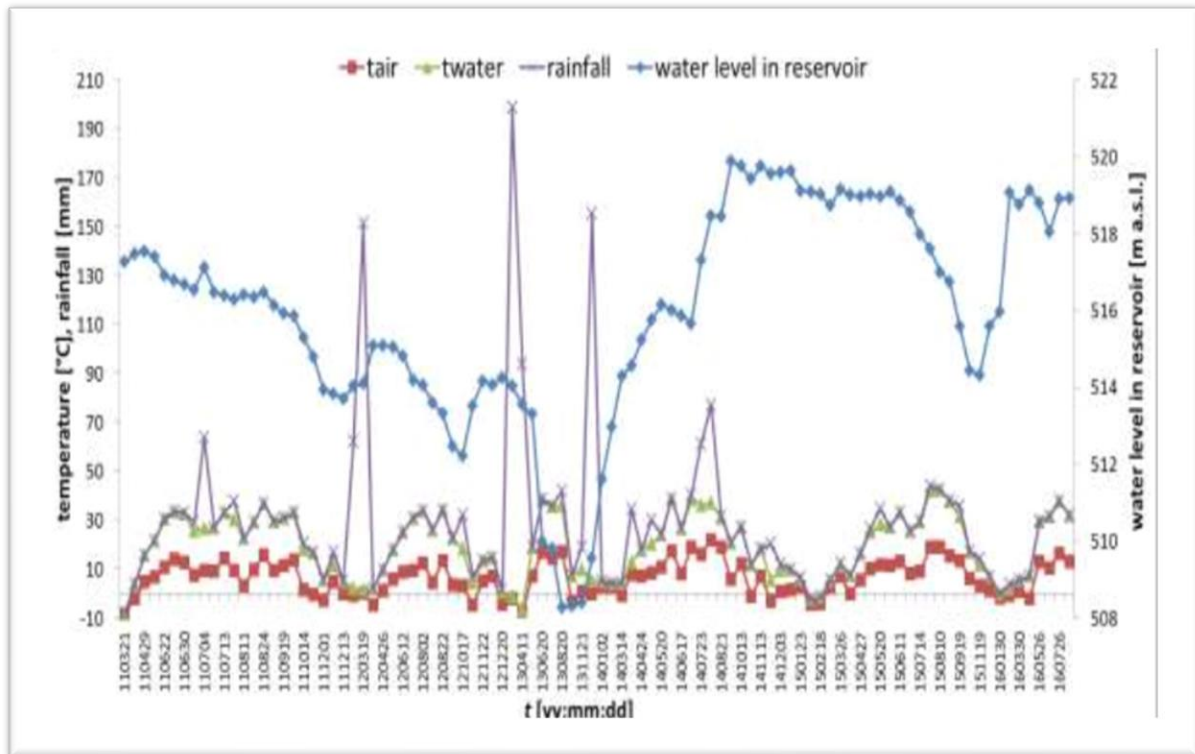
Fig. 4.3 Monitored variables with time (Pařílková et al, 2016)

4.3 Historical study of seepage problem

Because of leakage on the downstream dam face due to a technological indiscipline when filling dam layers during dam construction stage, a different composition of mixed soils; the grain sizes of soil with high difference (fine- gravelly grains) and bad compacting of soil during the construction stage, which led to permeability of the core and downstream dam face (Jareš and Krejčí, 2015). So that the reservoir was used to a limited level. The history of the seepage problem can be summed up as following:

1. December 1984   The first filling of the reservoir
2. February 1986   The first problems of leakage on the downstream dam face appeared at level 517.98 m a.s.l.
3. February 1987   The highest level of water (520 m a.s.l).
4. June 1987   The water level had been decreased because of leakage to (518 m a.s.l).
5. July 1987   Installing five vertical drainage wells PV7 till PV11 in the upper berm of dam.
6. July 1988   Installing drainage wells DV1, DV2 in the left side and DV3, DV4 in the right side with a length ranges from (85m) to (105 m).

26

7. August 1989   Excavating by grundomat machine and installing drain rib D2A.

8. November 1990   Installing the drain ribs D1, D2A, D2B, D3, D4, D5, D6, and D7 in the left side of lower berm, and D8B, D10A, and D11A in the right side of lower berm of the dam.

9. December 1991   Stopping the trial operations.

10. November 1992   Installing ten new drain ribs in lower berm of dam and three in upper berm of dam.

11. May 1996   Installing new drainage wells in the lower berm of dam.

12. February 1997   Starting measuring drainage wells level.

13. June 1997   Installing a second new drainage well in the lower berm of dam.

14. September 1998   Installing   a measuring well in the left side of lower berm.

15. April 1999   Installing three vertical drainage wells PV12 till PV14, (10 m) deep

16. June 1999   Installing six new drain ribs in lower and upper berm of dam.

17. July 1999   Remedial actions of spillway erosion.

18. August 1999   Replacing concrete canal pavement slab on the left side of dam toe.

19. May 2000   Automatic leakage measurement.

20. July 2002   Installing new drain ribs instead of non-functional ribs.

21. July 2003   Installing two new drain ribs in lower berm and bottom zone of dam.

22. September 2003   Replacing concrete canal pavement slab on the right side of dam toe.

23. November 2003   Remedial actions of the dam crest

24. June 2004   Connecting the pore pressure sensors to S.A.E system.

25. July 2004   Geotechnical investigation of dam crest and installing pore pressure sensors.

26. November 2009   Replacing gauges of pore pressure sensors.

27. October 2010   Geophysical measurements were made to investigate the heterogeneity of the material of the core.

28. June 2011   Geophysical measurements were made on the downstream dam face by NOZA company.

29. November 2012   Removing culvert downstream of the dam and checking the drills made from the dam crest to the gallery ceiling.

There were some steps to improve safety which had been developed to reconstruct the dam after extensive surveys in 2005. The major rehabilitation was commenced in period from September 2012 till October 2013 and it includes:

1- Remediation of central core of the dam by using a diaphragm wall

and jet grouting technology.

2- Protecting the surface of the dam by installing a new steel railing.

3- Renewing the roads, with a new sand-gravel and reinforced concrete. The project was completed by the end of October 2013.

30. September 2013   Monitoring is carried out regularly once a month.

31. February 2015 until February 2017   Seepages is appeared and inrush area reappeared at the downstream face of the dam.

4.4 Parameters of soil

Due to sensitivity analysis, some of parameters are assumed according to the specifications of the materials in dam. The material parameters used in modelling is shown in Tab (4. 2).

Parameters	Core	Zone 2b	Zone 2a	Zone 3	Subsoil	Diaphragm Wall / Jet pile	Mixture	Curtain	Drain	Bentonite
Hydrauli conductivity [m/day]	0.086	0.864	0.864	4.320	4.320	$0.864.10^3$	$0.864.10^4$	–	86.4	$0.864.10^5$
Unsaturated unit weight [kN/m³]	19	19	19	19	19	12.5	12.5	25	20	10.5
Saturated unit weight [kN/m³]	21	21	21	21	21	12.5	12.5	25	21	10.5
Young modulus [kN/m²]	20.10^3	70.10^3	70.10^3	70.10^3	70.10^3	25.10^3	500	40.10^6	100.10^3	400
Poisson's ratio [-]	0.3	0.2	0.2	0.2	0.2	0.25	0.4	0.1	0.15	0.4
Cohesion [kN/m²]	21	1	1	1	1	200	18	–	1	16
Friction angle [°]	1	33	33	33	33	–	–	–	37	–
Interface reduction [-]	0.7	1	1	1	1	1	1	1	1	1

Table. 4.2 Material properties

28

4.5 Reliability Analysis of Karolinka Dam

4.5.1 Analysis of seepage problem

All dams have some seepage because the impounded water seeks paths with weak resistance through the dam and its foundation. The seepage through an earthen dam generally is related to WL of the reservoir. When water seeps from the reservoir through the foundation, the soil erodes and this could result in creating piping through the dam. Seepage must be controlled in terms of both velocity and quantity. It is not an easy to convert the seepage problems into numerical counterpart because of the heterogeneity of the natural soils and the varying boundary condition. The seepage analysis is mainly in the interest of slope stability of the earthen dam. Most studies analysed the seepage problem through the sketching flow net, by assuming the water flows in the saturated zone. The calculation of the seepage has been simplified with numerical applications like FEM. The seepage analysis can be divided into:

A) *Steady state flow analysis*

The boundary conditions inside and outside the ground don't change with time. The storage function drops out and time dependent term disappears and only the coefficient of permeability is required. Darcy's law originally describes water movement in saturated soil. Also, it can be used for unsaturated soil (Richards, 1931) as follows:

$$q = -k.i \tag{4.1}$$

Where q is the discharge per unit area, i is the hydraulic gradient, and k is the permeability coefficient. The governing equation describing the water flow through a porous medium in steady state and obeying the Darcy's law can be written as:

$$\frac{\partial}{\partial x}\left(k_x \frac{\partial h}{\partial x}\right) + \frac{\partial}{\partial y}\left(k_y \frac{\partial h}{\partial y}\right) + \frac{\partial}{\partial z}\left(k_z \frac{\partial h}{\partial z}\right) = 0 \tag{4.2}$$

Where k_x, k_y and k_z are the permeability coefficient in x, y and z direction, respectively, h is piezometric height.

B) *Transient seepage analysis*

The transient state condition is a variable of time and degree of saturation of the soil, different inflow and outflow with time. The governing partial differential equation for seepage through a heterogeneous, anisotropic, saturated and unsaturated soil depending on the conservation of mass for a representative elemental volume. Concerning Darcy's law, the total stress remains constant

during a transient process and pore air pressure is atmospheric, the differential equation for the three-dimensional transient seepage can be written as follows (Thieu et al, 2001):

$$\frac{\partial}{\partial x}\left(k_x \frac{\partial h}{\partial x}\right) + \frac{\partial}{\partial y}\left(k_y \frac{\partial h}{\partial y}\right) + \frac{\partial}{\partial z}\left(k_z \frac{\partial h}{\partial z}\right) = m\gamma \frac{\partial h}{\partial t} \tag{4.3}$$

Where k_x, k_y and k_z are the permeability coefficient in x, y and z direction, respectively, h is piezometric height, m is the water storage and γ is unit weight.

4.5.2 Analysis of stability problem

A) Limit equilibrium (conventional slip circle analysis)

Limit equilibrium (LE) has been used for analysing the slope stability and geotechnical structures safety since 1930. LE methods are based on some assumptions about the sliding surface shape, and it is one of the most popular methods because of their simplicity, with no need for many parameters. The typical output from a LM analysis is SF. LM methods sum forces and moments related to an assumed slip surface passed through a soil mass. It assumes a slip surface and the soils along this surface providing shear resistance. Depending on the Mohr-Coulomb (MC) equation at the failure, the shear stress τ along the failure surface reaches the shear strength (Nash,1987), and the safety factor is:

$$F = \frac{\tau_f}{\tau} \tag{4.4}$$

$$\tau_f = c'_+ \sigma' \tan \varphi' \tag{4.5}$$

Where τ_f is failure shear strength of the soil, τ is shear stress of the soil, c' is effective cohesion of the soil, and ϕ' is effective friction angle. SF is assumed to be constant along the slip surface and can be defined in terms of stresses (total and effective), forces and moments, as illustrated in Figure (4.4)
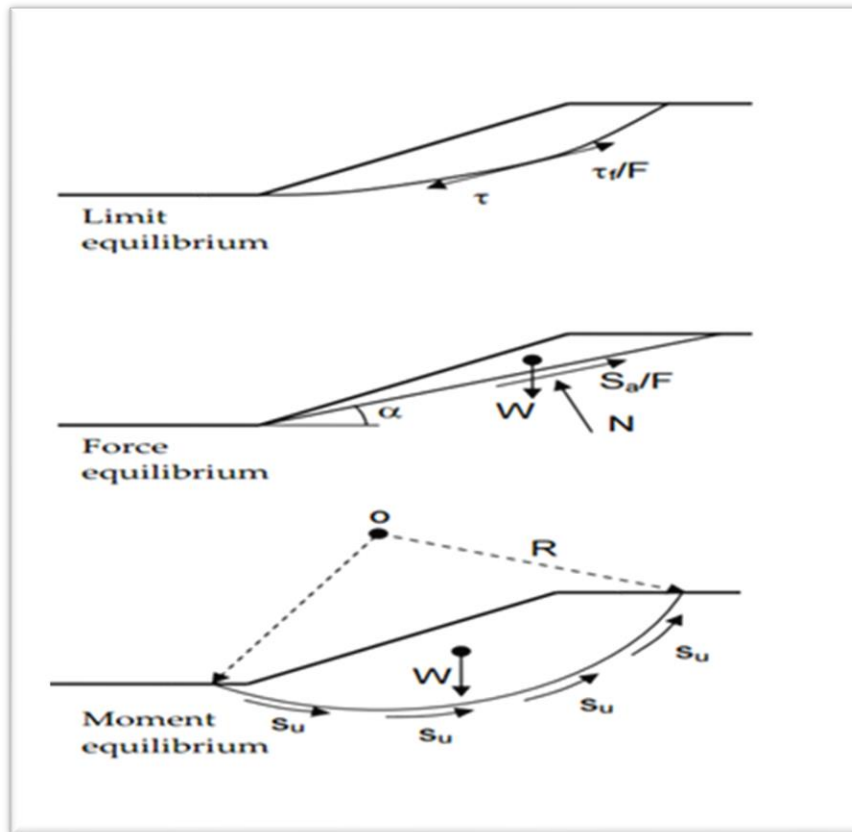
Fig. 4.4 Various definition of safety factor (Abramson et al, 2002)

B) Finite element method (shear strength reduction)

Although LE methods do not take into account the soil behaviour, it is important to make an initial stability assessment for simple problem geometries using LE software. Conversely, the problems of complex geometries, or those that require seepage analysis, consolidation and fully coupled flow-deformation analysis (FCFD) to analyse the development of deformation and pore water pressure as a result of time-dependent hydraulic boundary condition, FEM would be better to demonstrate the geometry of failure surfaces, clear the deformations in soils with their exact place, and simulate failure mechanism as well. In FEM, failure occurs naturally through the zones where the applied shear stress exceeds the shear strength, thus no assumption about the shape or location of the failure surface. Figure (4.5) illustrates the stresses that are imported from a finite element analysis into LE analysis.
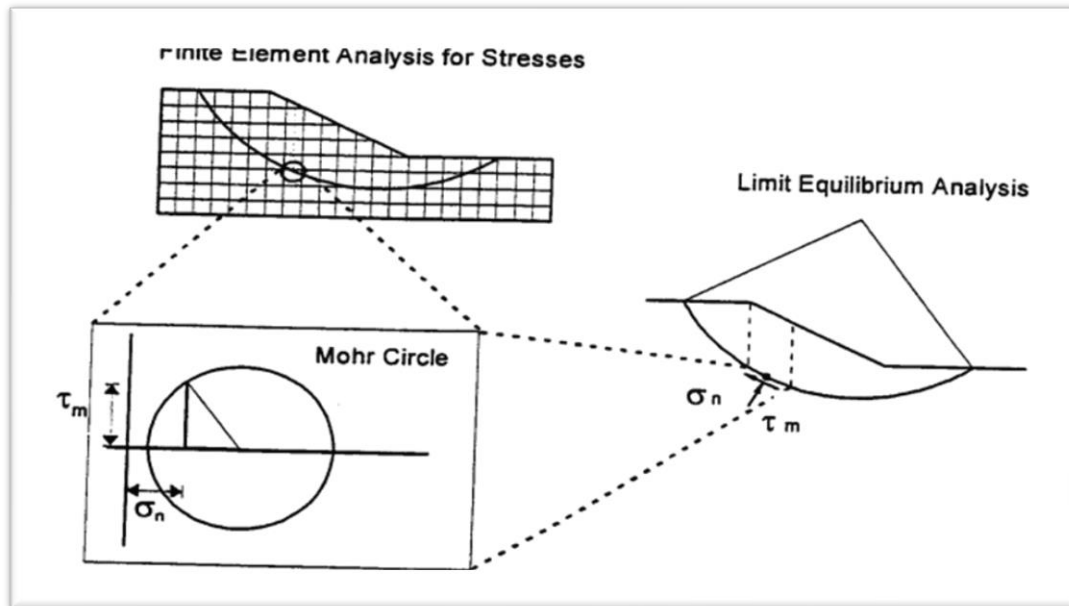
Fig. 4.5 Imported stresses from a finite element analysis into a limit equilibrium analysis
(Fredlun et al, 1999)

4.5.3 Analysis of cement autogenous shrinkage problem

The shrinkage expresses a time-dependent deformation which reduces the volume of elements in all directions during the hardening process of the element due to water loss. The value of shrinkage is influenced by temperature, humidity, elements dimensions, w/c factor, type and quantity of cement. Mineral admixtures such as fly ash is added as cementing materials, also affect the shrinkage strain by enhancing the pore refinement of the cement paste, and increase in capillary tension. As a result, more autogenous shrinkage; the change in volume due to the chemical process of hydration of cement, (Mazloom et al. 2000). The shrinkage causes cracking in the element because of strains and stresses which decrease an element's ability to ban the flow of water and effect on its strength (Lura, 2003).

4.6 Numerical approach

Because of the techniques development, it has been used numerical solution of geotechnical problems, which depend on the solution of the partial differential equations. The most popular numerical methods can be summed up as follows:

- **Finite Difference Method** (**FDM**): It is the oldest numerical method. It is based upon the application of a local Taylor expansion to approximate the differential equations. It is used to solve the problems, including linear and non-linear, time-independent and dependent

problems. In comparison with FEM, FDM is tough to implement in complex geometry, so in most of the cases, the accuracy of FDM increases with refining grid.

- **Finite Element Method** (**FEM**): It is a widely used because of flexibility in dealing with complex geometric domains, any type of loading, different types of material properties, various boundary conditions. On the other hand, it has some disadvantages. For example, it doesn't prove to be efficient for fluid dynamics problems also the time of computational is high. It is a method of solving continuous problems governed by differential equations. It is based on the discretization of a continuum into a number of elements which are connected at nodal points. Each element is assigned an element property with stiffness characteristics. This force displacement relationship is expressed as (Bhavikati, 2005):

$$\lfloor K \rfloor * \{\delta\} = \{F\} \qquad (4.6)$$

Where $\lfloor K \rfloor$ is the element stiffness matrix, $\{\delta\}$is the nodal displacement vector of the element and $\{F\}$ is the nodal force vector. In this study, the behaviour of the dam , foundation and the effects of the reconstructions have been analysed using FEM which is based on package Plaxis 3D.

4.6.1 Plaxis 3D software

It is a powerful and an advanced finite element software. It is intended to three-dimensional analysis of deformation, stability of soil structures under static and dynamic loading and groundwater flow. It is divided into:

• PLAXIS 3D Input: It includes geometry, materials set, initial and boundary condition and forming calculation phases.

• PLAXIS 3D Output: It includes the deformation, cross sections, and plot various relationships. It is used for post- processing of the calculation result

The continuum elements consist of 10 node tetrahedral elements. The domain is discretised into a mesh by elements. The mathematical system is connected to the soil for describing its behaviour.

4.6.2 Assumptions of material

➢ Homogeneous: The properties are not function of position.
➢ Continuum: There are no holes or voids.
➢ Isotropic and hydraulic conductivity are considered for each material.
➢ Elastic-Perfectly Plastic behaviour for the dam body and subsoil (Dawson et al, 1999).

➤ The strains are small.

➤ Mixture grouting is incompressible.

➤ Flow in the soil is ideal.

4.6.3 Constitutive model

The constitutive soil models have been developed, based on an experimental observations on the soil behaviour for modelling the stress- strain behaviour of soil. Plaxis includes many models involving specifice features, where are used for simulating non-linear and time-dependent behaviour of soils. The constitutive model used in this study is linear-elastic perfectly plastic with MC failure criterion. All expressions, formulas and input parameters of material and their models are described according to behaviour (Brinkgreve et al., 2017). MC Model involves five input parameters, those are elastic modulus E, poisson ratio v for soil elasticity and the friction angle φ, the cohesion c for soil plasticity, also the angle of dilatation ψ. MC model is a first-order to provide with a trusty result of soil behaviour (Brinkgreve et al. 2017). The material behaves elastically until all the shear strength have been mobilized (Brinkgreve, 2017). When reaching the yield criterion, all load increments will lead to plastic strains. MC failure criterion can be written as the equation for the line that represents the failure envelope (Labuz, Zang, 2012)

$$\tau = \sigma' \tan \varphi' + \acute{c} \tag{4.7}$$

Where τ is shear stress, σ' is effective normal stress, φ' is effective angle of internal friction and $\acute{c}$ is effective cohesion.
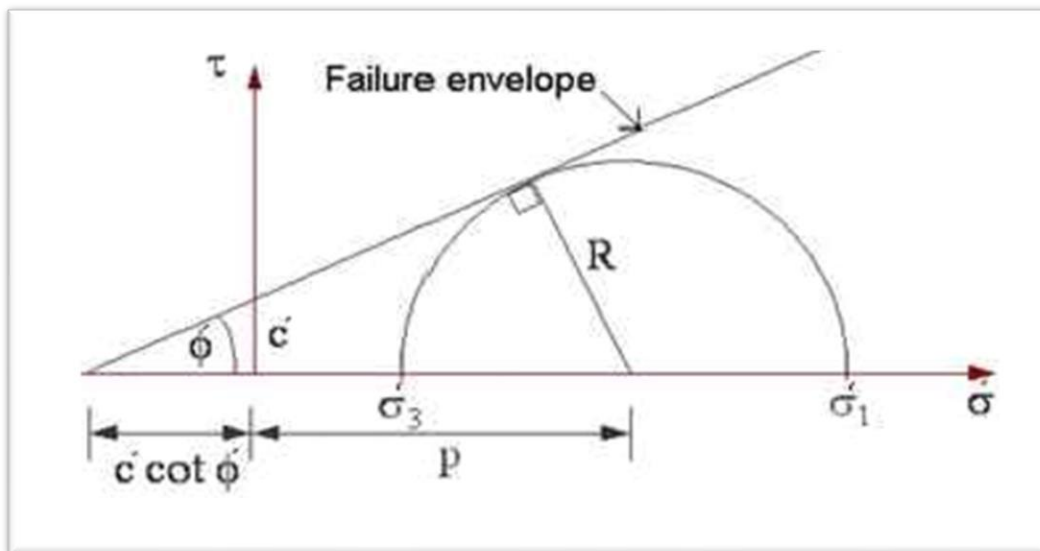

Fig. 4.6 Mohr diagram and failure envelope

For the third dimension, the failure surface in MC model occurs as hexagonal cone in the

principal stress space. Inside the surface elastic deformations will be developed until reached to elastic-plastic deformations. When the soil element has reached the stress surface, the elastic deformations goes to elastic-plastic state.
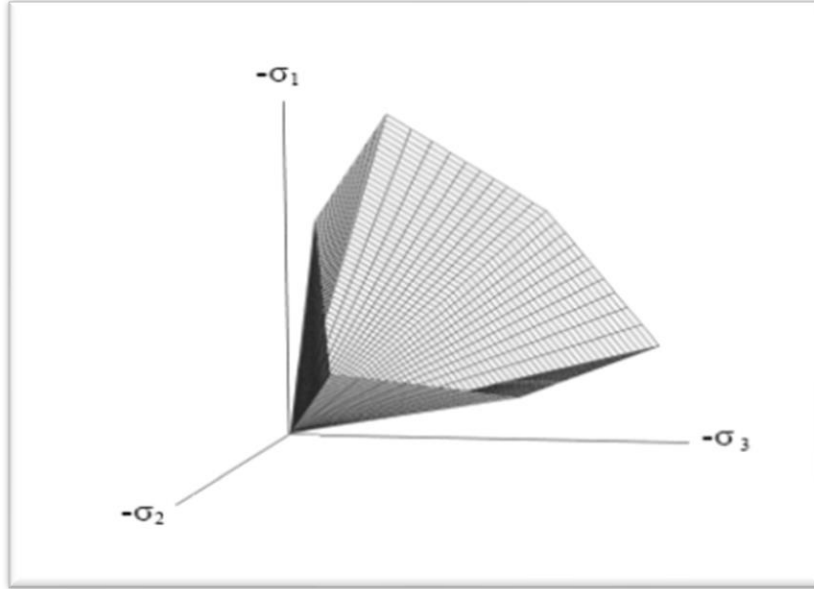

Fig. 4.7 Mohr-Coulomb yield surface in principal stress space (Potts et al, 2002)

Depending on Figure (4.6) it can be inferred:

$$\sin \acute{\varphi} = \frac{R}{\acute{C} \cot \acute{\varphi} + P} = \frac{\sigma'_1 - \sigma'_3}{\acute{C} \cot \acute{\varphi} + \frac{\sigma'_1 + \sigma'_3}{2}} \tag{4.8}$$

$$\frac{\sigma'_1 - \sigma'_3}{2} = \sin \acute{\varphi} \frac{\sigma'_1 + \sigma'_3}{2} + \acute{c} \cos \acute{\varphi} \tag{4.9}$$

$$\sigma'_1 - \sigma'_3 = \sin \acute{\varphi} \, (\sigma'_1 + \sigma'_3) + 2\acute{c} \cot \acute{\varphi} \tag{4.10}$$

$$\sigma'_1 = \sigma'_3 \left(\frac{1 + \sin \acute{\varphi}}{1 - \sin \acute{\varphi}}\right) + 2\acute{c} \left(\frac{\cos \acute{\varphi}}{1 - \sin \acute{\varphi}}\right) \tag{4.11}$$

As a result, the failure criterion can be expressed in terms of the relationship between the principal stresses (Trigonometric Functions):

$$\sigma'_1 = \sigma'_3 \tan^2 \left(\frac{\acute{\varphi}}{2} + 45\right) + 2\acute{c} \tan \left(\frac{\acute{\varphi}}{2} + 45\right) \tag{4.12}$$

Where σ'_1, σ'_3 are major and minor effective principal stress respectively. MC model is a reliable model and its parameters are well known and can be obtained from different soil tests.

4.6.4 Initial conditions

The initial conditions in general comprise the initial groundwater conditions, the initial geometry configuration and the initial effective stress state.

- Initial Displacements

The hydrodynamic analyses of dams assume at time t=0, the dam is in the state of static equilibrium and the initial displacements equal zero.

- Initial Ground Water Surface

The initial piezometric head in the domain (steady state flow) is equal to specified piezometric head.

- Initial stresses

The initial stress field is influenced by the material weight and the history of its formation. This stress state is usually characterized by an initial vertical effective stress and the initial horizontal effective stress, and they are related to the coefficient of lateral earth pressure K'_0 as follows:

$$\sigma'_v = \gamma.d \tag{4.13}$$

$$\sigma'_h = \sigma'_v.K'_0 \tag{4.14}$$

Where σ'_V is vertical effective stress, σ'_h is horizontal effective stress, K'_0 is coefficient of lateral earth pressure, and for coarse grained soil:

$$K'_0 = (1 - sin\,\varphi') \tag{4.15}$$

4.6.5 Boundary conditions

Boundary conditions are required at the boundaries of solution domain to define the limits and conditions in the cross-section that is being analysed. Setting up the boundary conditions in the model is a major step because the result is dependent on the chosen boundary conditions in the model.

There are two types of boundary conditions in hydrodynamic analysis of dams:

I.   Dirichlet conditions (specified head boundary)

It consists in specifying the known value of the variables, usually represents a body of surface water. In this case the function values are specified on boundaries. In the seepage analysis through the earthen dam, the Dirichlet boundary condition is dominant when the water head is specified on boundaries.

II.   Neumann conditions (specified flow boundary)

It consists in imposing the value of the derivative, which are WL gradient boundaries. In this case the function derivative values are specified on boundaries.

4.6.6 Soil parameters

Soil layers were modeled as three-dimensional continuum elements using MC model. For current study method B was considered for undrained calculation. It enables us to perform the undrained calculations considering effective stiffness parameters and undrained shear strength. Also mode drained was chosen to analys the coarse-grained materials (i.e., gravels, sands).

4.6.7 Structural elements in Plaxis 3D

Plate elements are structural objects with linear elastic in Plaxis 3D, and isotropic modelling is optional. The plate is used as a two dimensional structure element with 6 nodal triangles .The plate parameters are: thickness (d), unit weight (γ), plate modulus in both directions (E_1 and E_2), Poisson ratio (v), and shear modulus (G_{12}, G_{13} and G_{23}). The node-to-node anchors are one dimensional with two nodal line elements.

4.6.8 Interface element

The interaction between the structural element and the soil is modeled by mean of the interface. It is used to reduce the friction between the structural element and the soil. It is composed of pairs of nodes one belongs to the structure and second belongs to the surrounding soil. It is termed as R$_{inter}$, and its value ranges between 0.01 and 1. The value of 0.01 means no friction between the structural element and the soil and the value of 1.0 means the structural element and the soil is completely in contact as rigid, so soil and the structural component cannot slip one anothers. Values in between mean the friction is reduced by the given value of R$_{inter}$, and the structural element and the soil mass can slip between each other. The interface elements are presented between the wall and the soil depending on some recommendations (Schweiger et al, 2012).

4.6.9 Sensitivity analysis

It means studying the individual influences of each input parameter variation on output. The sensitivity analysis aims to show the influence of the change in the value of each input parameter on the values of output parameters, to define the most important parameters which have a significant effect on the output ones, thus they should be taken into consideration when it comes to the dam's safety. The method used in this study is One-at-a-time (OAT) method where all the parameters, except selected input parameter were kept constant (Iooss and Lemaitre, 2014). Meshing also affects the output parameter. Definitely for a complex geometry, a too fine meshing is uneconomical and takes a long time. On the other hand, too coarse meshing means bigger elements. That way fails to reach all stress points and the result is less accurate. Depending on the

average element size (AES) of the generated mesh, the effect of its value on the output parameter was studied with five different sizes of meshes (very fine, fine, medium, coarse and very coarse). In the case study, the most significant output parameter is SF from the beginning of reconstructions till the end.

4.6.10 Basic equations

- *Displacement state*

The three – dimensional state of stress-strain and deformations is defined as:

    a) Three Static Equations (Cauchy Equations):

$$\left(\frac{\partial \sigma_x}{\partial x}\right) + \left(\frac{\partial \tau_{xy}}{\partial y}\right) + \left(\frac{\partial \tau_{xz}}{\partial z}\right) + F_X = 0 \qquad (4.16)$$

$$\left(\frac{\partial \tau_{yx}}{\partial x}\right) + \left(\frac{\partial \sigma_y}{\partial y}\right) + \left(\frac{\partial \tau_{yz}}{\partial z}\right) + F_Y = 0 \qquad (4.17)$$

$$\left(\frac{\partial \tau_{zx}}{\partial x}\right) + \left(\frac{\partial \tau_{zy}}{\partial y}\right) + \left(\frac{\partial \sigma_z}{\partial z}\right) + F_Z = 0 \qquad (4.18)$$

Where F_x, F_y, F_Z denote the body forces per unit volume in *x, y, z* directions respectively.

    b) Six physics equations (Hook Equations):

$$\varepsilon_x = \frac{1}{E}\left(\sigma_x - v\left(\sigma_y + \sigma_z\right)\right) \qquad \gamma_{xy} = \frac{\tau_{xy}}{G} \qquad (4.19)$$

$$\varepsilon_y = \frac{1}{E}\left(\sigma_y - v(\sigma_z + \sigma_x)\right) \qquad \gamma_{yz} = \frac{\tau_{yz}}{G} \qquad (4.20)$$

$$\varepsilon_z = \frac{1}{E}\left(\sigma_z - v\left(\sigma_x + \sigma_y\right)\right) \qquad \gamma_{zx} = \frac{\tau_{zx}}{G} \qquad (4.21)$$

- **Static equilibrium of continuum**

The equation (4.22) expresses the static equilibrium of continuum (Brinkgreve et al, 2014)

$$(4.22)$$
$$L^T \sigma + b = 0$$

$$
L^T = \begin{bmatrix} \frac{\partial}{\partial x} & 0 & 0 & \frac{\partial}{\partial y} & 0 & \frac{\partial}{\partial z} \\ 0 & \frac{\partial}{\partial y} & 0 & \frac{\partial}{\partial x} & \frac{\partial}{\partial z} & 0 \\ 0 & 0 & \frac{\partial}{\partial z} & 0 & \frac{\partial}{\partial x} & \frac{\partial}{\partial x} \end{bmatrix}
$$
(4. 23)

Where L^T is the transpose of differential operator, σ is stress vector, and b is body forces vector.

- **Stress-Strain equation**

The relation between strain and displacement can be formatted as (Galavi 2010):

$$\varepsilon_{tot} = L\,u$$
(4.24)

$$\varepsilon_{tot} = \varepsilon_p + \varepsilon_e$$
(4.25)

Where u is displacement vector, ε_{tot} is strain vector, and ε_p, ε_e plastic and elastic strain respectively

The general relation between ε and σ can be formatted as (Galavi 2010):

$$\sigma = D^e\,\varepsilon_e$$
(4.26)

$$
D^e = \frac{E}{(1+v)(1-2v)} \begin{bmatrix} 1-v & v & v & 0 & 0 & 0 \\ v & 1-v & v & 0 & 0 & 0 \\ v & v & 1-v & 0 & 0 & 0 \\ 0 & 0 & 0 & \frac{1-2v}{2} & 0 & 0 \\ 0 & 0 & 0 & 0 & \frac{1-2v}{2} & 0 \\ 0 & 0 & 0 & 0 & 0 & \frac{1-2v}{2} \end{bmatrix}
$$
(4.27)

Where D^e is material stiffness matrix.
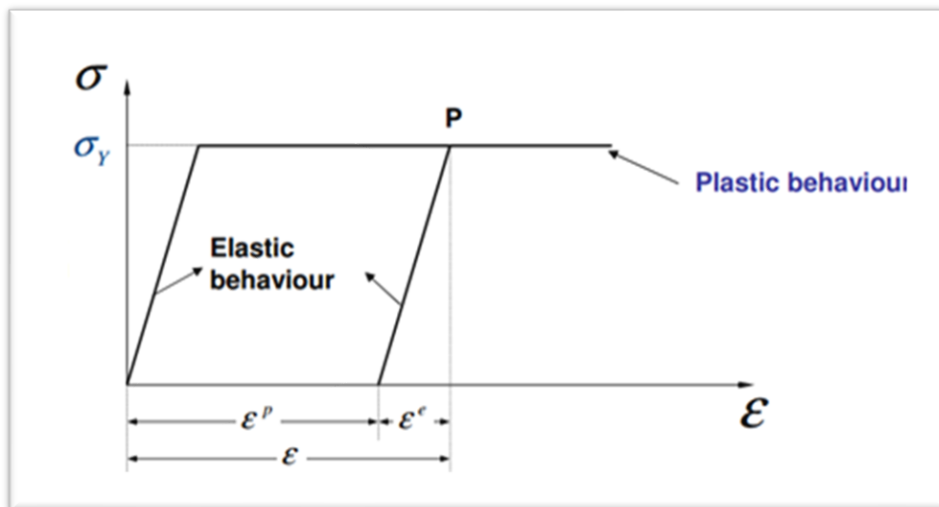
Fig. 4.8 Mohr-Coulomb soil modelling (Benz, 2007)

Plastic strain as (Benz, 2007) is:

$$\varepsilon_p = \lambda \frac{\partial g}{\partial \sigma i} \qquad (4.28)$$

Where λ is a controller of magnitude of plastic deformation and $\frac{\partial g}{\partial \sigma i}$ is a controller of direction of the plastic deformations.

λ is a non-negative multiplier when plastic yielding occurs, and it is zero for elastic and unloading states. Multiplier λ has no further physical meaning.

To distinguish elastic state from plastic state, a yield criterion is expressed to evaluate if strains will be plastic or elastic, it is a function of stress, cohesion and friction angle:

$$f(\sigma, c, \varphi) \lessgtr 0 \qquad (4.29)$$

- **Ground water flow equation**

  ➢ Constitutive Equation: Darcy's Law (see (4.2)) (Brinkgreve et al, 2014):

$$\begin{bmatrix} q_x \\ q_y \\ q_z \end{bmatrix} = - \begin{bmatrix} k_x & 0 & 0 \\ 0 & k_y & 0 \\ 0 & 0 & k_z \end{bmatrix} \begin{bmatrix} \frac{\partial h}{\partial x} \\ \frac{\partial h}{\partial y} \\ \frac{\partial h}{\partial z} \end{bmatrix} \qquad (4.30)$$

- **Safety factor equation**

SF is calculated by using Phi-c reduction theory, where specific soil parameters are gradually reduced to failure. The parameters c and $tan\ \varphi$ are decreased gradually and SF is calculated by the eq (4.31). Where C and $tan\ \varphi$ are the real parameters and they are decreased until a clear failure (Brinkgreve et al, 2014):

$$SF = \frac{tan\ \varphi}{tan\ \varphi_{red}} = \frac{C}{C_{red}} \qquad (4.31)$$

4.6.11 Dynamic analysis of drilling rod

The dynamic calculation is based on the time-dependent movement of a volume under the influence of a dynamic load as follows:

$$M\ddot{u} + C\dot{u} + Ku = F \qquad (4.32)$$

Where M is the mass matrix, $u, \dot{u}, \ddot{u}$ are relative nodal displacement, velocity and acceleration respectively, C is the global damping matrix, K is the stiffness matrix and F is the load vector.

4.6.12 The cement shrinkage

The shrinkage of the cement (Autogenous 0,4 cm^3/100 gr cement) was modelled by applying a contract surface to the diaphragm wall in hard state (Tazawa, 1997).

4.7 Numerical solution in Plaxis 3D

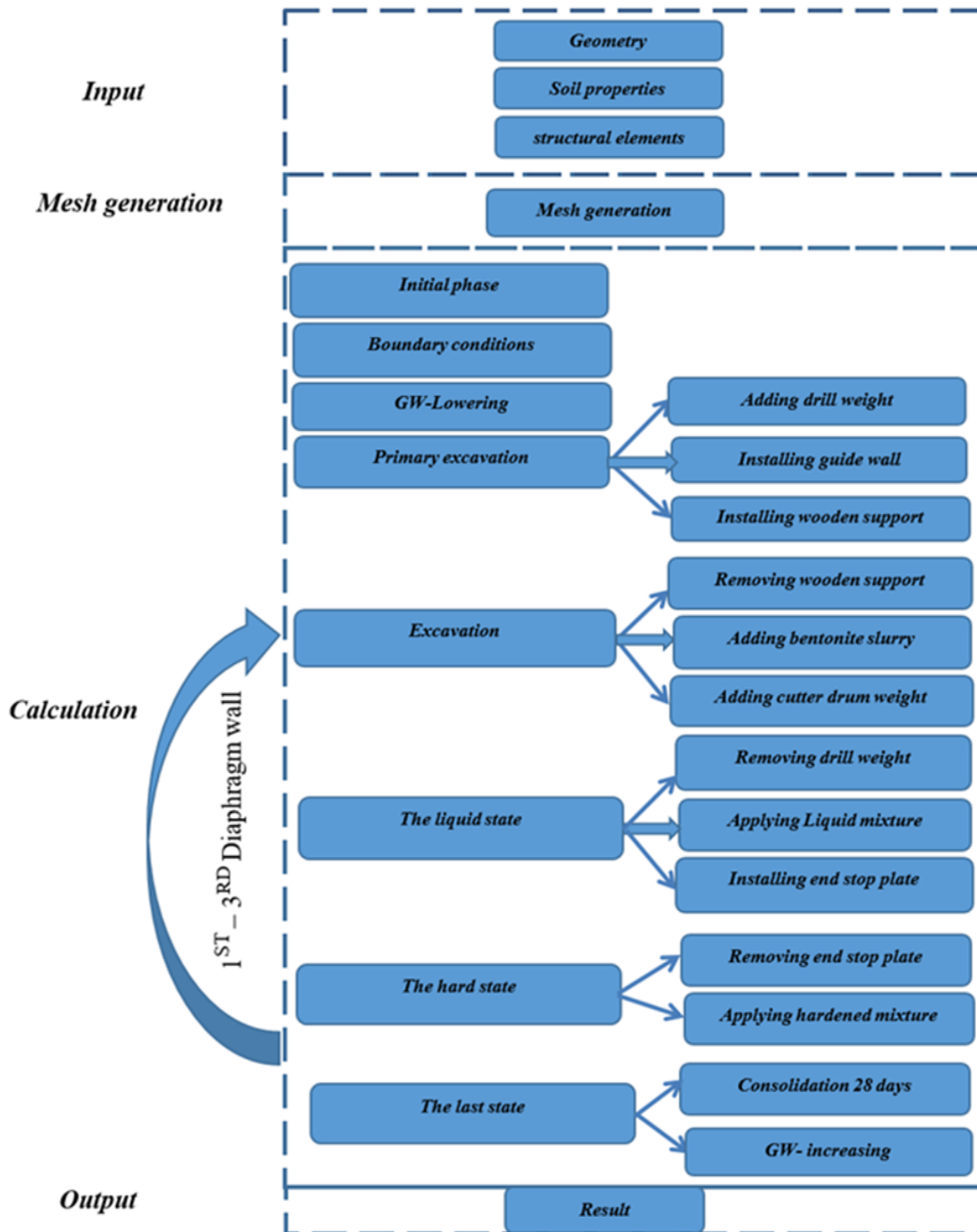Creating the model in the program Plaxis can be summarized in four phases (Fig. 4.9).

Fig. 4.9 The calculation steps in Plaxis

5 THE PRACTICAL PART

5.1 Numerical modelling of diaphragm wall

The diaphragm wall was constructed in 2013 after an intensive investigation were carried out on the dam body and its foundation, and as the result of exchanging experts and opinions, the final recommendation is to construct a diaphragm wall from self-hardening cement bentonite suspension along the entire length of the dam. It was suggested and conducted the following technical parameter:

- The total length of the diaphragm walls is 301.75 m with total area of 4777m^2
- The depth of the diaphragm walls ranges from 10.50 m to 19.30 m.
- The width of the diaphragm wall is 0.60 m.
- The length of the diaphragm wall is 3.60 m.

Figure (5.1) shows longitudinal section through the Karolinka dam, Figure (5.2) shows the layout plan for the entire Karolinka dam, and Figure (5.3) shows the cross section of the Karolinka dam.
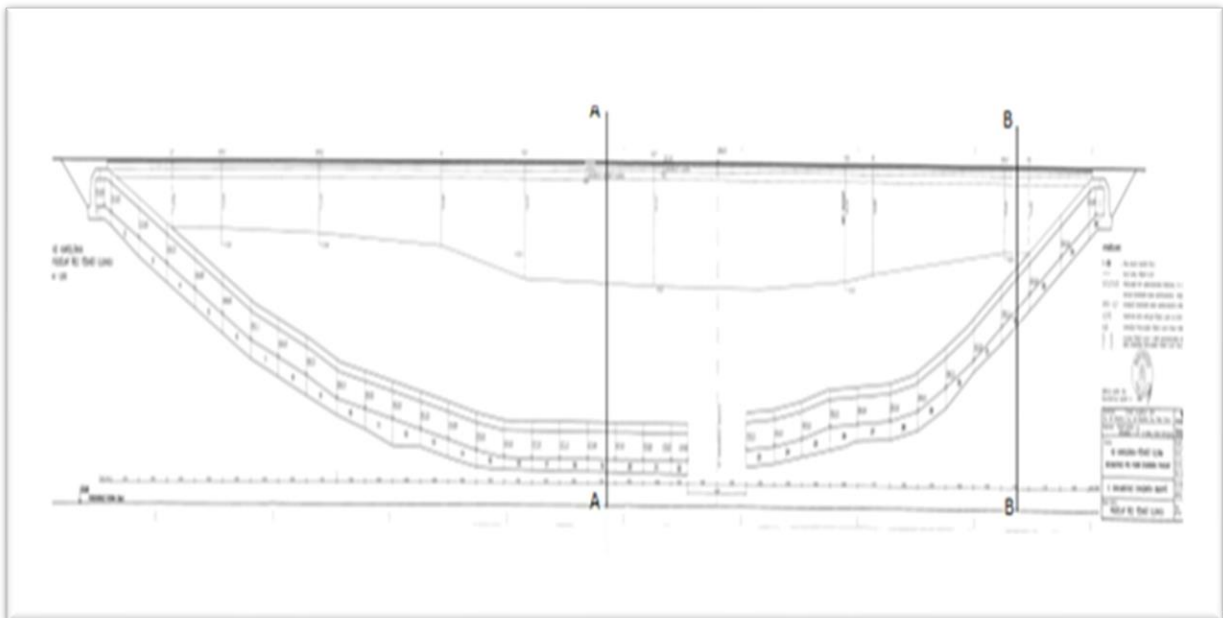
Fig. 5.1 The longitudinal section through the Karolinka dam including constructed wall
(Pařílková et al, 2016)
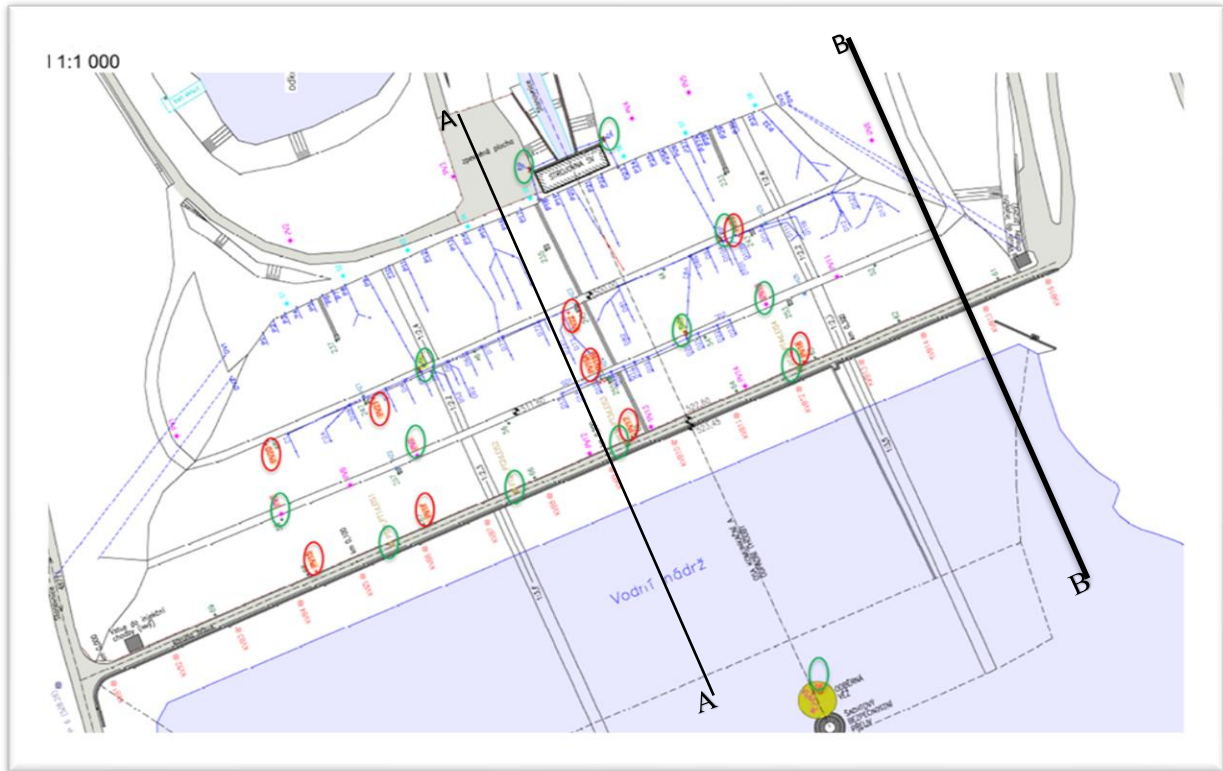
Fig. 5.2 The layout plan of the Karolinka dam with monitoring system (Pařílková et al, 2016)
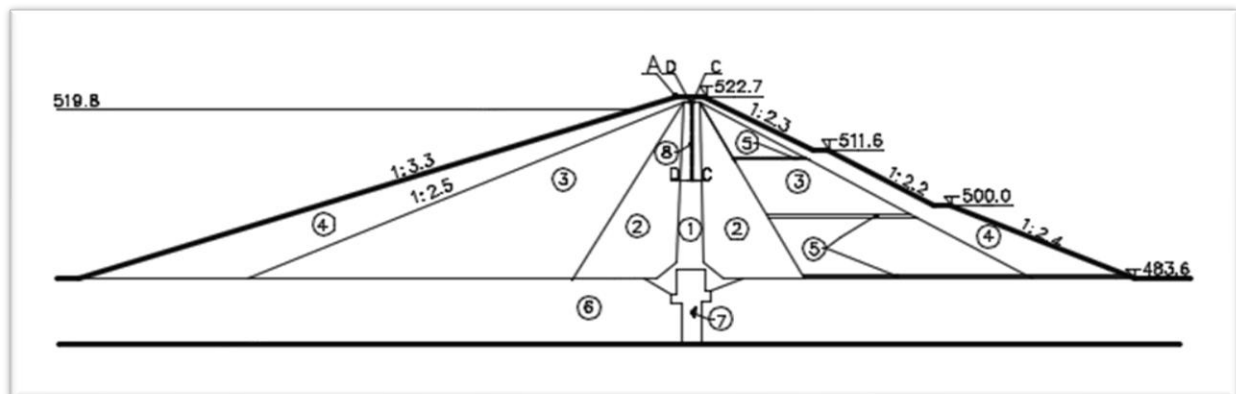
Fig. 5.3 Cross section A-A of the Karolinka dam

Legend

1. Core Clay gravelly, 2. Zone 2B Gravel with fine –grained soil, 3. Zone 2A Gravel with loam,
4. Zone 3 Gravel with fine-grained soil, 5. Gravel Drain, 6. Gravel with loam, 7. Curtain Grouting,
8. Diaphragm wall.

5.1.1 Formulation of problem

- *Variables*

The three-dimensional problem (3D) of stress-strain and displacement depends on these variables:

Six components of Stress

$$\{\sigma\} = \left(\sigma_x, \sigma_y, \sigma_z, \tau_{xy}, \tau_{yz}, \tau_{zx} \right)^{\mathrm{T}} \tag{5.1}$$

Six components of strain

$$\{\varepsilon\} = \left(\varepsilon_x, \varepsilon_y, \varepsilon_z, \gamma_{xy}, \gamma_{yz}, \gamma_{zx} \right)^{\mathrm{T}} \tag{5.2}$$

Three components of displacement

$$\{\vec{U}\} = \left(u, v, w \right)^{\mathrm{T}} \tag{5.3}$$

The pore water pressure

$$\{p_w\} = p_w \tag{5.4}$$

- *Boundary conditions*

The Boundary conditions have to be defined to simulate the case studied as much as possible. The boundary conditions of case study were defined at the border area
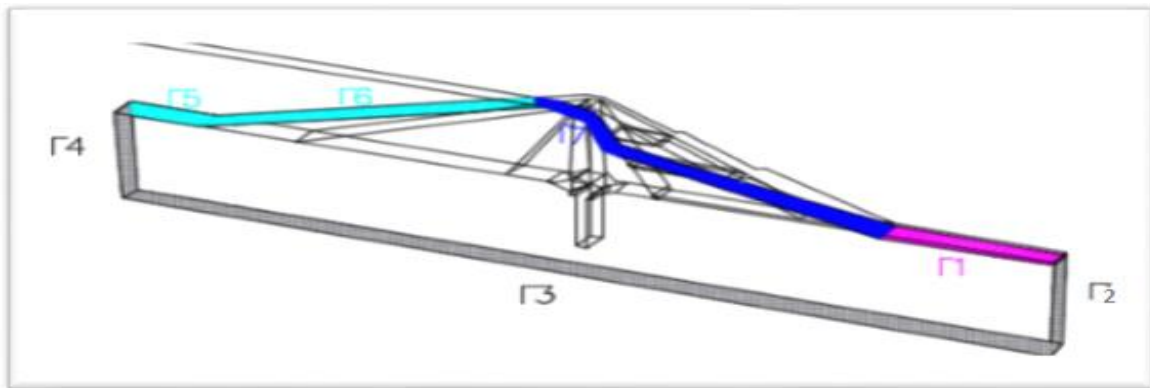
Fig. 5.4 Boundary conditions of the case study

The Figure (5.4) shows the boundary condition of case study. The prescribed displacement at borders $\Gamma_{2, 3, 4}$ assumed to be zero :

$$U|\Gamma_{2, 3, 4} = 0 \tag{5.5}$$

The value of water head at borders $\Gamma_{1, 5, 6, 7}$ assumed to be:

$$h|\Gamma_1 = H_1(t) \tag{5.6}$$

$$h|\Gamma_{5, 6} = H_2(t) \tag{5.7}$$

$$h|\Gamma_7 = Z(x, y, t) \tag{5.8}$$

Where $H_1(t)$, $H_2(t)$ are known piezometric heads in borders Γ_1, $\Gamma_{5, 6}$ respectively and $Z(x, y, t)$ is the free surface water in studied boundary.

The Neumann boundary condition for flow:

$$\left(k_{ij} \frac{\partial h}{\partial x_i}\right) n_i |\Gamma_{2, 4} = q_n \tag{5.9}$$

$$\left(k_{ij} \frac{\partial h}{\partial x_i}\right) n_i |\Gamma_3 = 0 \tag{5.10}$$

$$\left(k_{ij} \frac{\partial h}{\partial x_i}\right) n_i |\Gamma_7 = 0 \tag{5.11}$$

Where n_i is normal vector in directions x, y, z, q_n is specified seepage in the studied boundary, and h is hydraulic head.

- *Initial conditions*

  ➢ *Initial displacements*

  The initial value of the displacements equals zero.

  ➢ *Initial ground water surface*

$$h_{p,0} = H_0 \tag{5.12}$$

Where $h_{p,0}$ is initial piezometric head, and H_0 is specified piezometric head.

  ➢ *Initial Stresses*

Plaxis allows calculation of the initial stress state to be carried out automatically using the coefficient of earth pressure K'_0

$$\sigma'_h = \sigma'_v . K'_0 \tag{5.13}$$

Where σ'_v is the vertical effective stress, σ'_h is the horizontal effective stress, and K'_0 is the coefficient for lateral earth pressure (Brinkgreve et al., 2017).

5.1.2 Numerical solution

The numerical technique used in this study is the FEM which is performed by the program Plaxis.

- **Mesh generation and boundary conditions**

In this modelling, 10-node tetrahedral elements for soil elements were used Fig (5.5). The well-refined mesh is generated with extra refinement to specific clusters. The domain is discretised into a mesh by 28702 elements through placement of nodal points 44169. With respect to the boundary condition in Plaxis 3D, the top (Z_{max}) boundaries set to free and the bottom (Z_{min}) is

set to fixed. Whereas the right (X_{max}), left (X_{min}), and boundaries: (Y_{min}, Y_{max}) are set to normally fixed as well. In the ground water flow boundary set boundaries: $(Y_{min,max})$, and (Z_{min}) to closed. The remaining boundaries are open.
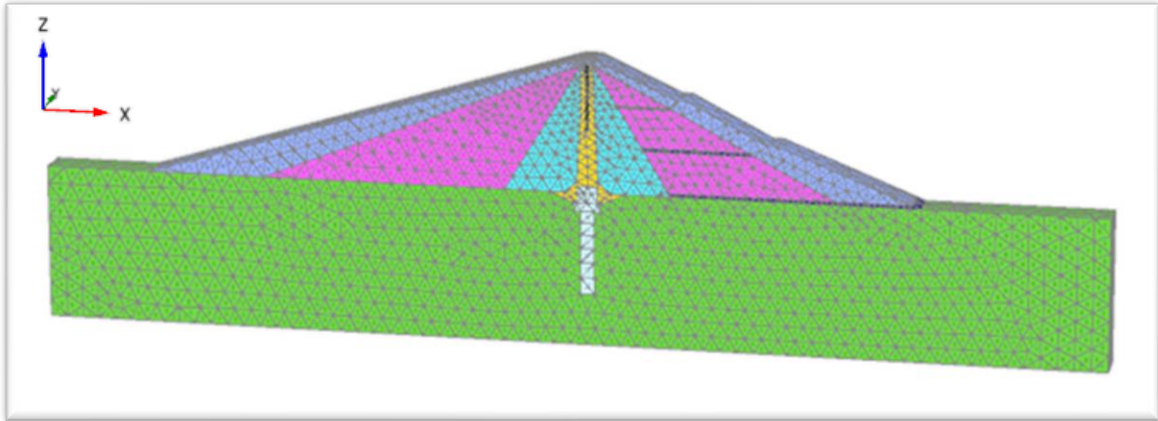

Fig. 5.5 Generated mesh

- **Structural (plate- support) elements in Plaxis 3D**

The parameters used in modelling the structural elements are presented below in Tab (5.1)

Table 5.1 Plate and Support parameters

Element	d	γ	E_1	E_2	ν	G_{12}	G_{13}	G_{23}
	[m]	[kN/m³]	[kN/m²]	[kN/m²]		[kN/m²]	[kN/m²]	[kN/m²]
End stop	0.02	78	2 E⁸	2 E⁸	0.1	9 E⁷	9 E⁷	9 E⁷
Support	0.05	9	15 E⁶	15 E⁶	0.2	6 E⁶	6 E⁶	6E⁶

Table 5.2 Beam parameters

Element	A	γ	E	I_3	I_2
	[m²]	[kN/m³]	[kN/m²]	[m⁴]	[m⁴]
Beam	8E⁻³	9	15E⁶	5E⁻⁶	5E⁻⁶

- **Modelling procedure**

The analysis has simulated the main stages of construction as follows:
1- Constructing the guide wall and the supports.
2- The sequential excavating with the supporting slurry fluid.
3- Using joint construction methods for diaphragm wall construction by adding end stop plate.

4- Modifying the geotechnical parameters in the volume of core affected by the treatment.

5- Activation of all diaphragm walls and their interfaces.

Figure (5.6), shows the construction sequence modelling. The modelling procedures are summarized as follows:

1. Decreasing WL by ten meters in ten days.

2. Preliminary excavation to (1.5 m) with adding weight of drill, and installing the guide wall.

3. Installing the support elements.

4. Removing the supports and adding weight of cutter drum which digs down to tip elevation, with bentonite slurry.

5. Installing end stop plate, and casting the liquid mixture while removing the bentonite slurry.

6. Curing liquid mixture in the wall number 1 by applying a hardened mixture in shrinkage state.

7. Appling the same modelling procedures to construct wall No. 3 then No 2.

8. Increasing WL by ten meters in fifteen days.

Fig. 5.6 Diaphragm wall construction sequence
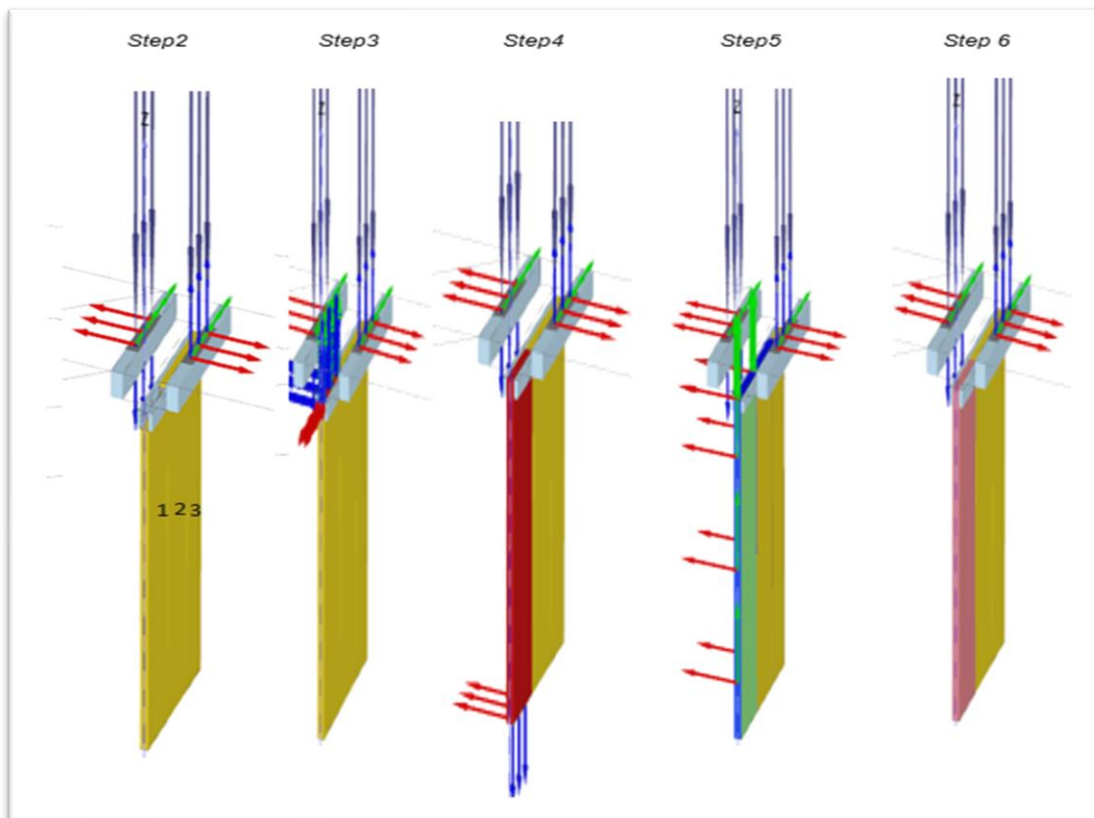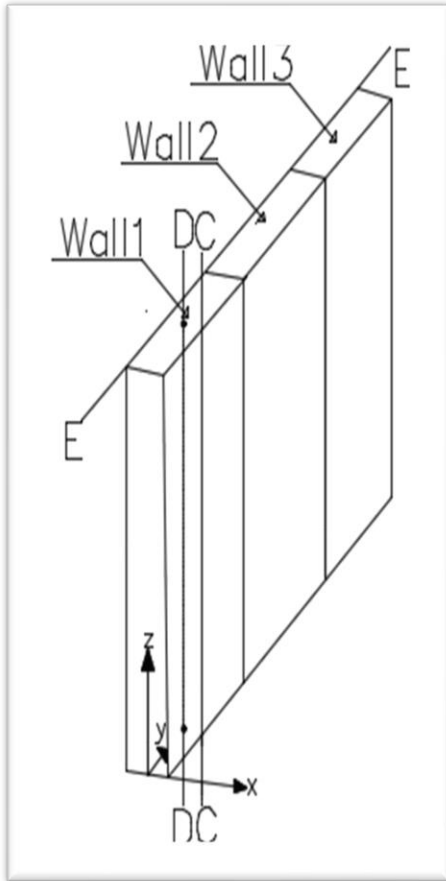
Fig. 5.7 Cross -Section lines   **Fig. 5.8** Top view of the dam crest
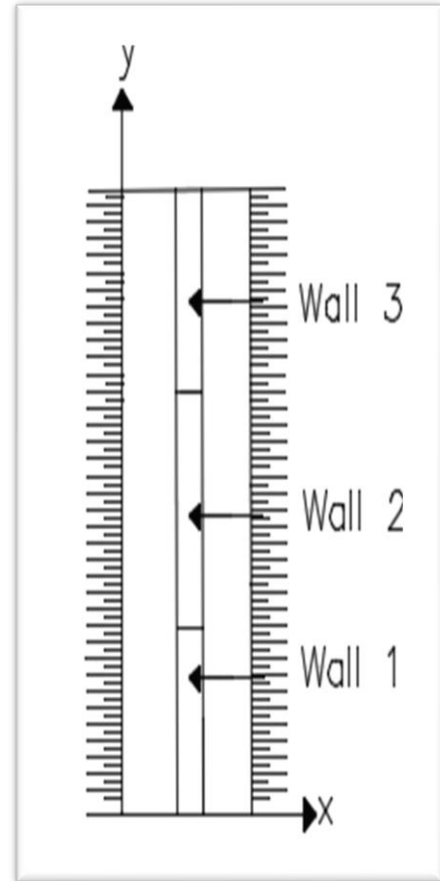
5.2 Numerical modelling of piles

Additional sealing has been conducted at both end of the dam (2×25 m long) by using jet pile with a diameter of 1 m and overlap of 0.2 m, from a cement- bentonite mixture.

5.2.1 Formulation of problem

- **Variables**

The three-dimensional problems (3D) of stress-strain and displacement depend on these variables

Six components of stress

$$\{\sigma\} = \left(\sigma_x , \sigma_y , \sigma_z , \tau_{xy} , \tau_{yz} , \tau_{zx} \right)^{\mathrm{T}} \qquad (5.1), (5.14)$$

Six components of strain

$$\{\varepsilon\} = \left(\varepsilon_x , \varepsilon_y , \varepsilon_z , \gamma_{xy} , \gamma_{yz} , \gamma_{zx} \right)^{\mathrm{T}} \qquad (5.2), (5.15)$$

48

Three components of displacement

$$\{\vec{U}\} = (u, v, w)^{\text{T}}$$

(5.3), (5.16)

The pore water pressure

$$\{p_w\} = p_w$$

(5.4), (5.17)

- **Boundary conditions**

Depending on Dirichlet and Neumann boundary conditions, the boundary conditions of case study were defined at the border area.
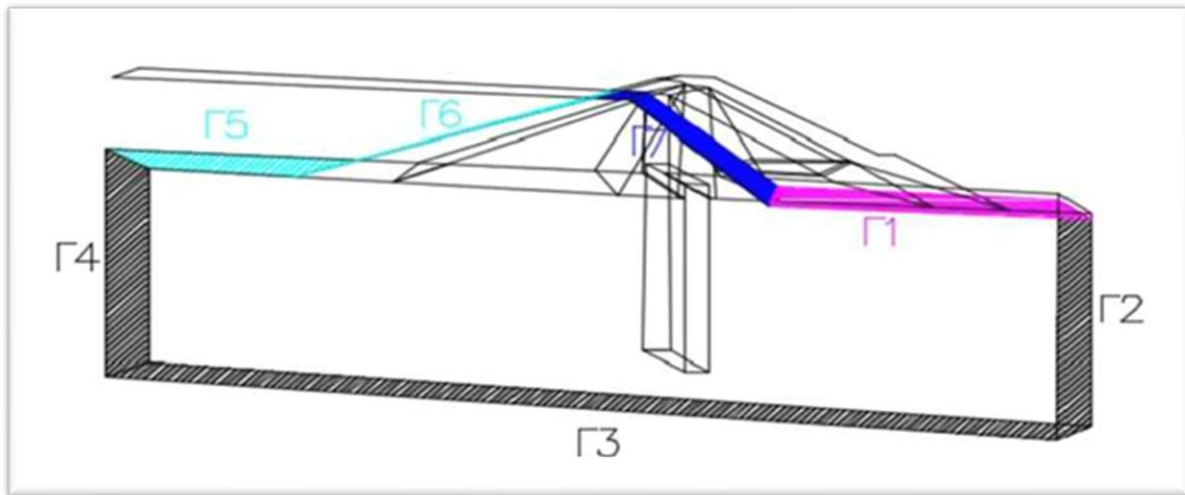
Fig. 5.9 Boundary conditions of case study

Figure (5.9) shows the boundary condition of case study (Karolinka dam). The prescribed displacement at border $\Gamma_{2,\ 3,\ 4}$ assumed to be :

$$U|\Gamma_{2,\ 3,\ 4} = 0$$

(5.5), (5.18)

The value of water head at border $\Gamma_{1, 5, 6, 7}$ is assumed to be:

$$h|\Gamma_1 = H_1(t)$$

(5.6), (5.19)

$$h|\Gamma_{5,\ 6} = H_2(t)$$

(5.7), (5.20)

$$h|\Gamma_7 = Z(x, y, t)$$

(5.8), (5.21)

Where $H_1(t)$, $H_2(t)$ are known piezometric heads in borders Γ_1 , $\Gamma_{5,\ 6}$ respectively and $Z(x, y, t)$ is the free surface water in studied boundary.

The Neumann boundary condition for flow:

$$\left(k_{ij} \frac{\partial h}{\partial x_i}\right) n_i \big|_{\Gamma_{2,\ 4}} = q_n \qquad\qquad (5.9), (5.22)$$

$$\left(k_{ij} \frac{\partial h}{\partial x_i}\right) n_i \big|_{\Gamma_3} = 0 \qquad\qquad (5.10), (5.23)$$

$$\left(k_{ij} \frac{\partial h}{\partial x_i}\right) n_i \big|_{\Gamma_7} = 0 \qquad\qquad (5.11), (5.24)$$

Where n_i is normal vector in directions x, y, z , q_n is specified seepage in the studied boundary, and h is hydraulic head.

- **Initial conditions**

Initial displacements

The initial value of the displacements equal zero.

Initial ground water surface

$$h_{p,0} = H_0 \qquad\qquad (5.12), (5.25)$$

Where $h_{p,0}$ is initial piezometric head in the domain (steady state flow), and H_0 is specified piezometric head.

Initial stresses

The initial stress field is generated by means of the K'_0 procedure using the given (default) K'_0 value in the sub-soil.

$$\sigma'_v = \gamma.d \qquad\qquad (5.26)$$

$$\sigma'_h = \sigma'_v.K'_0 \qquad\qquad (5.13), (5.27)$$

Where σ'_V is the vertical effective stress, σ'_h is the horizontal effective stress, and K'_0 is the coefficient for lateral earth pressure (Brinkgreve et al., 2017).

5.2.2 Numerical solution

The numerical technique used in this study is FEM that was performed by the program Plaxis. Fig (5.10) shows the cross-section B-B of the dam.
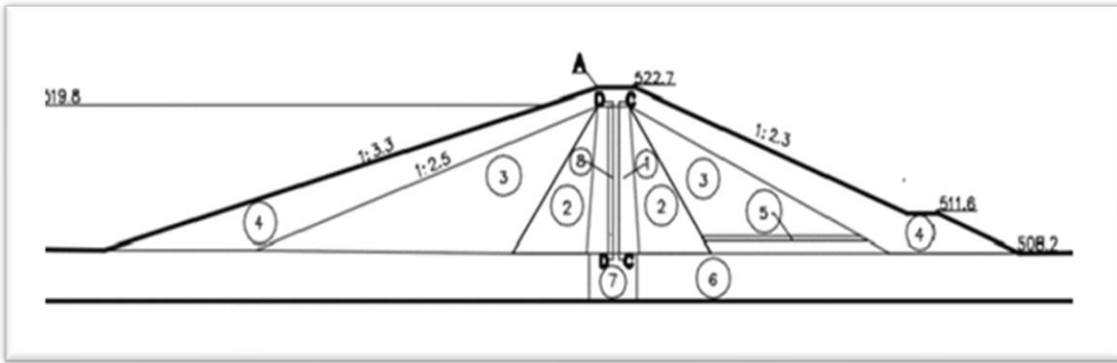
Fig. 5.10 The Cross section B-B of the Karolinka dam

Lenged

1. Core Clay gravelly, 2. Zone 2B Gravel with fine –grained soil, 3. Zone 2A Gravel with loam, 4. Zone 3 Gravel with fine-grained soil, 5. Gravel Drain, 6. Gravel with loam, 7. Curtain Grouting, 8. Pile.

- **Mesh generation and boundary conditions**

In this modelling, 10-node tetrahedral elements for soil elements were used Fig (5. 11). A sufficient and well-refined mesh by 32076 elements and 52380 nodal points was generated. The top (Z_{max}) boundaries set to free and the bottom (Z_{min}) is set to fixed, whereas the right (X_{max}), left (X_{min}), and boundaries: (Y_{min}, Y_{max}) are set to normally fixed as well. In the ground water flow boundary set boundaries: $(Y_{min,max})$, and (Z_{min}) to closed. The remaining boundaries should be open.
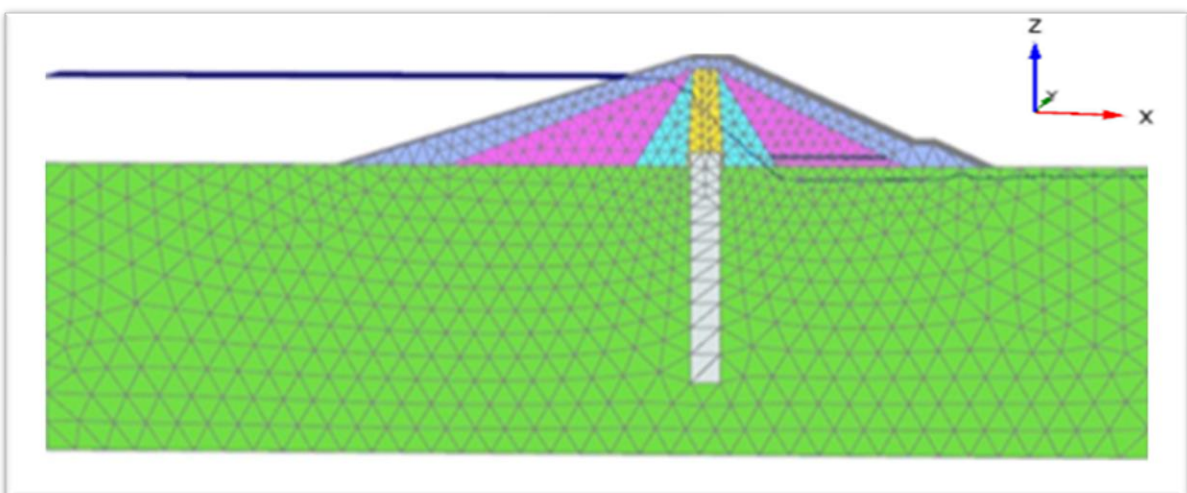
Fig. 5.11 Generated mesh

- **Dynamic analysis of jet rod**

The dynamical module of Plaxis is used. The circular motion can be represented as harmonic motion (LibreTexts, 2018). In other words, the rotational motion of jet rod has been converted to the harmonic to perform dynamic analysis by Plaxis program. Depending on ČSN EN 12716 (731072) to define a parameters of jet grouting method. The rod rotation is (6-20 r/sec) and therefore the frequency equals 0.02 Hz. So, the displacement can be calculated during rotation by Plaxis with some simplifying.

- **Investigation of the failure state**

The failure criterion can be expressed in terms of the relationship between the principal stresses:

$$\sigma'_1 = \sigma'_3 \tan^2\left(\frac{\phi}{2} + 45\right) + 2\acute{c}\tan\left(\frac{\phi}{2} + 45\right) \qquad (4.12), (5.28)$$

Where σ'_1, σ'_3 are the major and minor effective principal stress respectively.

- **Jet grouting procedure**

Figure (5.12) shows the construction steps can be summed up as following:

1. Decreasing WL by ten meters in ten days.

2. Adding the weight of the drill.

3. Build the piles (1, 3, 5) as volume cylinder with adding interfaces, moment and forces in liquid state.

4. Curing liquid mixture by applying a hardened mixture.

5. Applying the same modelling procedures to the piles (2, 4, 6).

6. Increasing WL by ten meters in fifteen days.
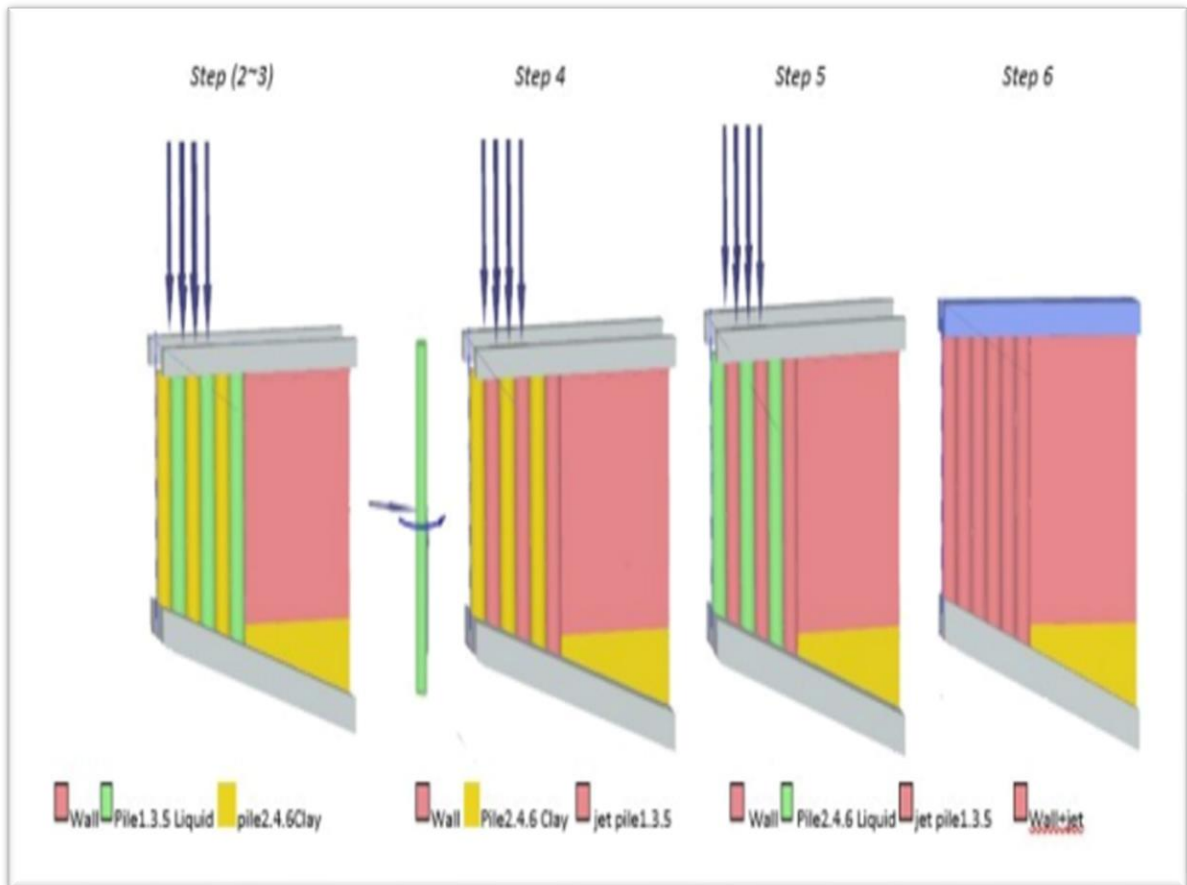
Fig. 5.12 Pile construction sequence
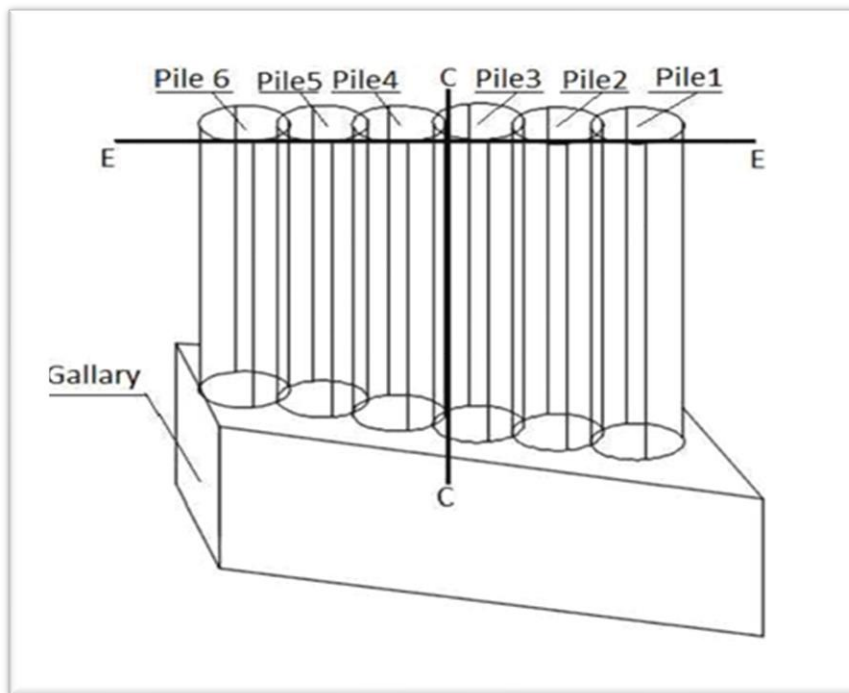
Fig.5.13 Cross -Section line

53

6 RESULTS AND DISCUSSION

6.1 Diaphgram wall

6.1.1 Ground water head

Figures(6.1) and (6.2), show the variations of ground water head during decrease and increase water respectively. This result was concluded depending on FCFD analysis which analyses the development of deformation and pore water pressure as a result of time-dependent hydraulic boundary condition . In other words, it takes into account the permeabilities, the change of pore water pressure, and time.
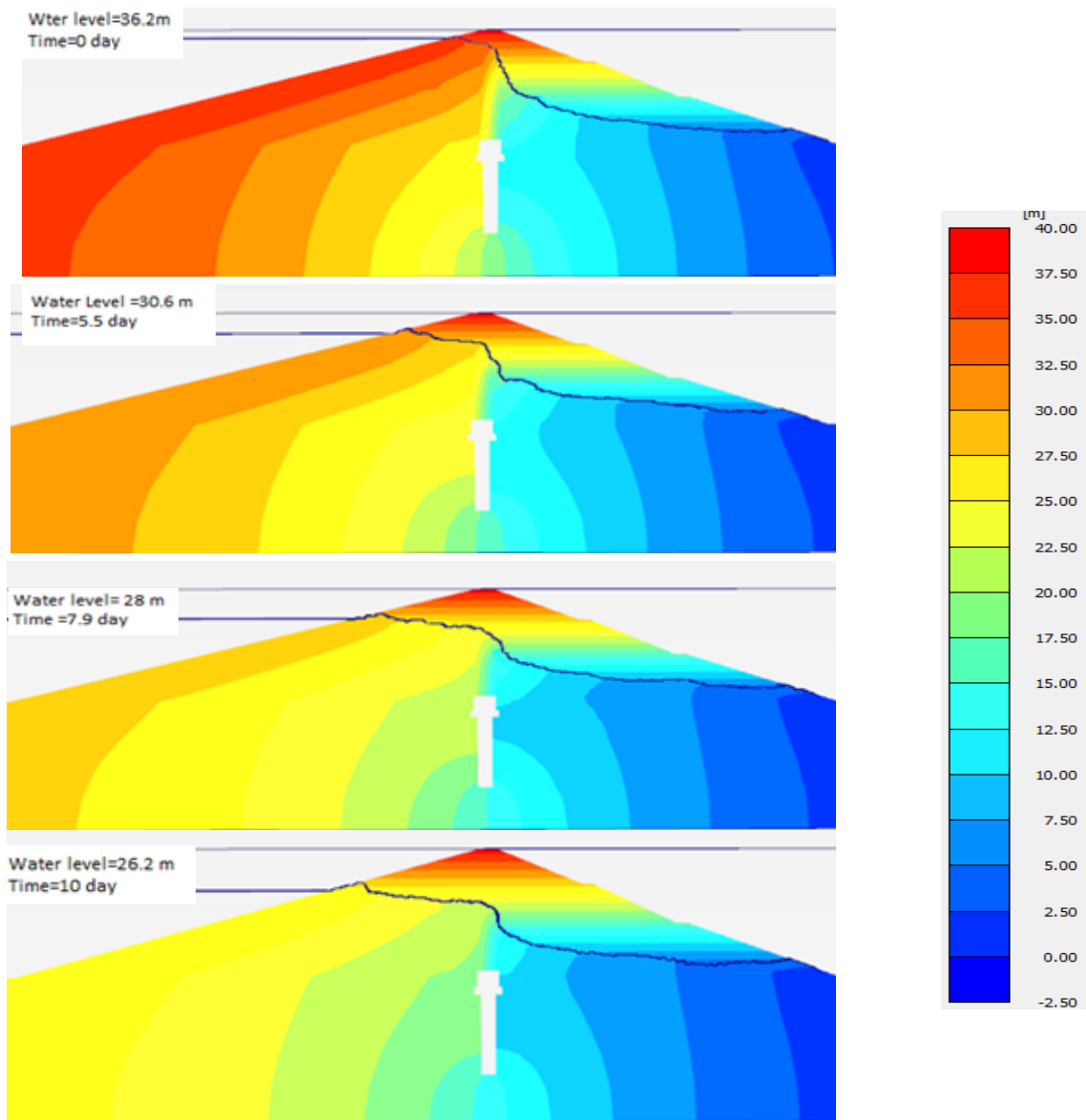
Fig. 6.1 Variations of ground water head (decrease WL)
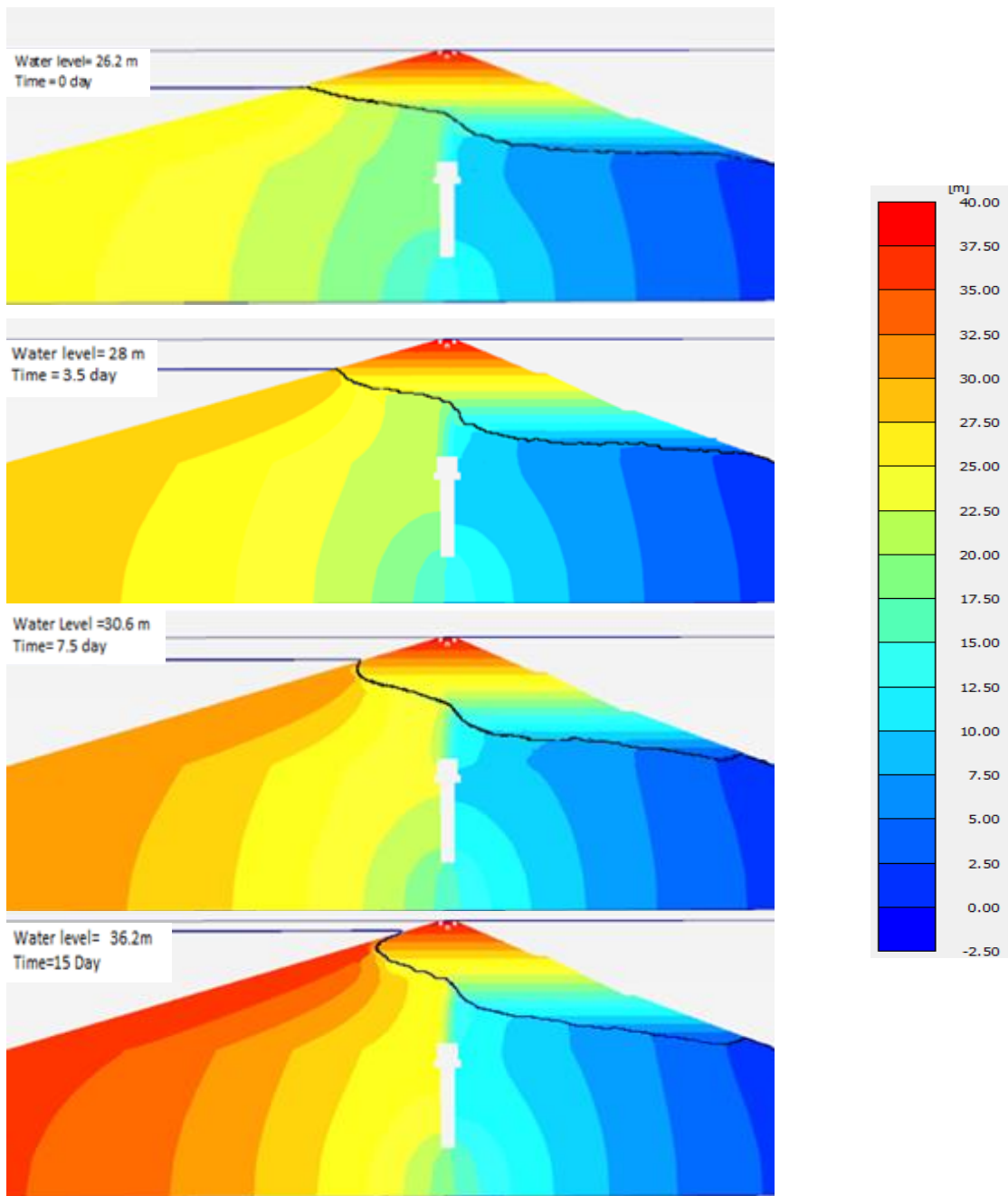
Fig. 6.2 Variation of ground water head (increase WL)

6.1.2 The total displacement

Displacement results are expressed in Figures (6.3), and (6.4) which show the horizontal displacement with respect to the time (drawdown-fill) respectively at crest point A (see Figure 5.7). The maximum value of the horizontal displacement reached 32 mm during decreasing WL and 23.5 mm during increasing WL. Depending on some recommendations the level of water was

decreased by one meter per day within ten dayes, and after reconstruction it was increased by ten meters in fifteen days (ČSN 75 2310). As a result, the construction of wall and controlling (discharge-charge) by the appropriate period for decreasing and increasing water level in the reservoir lead to decrease displacement and increase stability of the dam.
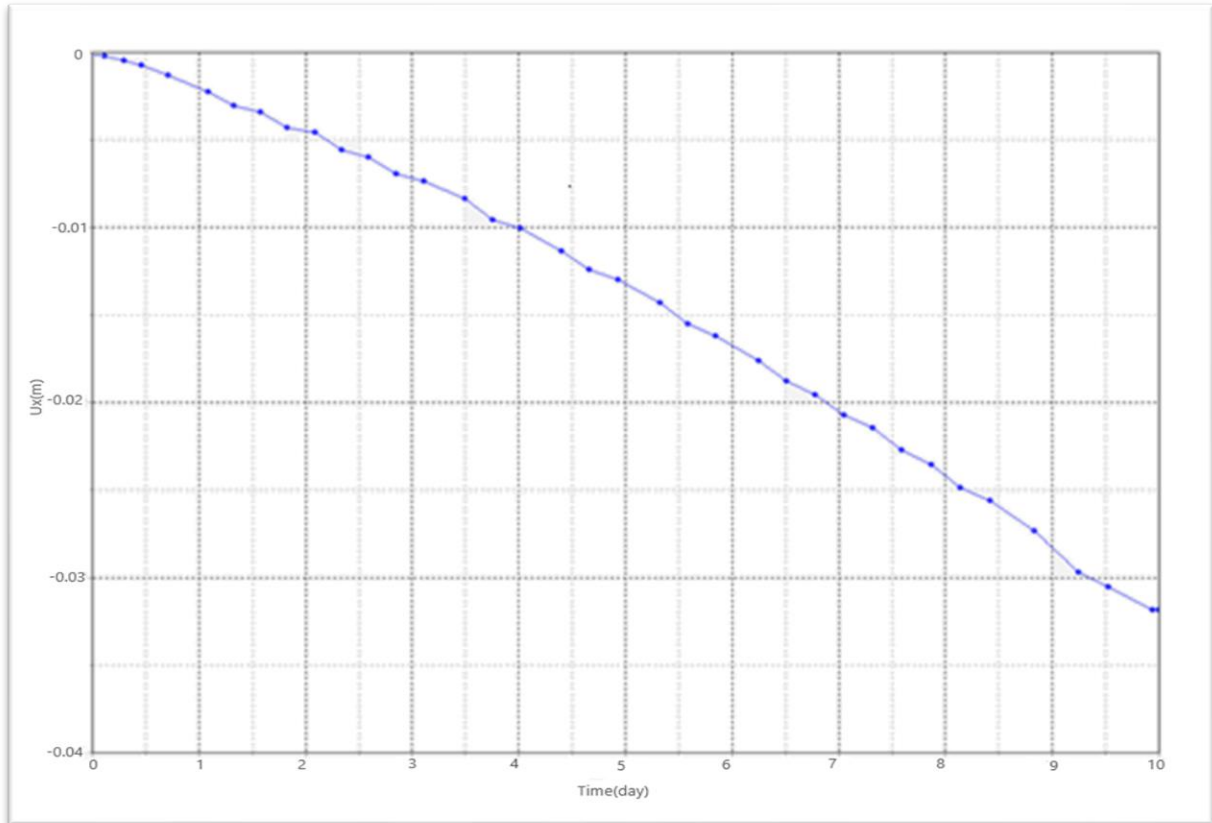
Fig. 6.3 Horizontal displacement-time (decrease water) history at point A (-2.5, 0, 39)

56
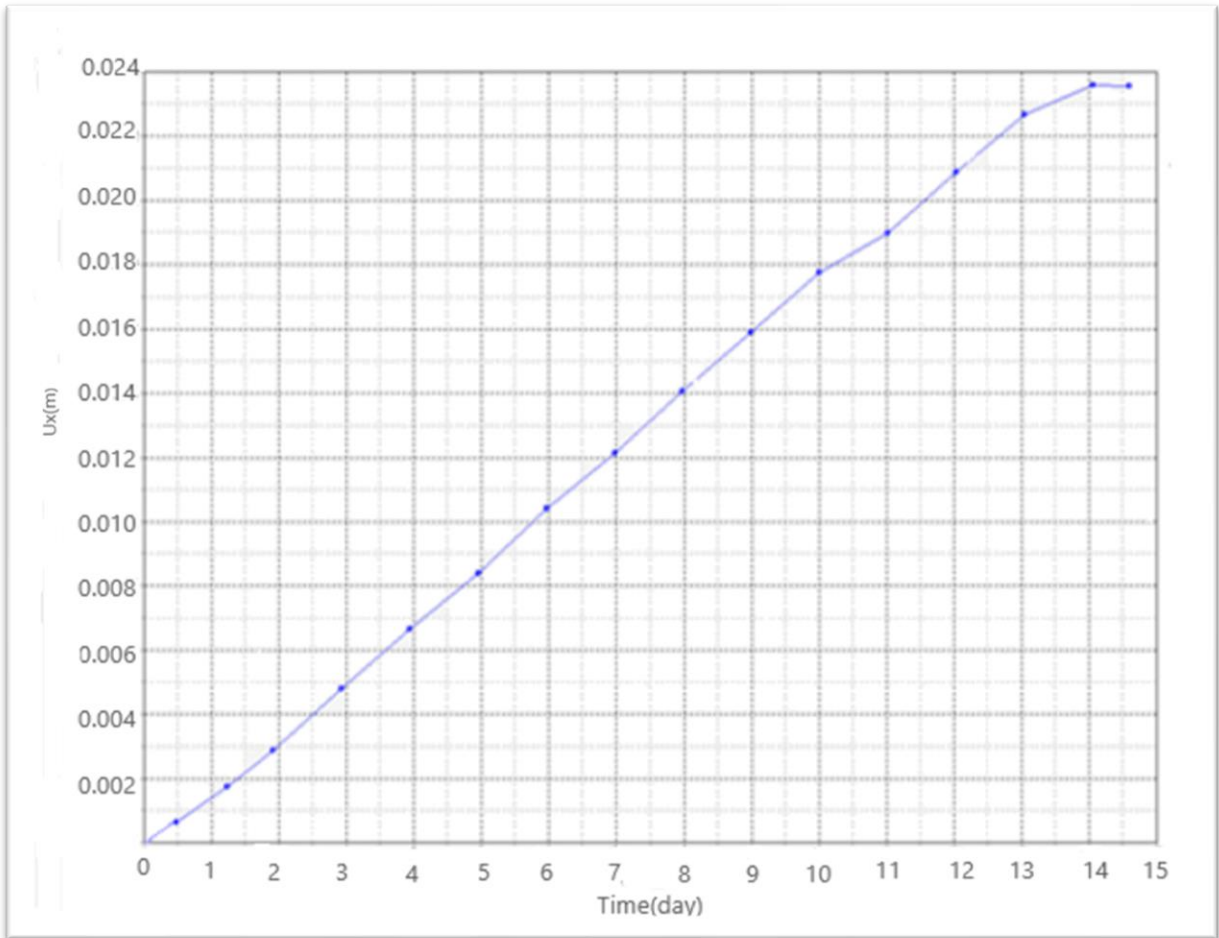
Fig. 6.4 Horizontal displacement-time (increase water) history at point A (-2.5, 0, 39)

Figure (6.5) shows the displacement distribution with depth at line cross section C-C Figure (5.7) during wall construction process. It is clear that the maximum value of the displacement occurred almost in the upper one-third of the wall height and the maximum value of displacement about 0.5 % of the wall thickness, so it is relatively small.
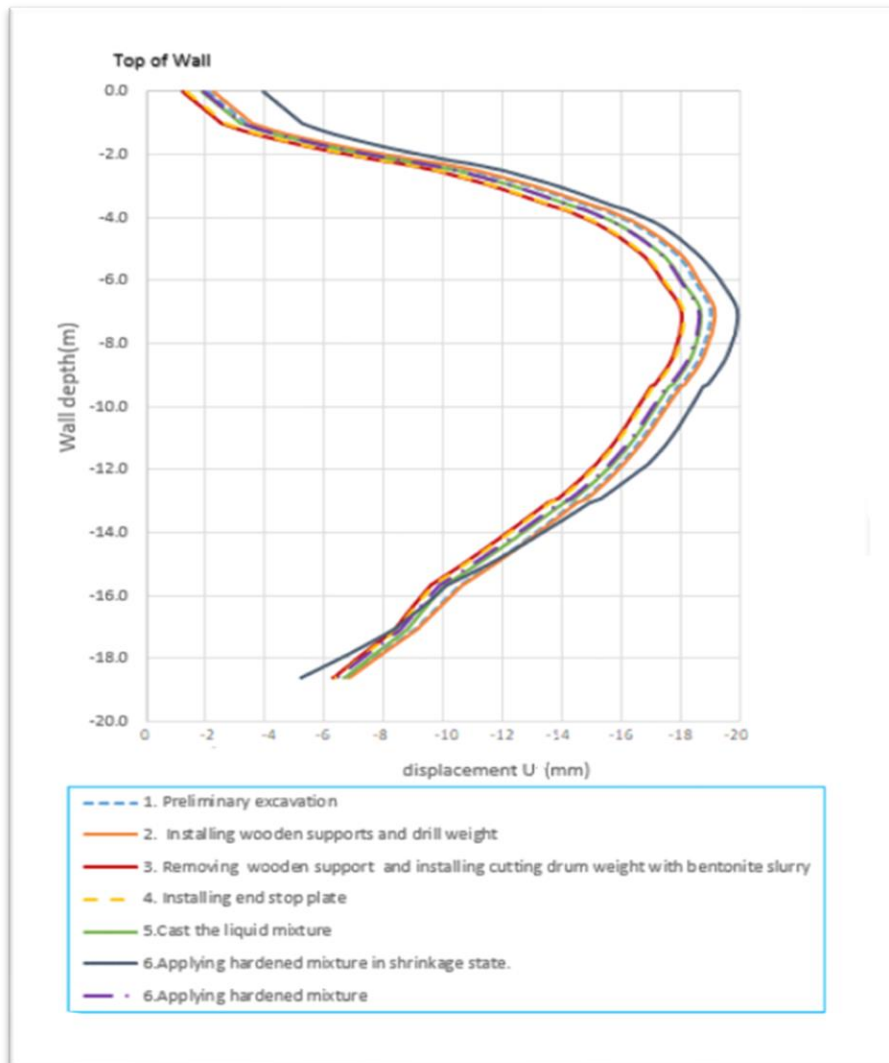
Fig.6.5 The displacement along the line cross section C-C

(construction wall 1)

Figure (6.6), shows the variation of vertical displacement with wall depth at line cross section D-D (see Figure 5.7). There is a convergence of two results whether we support with end plate stop or not.The end plate is used to secure a correct geometrical continuity of the wall.
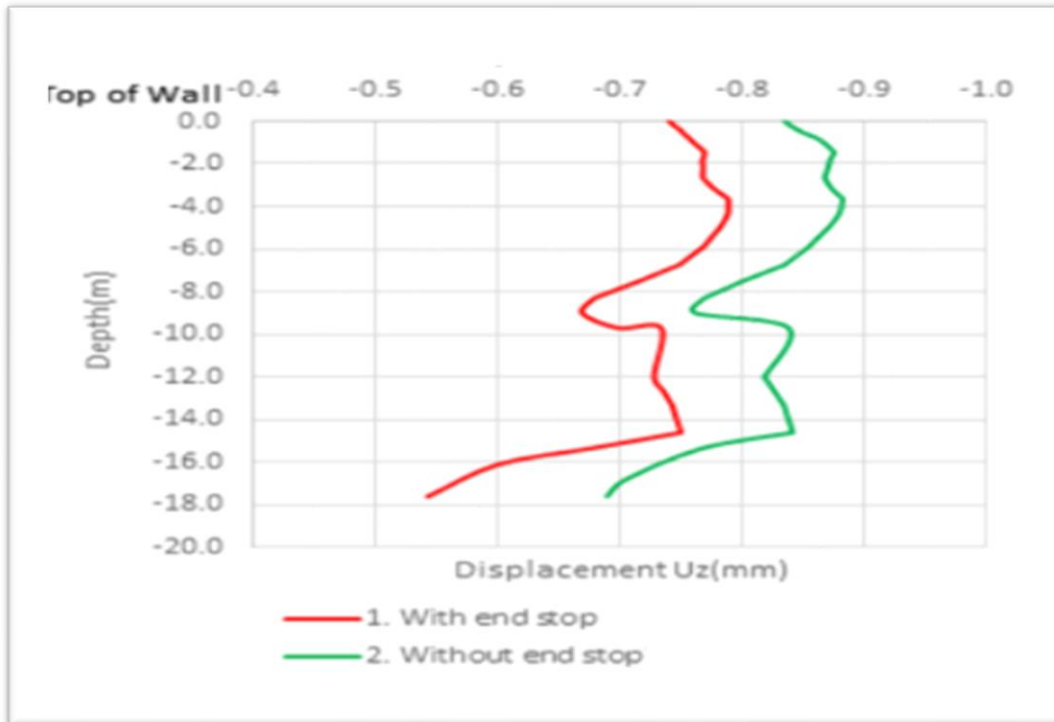
Fig. 6.6 Variation of vertical displacement with wall depth

Figure (6.7) shows the variation of total displacement with loading time associated with machine weight at dam crest. As a result, the displacement increases with the loading time in both cases: 1- The weight of the machine is (83.6) tons, 2- The weight of the machine is (120 tons) There is no significant difference in the values of the displacement in both cases. The maximum value for the first weight is 10.7 mm, and for the second one is 13.4 mm. The machine of (83.6 tons) weight will be more appropriate when it comes to economical options.
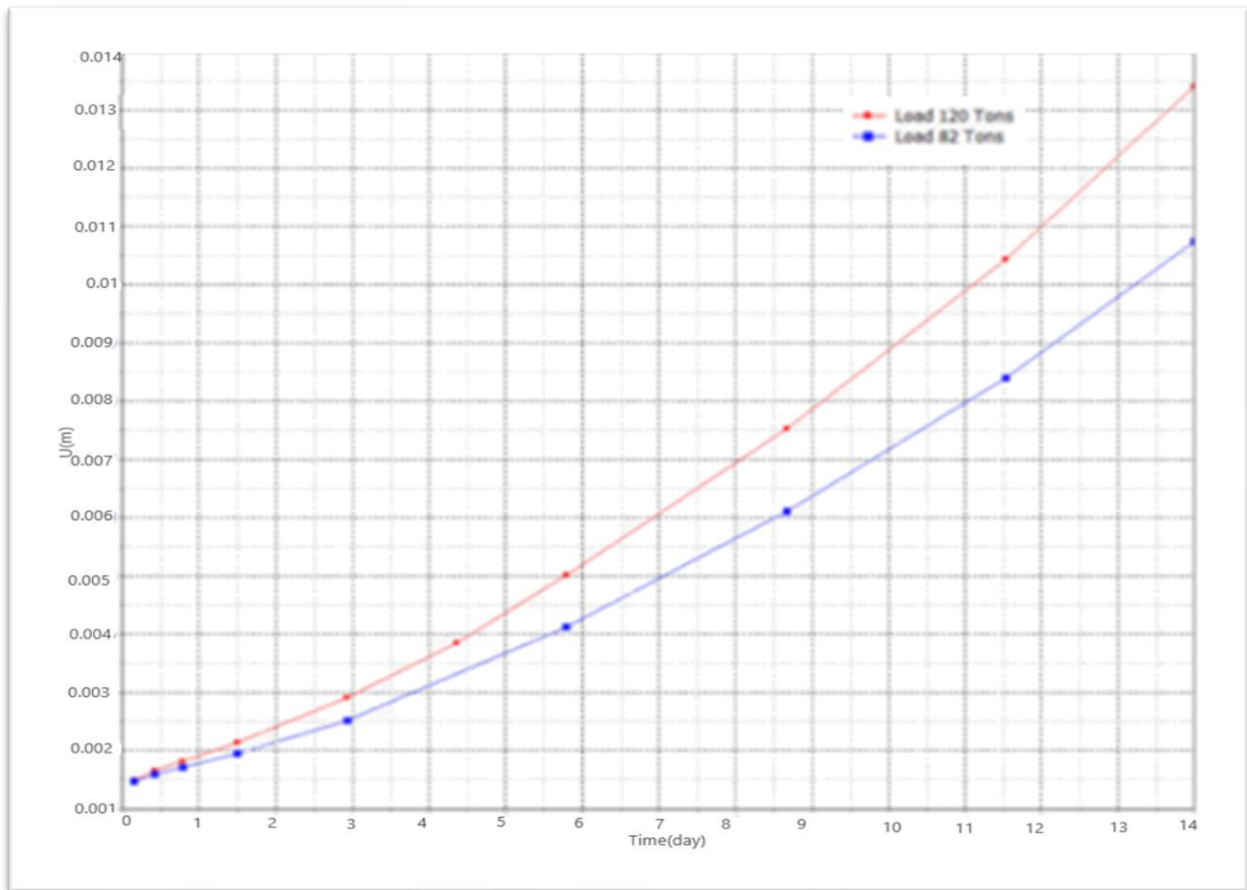
Fig. 6.7 Variation of total displacement with loading time

━◆━ Load 83.6 Tons ━◆━ Load 120 Tons

6.1.3 Safety factor

Figures (6.8) and (6.9) depict that the most critical surface in the initial state is deep with a large radius. Also it is less deep with smaller radius in the last state. It is found to be near the upper part of the core and berm before reconstructions so any remedial steps applied to lower the seepage at the clay will have essential improvement in FS. The value of SF increases in this analysis, it goes from 1.48 to 1.56. Figure (6.10) shows the safety factor for studied situations. It is noted that the variation of water level (decrease- increase) affects safety factor because of water movement in the soil pores, thus reducing the effective stress, soil strength and stability. The sudden drop of safety factor value is normal in c/phi reduction. During the incremental reduction of C and/or Phi an excessive displacement occurs and results in a lower Msf than that in the previous increment or step. Plaxis will continue to adjust the incremental change in C and/or Phi as if it is looking for the minimum safety factor.
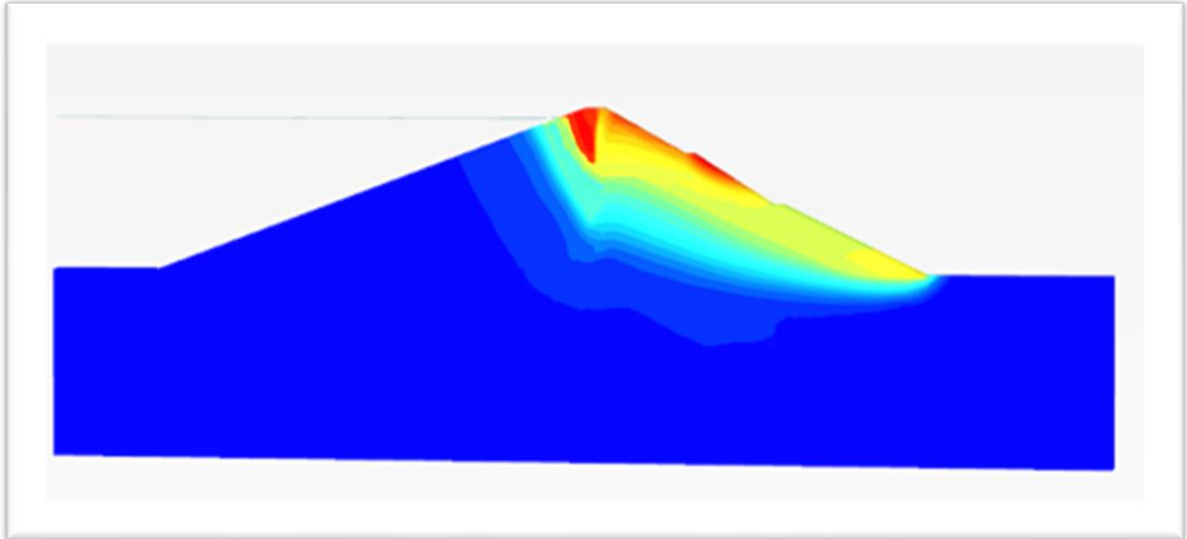
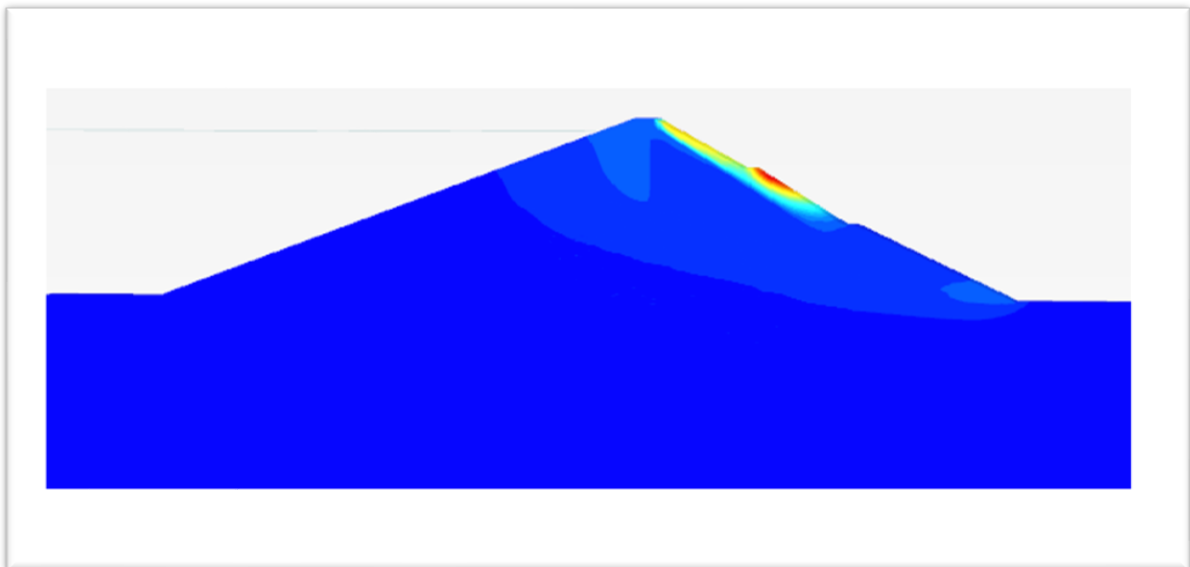**Fig. 6.8** Slip surface at failure (Initial state), **FS =1.48**

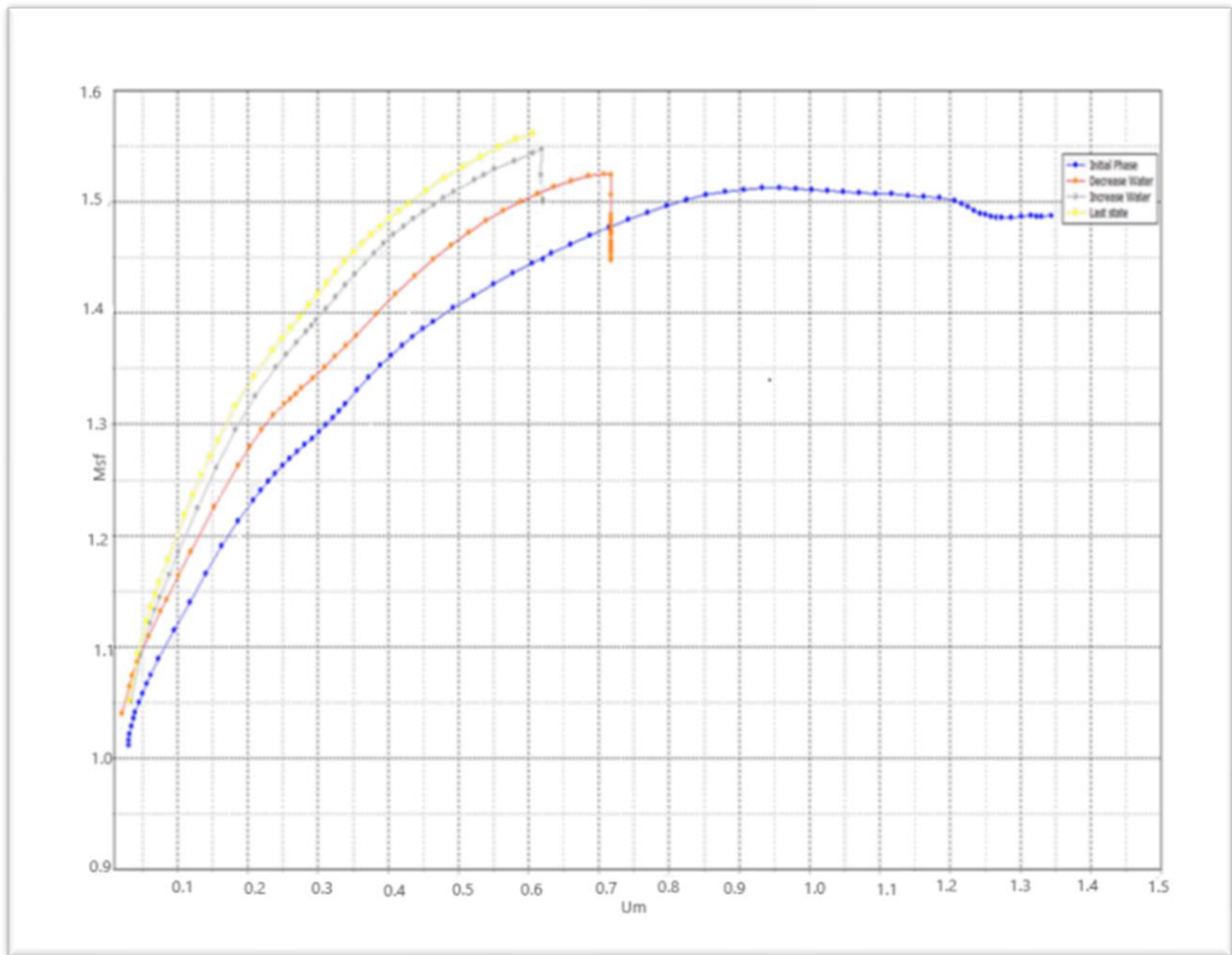**Fig. 6.9** Slip surface at failure (Last state), **FS =1.56**

Fig. 6.10 Evaluation of safety factor
━━ Initial state ━━ Decrease WL ━━ Increase WL ━━ Last state

6.1.4 Ground water flow

1. Figures (6.11) (6.12), show the variation of ground water flow during decrease WL (before reconstruction) and increase WL (after reconstruction) respectively. The obtained results see (figure (6.12)) show that the seepage in the core at studied cross section was decreased to smallest value after reconstructions(increase WL). And this leads to increase the value of SF. In other words, when WL does not enter into the failure surface the stability of slop increases. So SF of dam can be increased by preventing the water from penetrating the slopes by means of drainage techniques.

Elapsed Time 0 days

Groundwater flow |q| (scaled up 200 times)

Maximum value = 0.1884 m/day

Minimum value = 0.000 m/day

Total discharge is 1.604 m³/day

Elapsed Time 3.3 days

Groundwater flow |q| (scaled up 200 times)

Maximum value = 0.1530 m/day

Minimum value = $8.485*10^{-6}$ m/day

Total discharge is 0.8826 m³/day

Elapsed Time 5.17days

Groundwater flow |q| (scaled up 200 times)

Maximum value = 0.1172 m/day

Minimum value = 0.000 m/day

Total discharge is 0.5331 m³/day

Elapsed Time 10 days

Groundwater flow |q| (scaled up 200 times)

Maximum value = 0.06892 m/day

Minimum value = $7.542*10^{-6}$ m/day

Total discharge is 0.06001 m³/day

Fig. 6.11 Variation of ground water flow (decrease WL)

Elapsed Time 0 days

Groundwater flow |q| (scaled up 200 times)
Maximum value = $0.9125*10^{-3}$ m/day
Minimum value = 0.000 m/day
Total discharge is $1.357*10^{-3}$ m³/day

Elapsed Time 5 days

Groundwater flow |q| (scaled up 200 times)
Maximum value = 0.01053 m/day
Minimum value = 0.000 m/day
Total discharge is $-0.3842*10^{-3}$ m³/day

Elapsed Time 10 days

Groundwater flow |q| (scaled up 200 times)
Maximum value = 0.03239 m/day
Minimum value = 0.000 m/day
Total discharge is 0.01361 m³/day

Elapsed Time 15 days

Groundwater flow |q| (scaled up 200 times)
Maximum value = 0.1322 m/day
Minimum value = 0.000 m/day
Total discharge is 0.06490 m³/day

Fig. 6.12 Variation of ground water flow (increase WL)

64

6.2 Jet grouting

6.2.1 Ground water head

Figures (6.13) (6.14), show the variation of ground water head during decrease and increase water respectively, taking into consideration the influence of pore water pressure variations with the time.
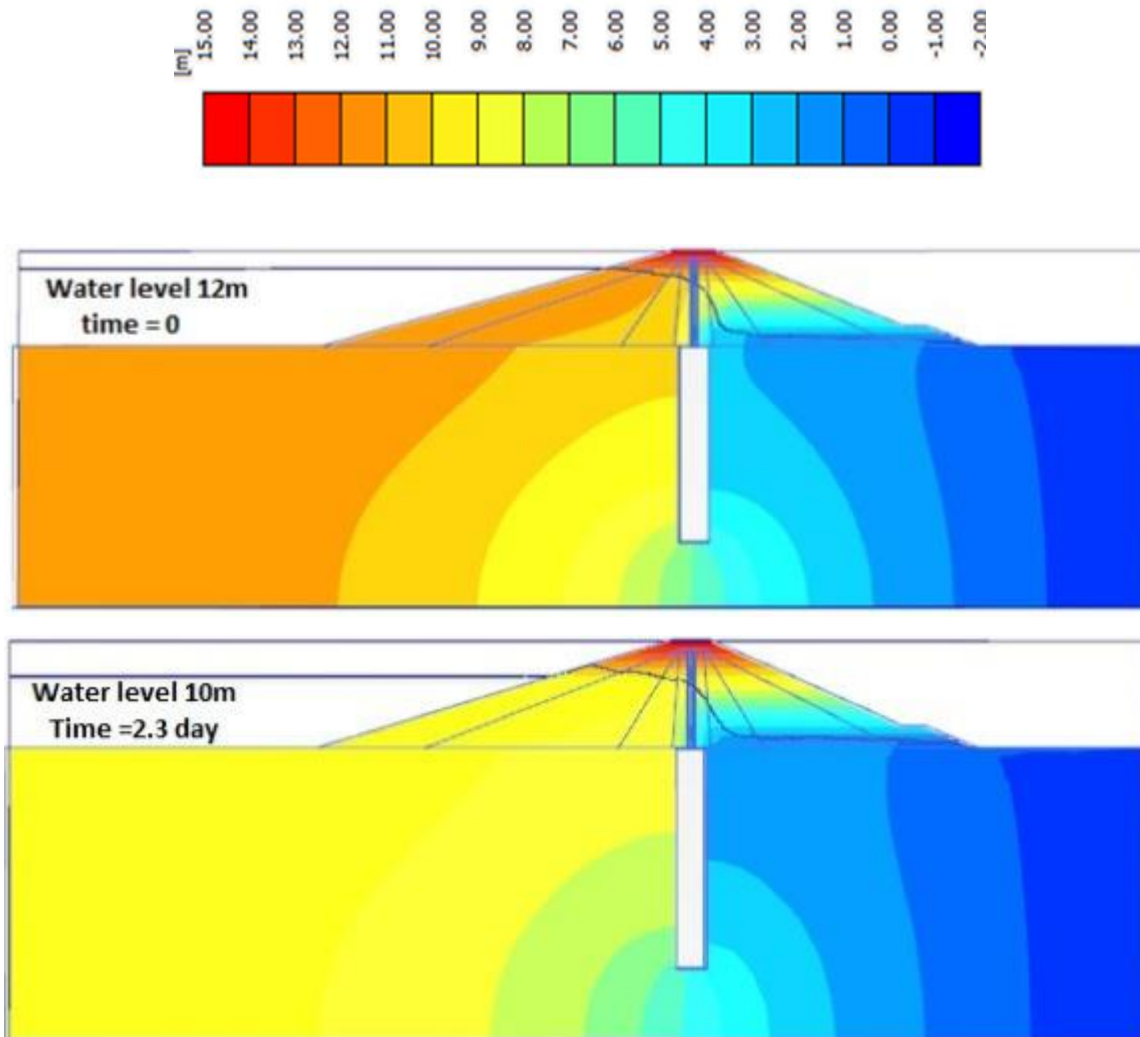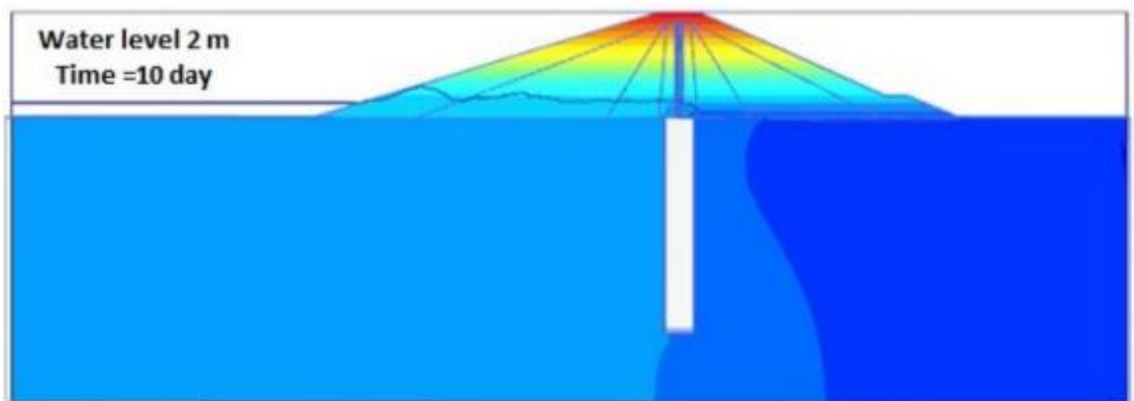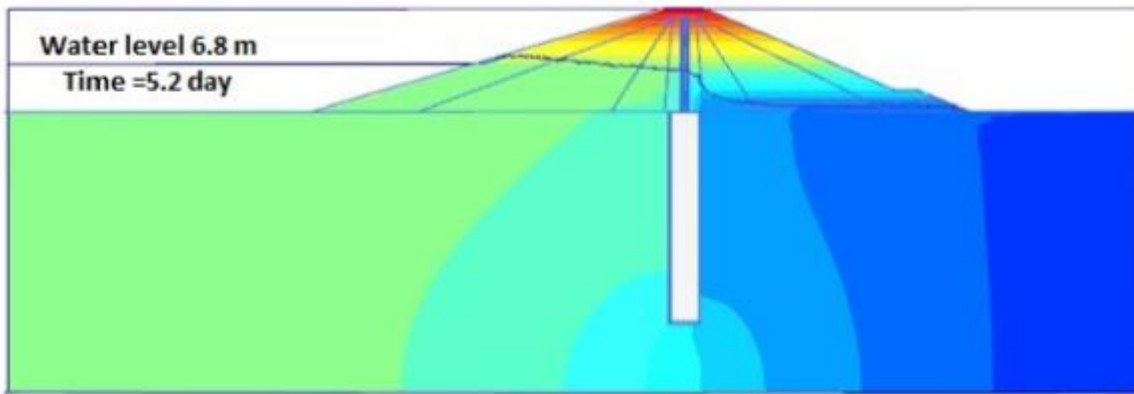
Fig. 6.13 Variation of ground water head (decrease WL)
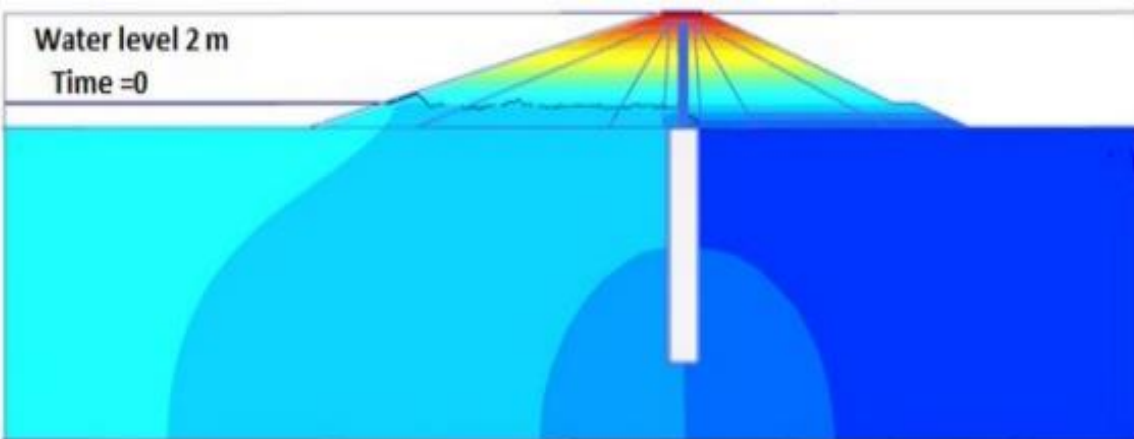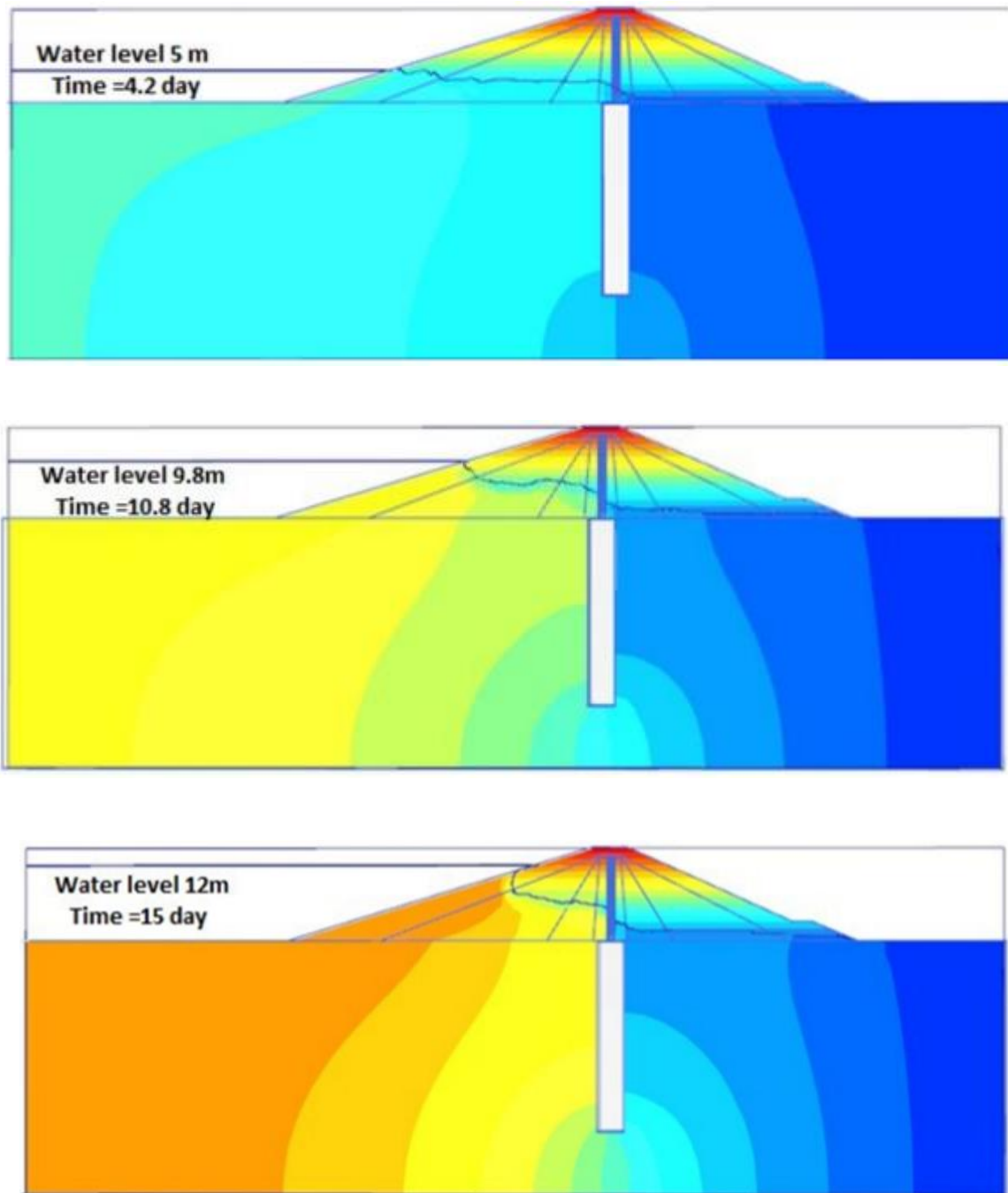
Fig 6.14 Variation of ground water head (increase WL)

6.2.2 The total displacement

The displacement result is expressed in the Figures (6.15) ~ (6-18). Figure (6.15), shows the horizontal displacement distribution with depth at line cross section C-C Figure (5.13). It is clear that the maximum value of horizontal displacement reached 17.5 mm during decrease WL in reservoir, and 10.9 mm during increase the water. On the other hand, there is no significant

horizontal displacement in the last state.
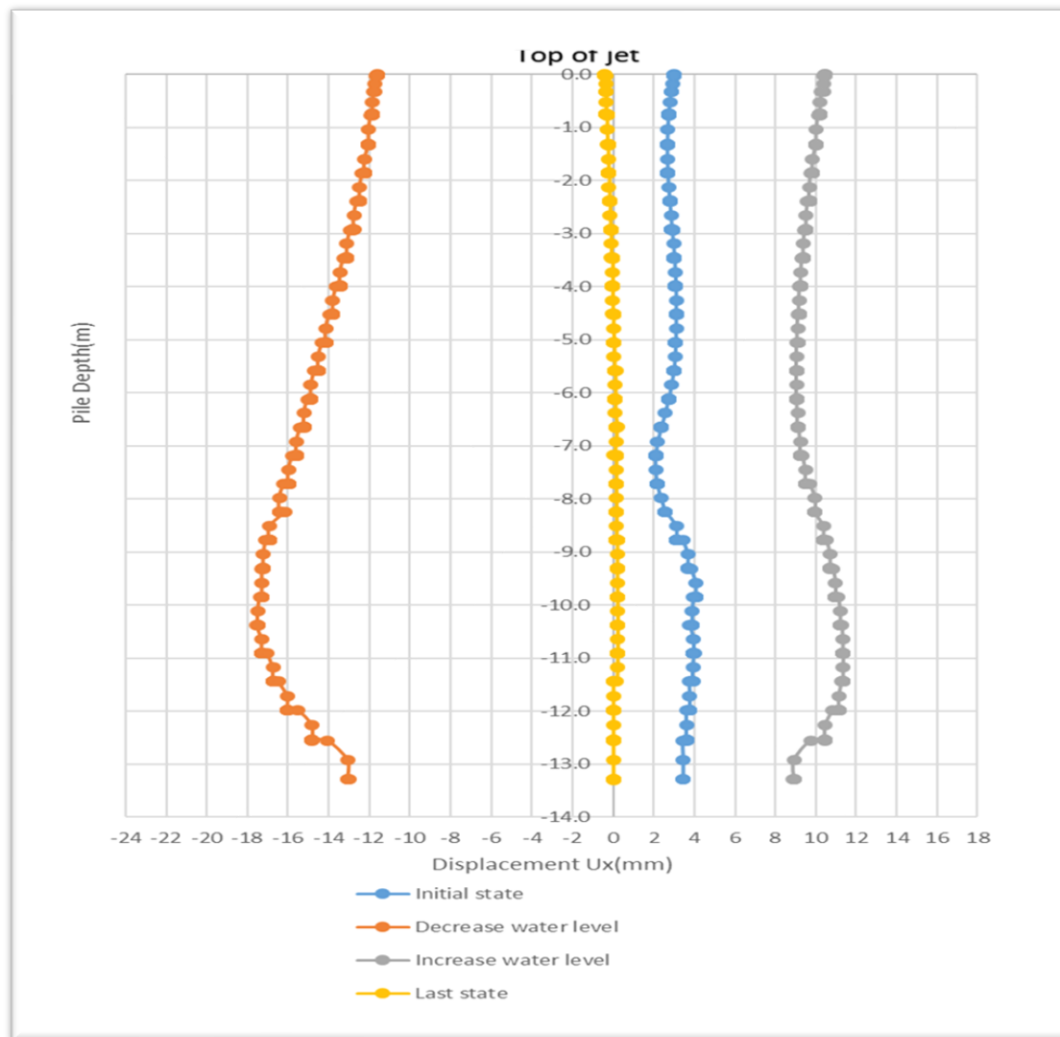
Fig 6.15 The horizontal displacement along the line cross section

C-C (construction pile 1, 3,5)

Figure (6. 16), shows the variation of total displacement with the loading time associated with the machine weight at dam crest. The weight has no effect on the dam state and the displacement resulting from its loading can be ignored.
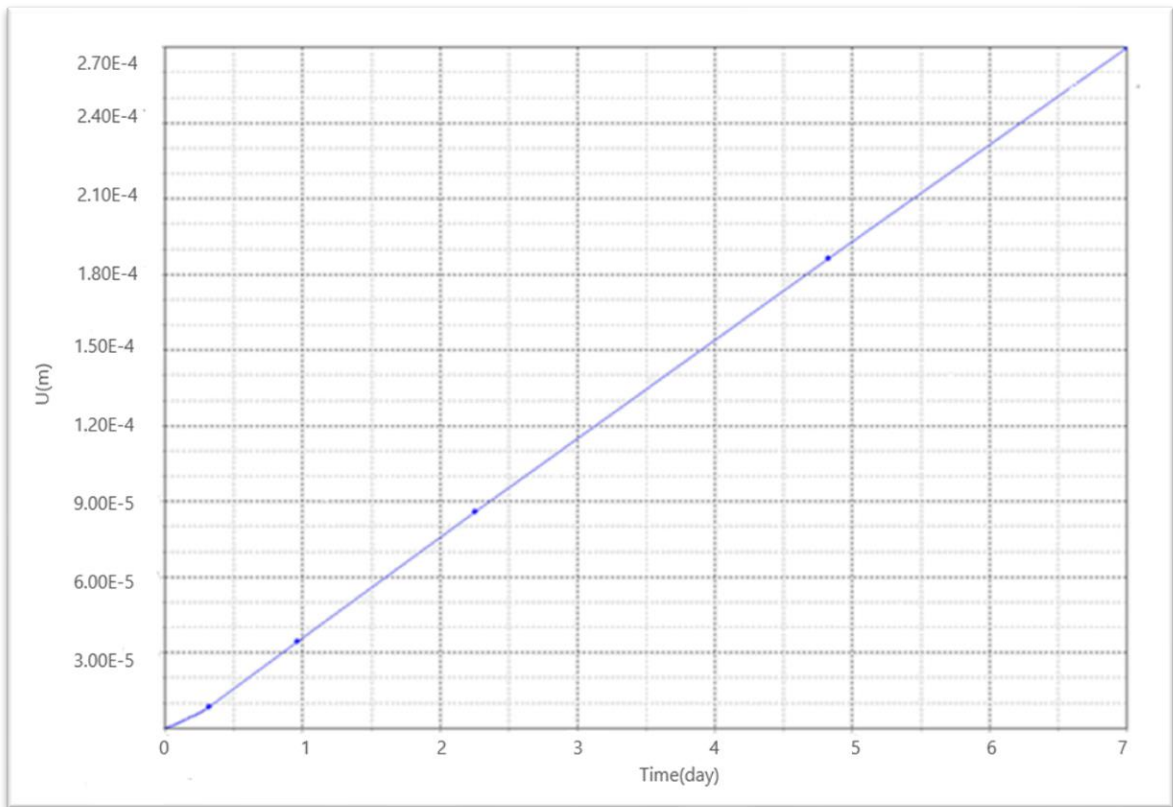
Fig 6.16 Variation of total displacement with loading time

Figures (6.17) and (6.18), show the horizontal and vertical displacement with section length E-E Figure (5.13). during construction piles (1, 3, 5). It is clear that the horizontal and the vertical displacement at crest dam along the line cross section E-E are approximately equal to zero. In other words, no additional risk during jet grouting process.
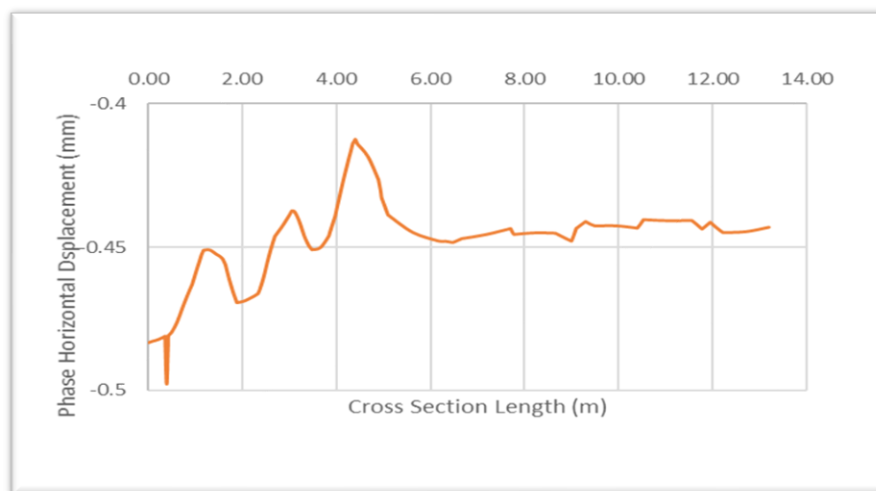
Fig 6.17 Horizontal displacement at crest dam along the line cross section E-E

(construction pile 1, 3, 5)
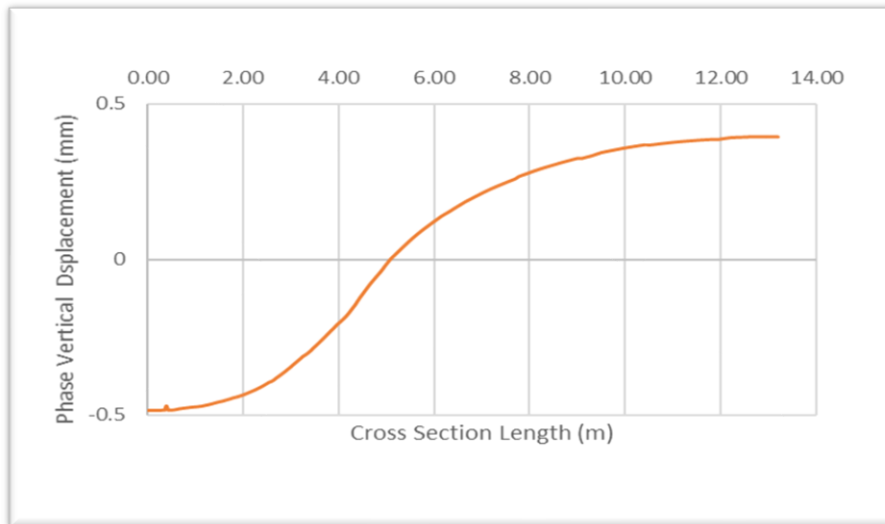
Fig 6. 18 Vertical displacements at crest dam along the line cross section E-E

(construction pile 1, 3, 5)

6.2. 3 Safety factor

The failure surfaces generated from the analysis are given in Fig (6.19) and (6.20). The failure is shallow, flatter with a small radius in both stages (initial state. last state) and the most critical surface in both stages is at the top of the dam. with the little difference in its shape can be ignored. Figure (6.19) shows evaluation of safety factor. SF even goes a little bit as up as 1.62 for the last state.
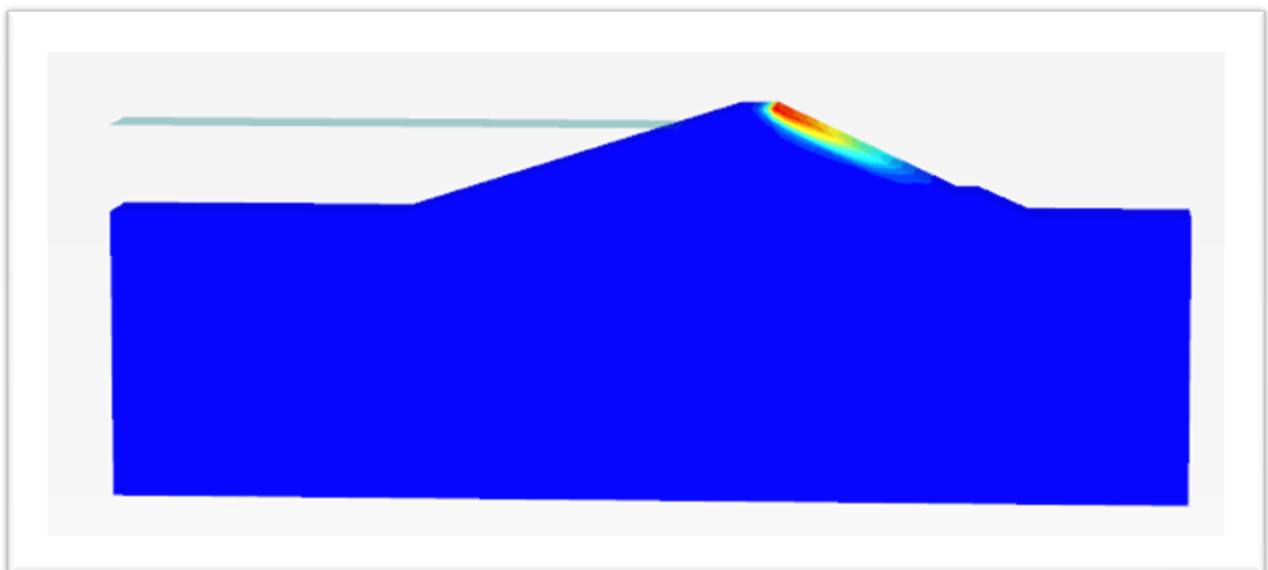
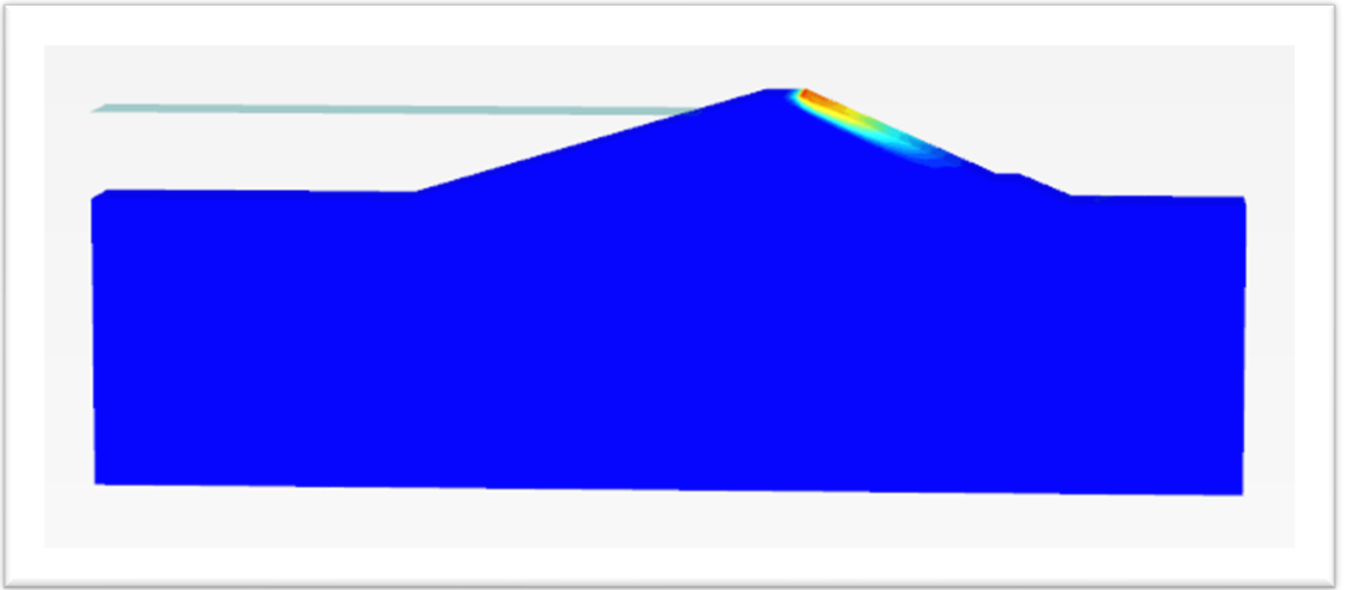**Fig. 6.19** Slip surface at failure (Initial state), **FS =1.60**

Fig. 6.20 Slip surface at failure (Last state), **FS =1.62**
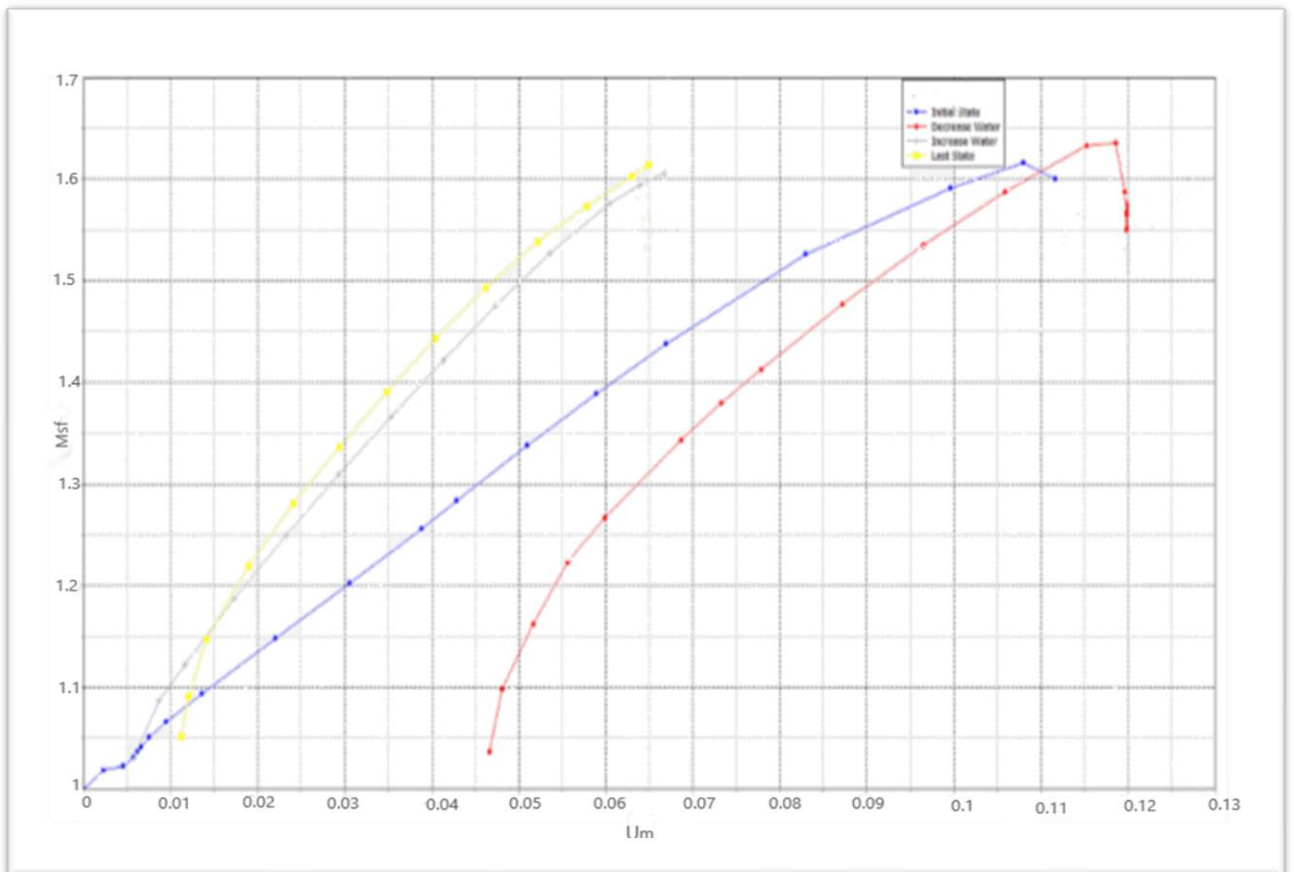

Fig. 6.21 Evaluation of safety factor

—◆— Initial state —◆— Decrease WL —◆— Increase WL —◆—Last stat

6.2.4 Stress state

Figure (6.22), shows the status of principal stresses for all points considered in the connection zone at line cross section C-C Figure (5.13) MC failure envelope is drawn for core (clay). According to this figure, the minor principal stress is compressive in all connection zone, so no probability of hydraulic fracture occurrence in the connection zone, and the failure of the core does not occur for the connection system.
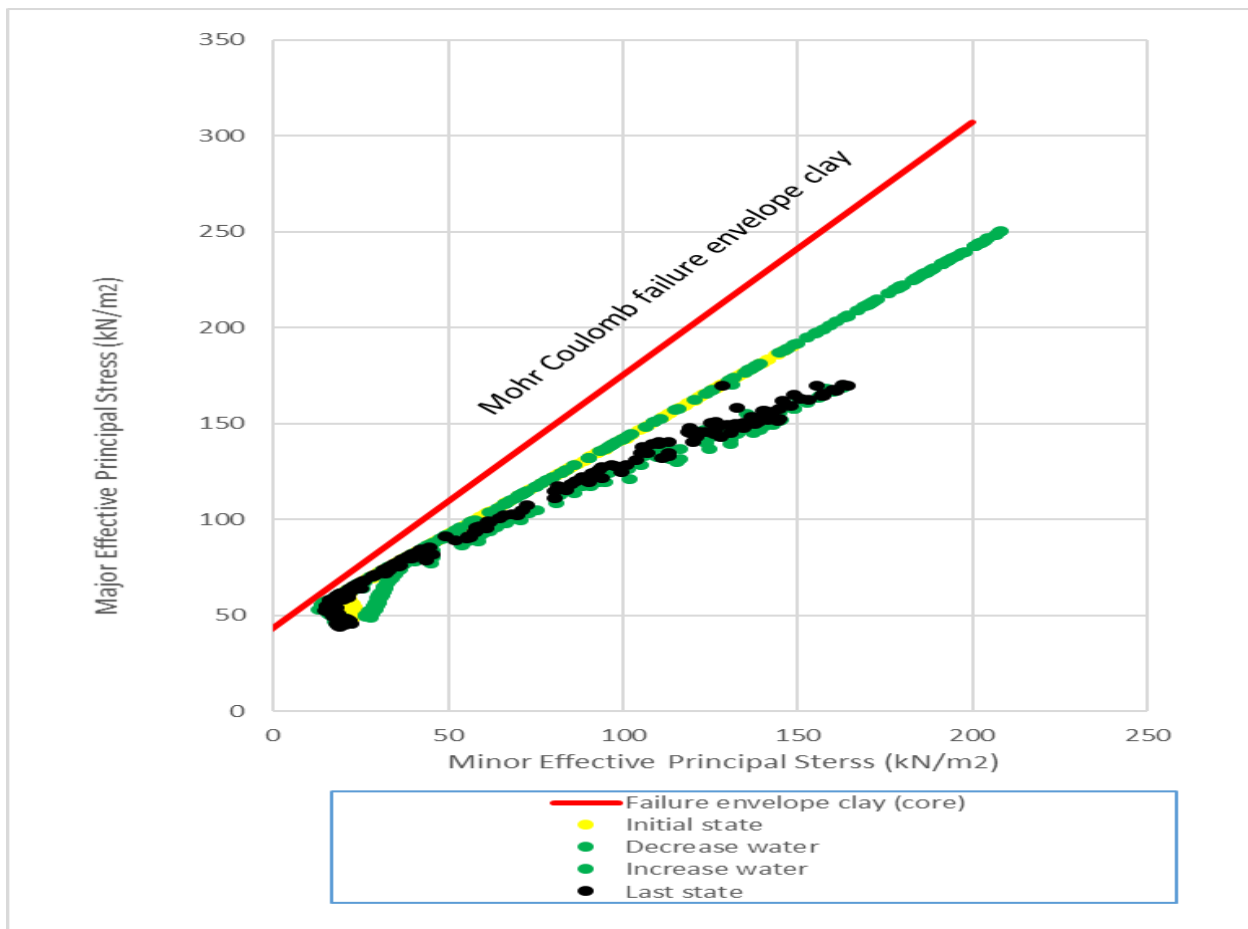

Fig 6.22 The investigation of the failure for grouting system in the core

6.2.5 Dynamic analysis

Figure (6.23) shows the horizontal displacement at a distance of 2.5 metres from the source point. The displacement swings within the first four seconds of the dynamic time at (-2.7mm - 2mm) then dampes gradually, thus no obvious displacement at studied distances.
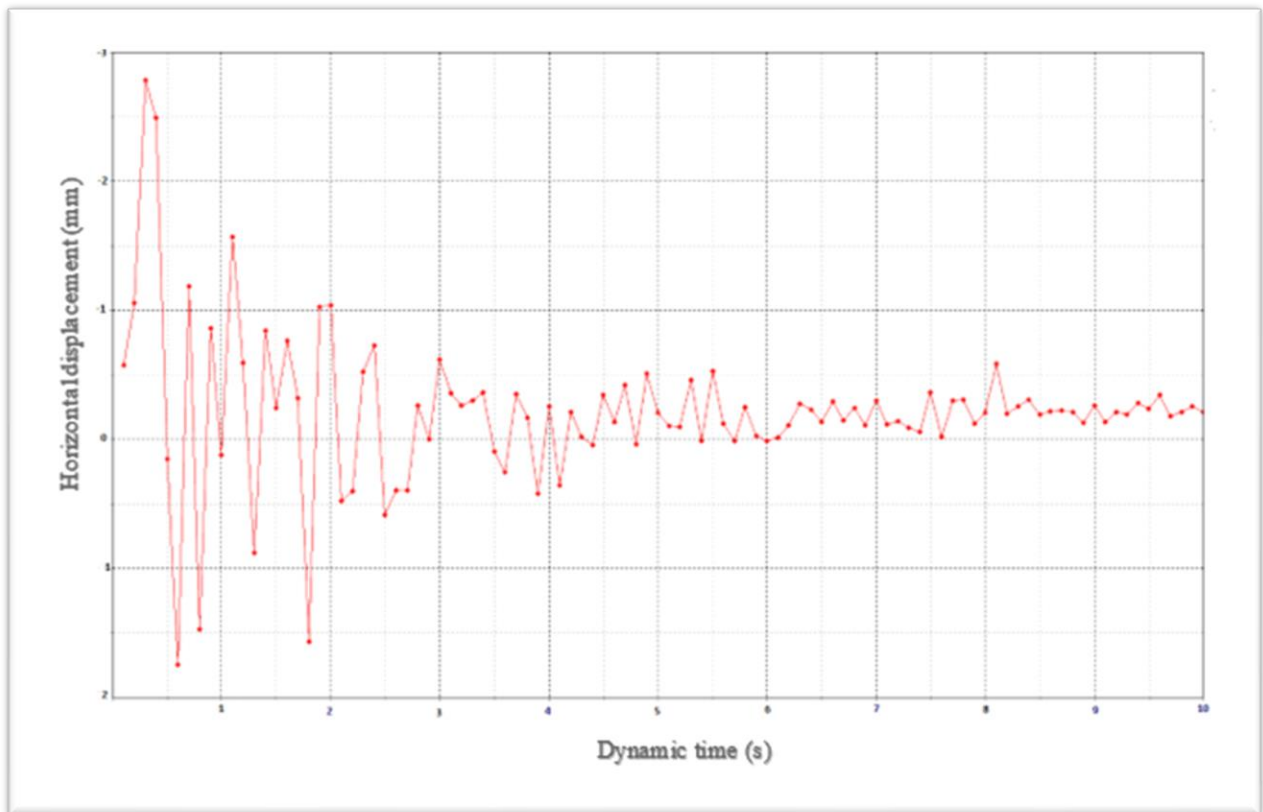
Fig 6.23 Horizontal displacement at crest dam

6.3 Sensitivity analysis (Diaphgram wall)

6.3.1 Effect of elasticity modulus and cohesion on safety factor

To study the effect of soil elasticity modulus and cohesion on the value of SF, the analyses were performed by the program Plaxis 3D where each of cohesion and elasticity modulus of all layers of the dam materials are changed independently with the same ratio, paying attention to keep these changes of these values in the allowable range for each soil material. In the first analysis the initial value was divided by 1.4, and in other analysis it was multiplied by 1.28, 1.56 and 1.85. The Figure (6. 24) shows the obtained values of these analyses. SF increases gradually with increasing both the elasticity modulus and cohesion. On the other hand, the cohesion has a bigger effect on SF than elasticity modulus. The appropriate determination of both cohesion and elasticity modulus have a significant role on determination of SF.

73

Table. 6.1 Relative change of safety factor

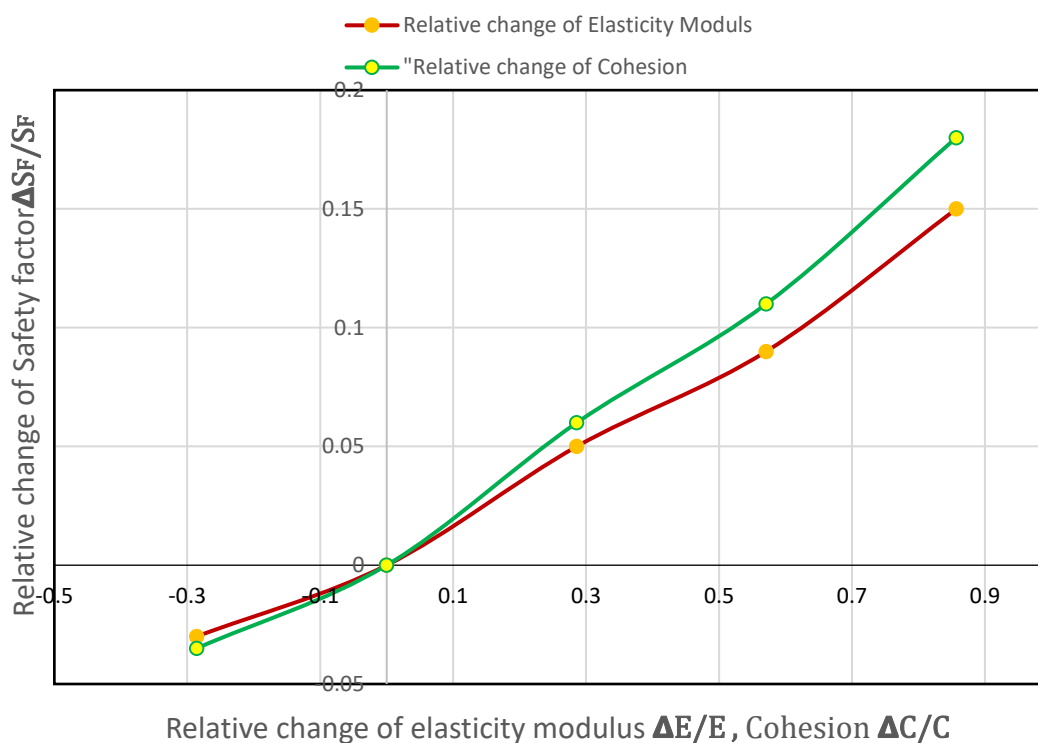| Rate of cohesion, elasticity modulus change	ΔSF/SF	
	Cohesion	Elasticity modulus
The initial state divided by 1.4	-0.04	-0.035
The initial state	0	0
1.28 times of the initial state	0.06	0.05
1.56 times of the initial state	0.11	0.09
1.85 times of the initial state	0.18	0.15

Fig. 6.24 Sensitivity analysis results

6.3.2 Effect of mesh size on safety factor

The effect of the element size was studied using five different sizes of meshes (very fine, fine, medium, coarse and very coarse). Fig (6.25), shows the influence of the element size on SF. It is clear that for the finer division, the variation of SF almost vanishes and this matches with the source data of (Application, 2001) . Thus, when we refine it more, there will be no further effects on the value of SF.
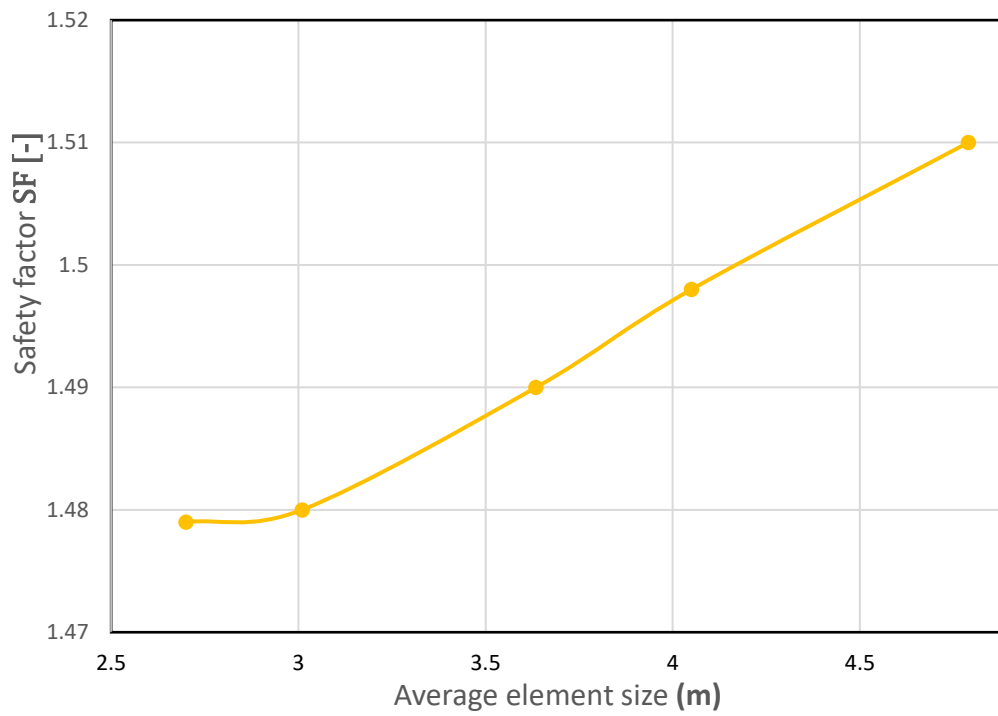
Fig. 6.25 Influence of mesh size on safety factor

7 CONCLUSIONS

The sealing is increasingly used as an integral factor of dam settlement. The last studies have proved the effectiveness of the sealing in dealing with many soils' problems. I have worked to study the effect of the sealing on soil permeability and safety factor, and find out a relation between process stages and the soil deformation, taking into account the sudden configuration of the excess pore pressure due to decreasing and increasing of water level, loading of weight equipment, and mixture prompt pumping process.

This study reports the ability of the sealing to reduce water flow and increase stability of the dam. It investigates the potential effect of the sealing on the studied dam. This work shows the valuation of safety factor during reconstruction stage of Karolinka dam, and minimize the efforts when verifying the safety of slopes in site, in addition to performing designs of excavating works. It presents some charts to facilitate the site work.

It is clear in our case study that satisfying changes of the soil state before and after sealing can be noticed. It is quite difficult to model the case study without specified material properties, so some reasonable values should be input. In this study, a numerical investigation is conducted using Plaxis software which is based on the (FEM), and the results are compared to the experimental and analytical data performed by Vodni dila -TBD company. The main findings in this study can be summarized as follows:

Diaphragm wall:

1. The prediction of this study for the vertical displacement at crest dam (diaphragm wall installing) is (8.2mm), which is comparable to measured value (12.2 mm) in the field measurement of displacement. The total displacement due to an impact of loading drill is (13mm), which is comparable to calculated value (8mm). Also the horizontal displacement is (23.4 mm) which is comparable to (35.1mm) of the horizontal displacement in the field measurement and analytical data performed by Vodni Dila-TBD company (Hodák, 2014).

2. The horizontal displacement at the point A (-2.5,0,39) during decreasing water reaches its height value (32 mm), and during increasing water is (23.5 mm), due to the influence of water load and pore water pressure variations with the time.

3. Adding end stop plate is important to secure a correct geometrical continuity of the wall.

4. There is no obvious difference in the displacement due to the impact of weight machines (83.6 tons, 120 tons). The machine of (83.6 tons) weight will be more appropriate when it comes to economical options.

5. The most critical surface in both cases (initial state, last state) is near the upper part of the core and berm so any remedial step is applied to lower the seepage at the clay will have essential improvement in SF.

6. The value of safety factor before reconstruction stages is (1.48), which is compared to the calculated value depended on: **1**- the shape of failure surface, 2- the data taken from measuring well, **3-** Bishop method, equals (1.498) (Bednárová and Grambličková, 2006).

7. The results of safety factor consider the cross-section positions in two cases: **1-** in the middle (diaphragm wall case), **2-** in the end of dam (jet grouting case). The results show that the value of safety factor in the middle of dam -where the highest height- equals (1.48).   On the other hand, the highest value of the safety factor in the end of dam -where the lowest height-equals (1.6). As a result, the height of dam has a clear impact on the value and shape of the failure surface and the safety factor.

8. The value of safety factor before reconstruction stage is (1.48) and after reconstruction is 1,56 and this result is compatible with the traditionally required value of 1.5 (ČSN 75 2410). As a result, diaphragm wall is an effective technology to improve dam stability (Fathani and Legono, 2011).

9. It is noted that the variation of WL (decrease- increase) affects SF because of water movement in the soil pores, thus reducing the effective stress, soil strength and stability.

10. According to the seepage problem, the obtained results show, that the seepage at studied cross section has been controlled after reconstruction. So, the safety factor of dam can be increased by preventing the water from penetration into the slope by means of drainage techniques.

11. According to the result of sensitivity analysis, it is clear that the safety factor increases gradually with increasing both the elasticity modulus and cohesion. On the other hand, the fine mesh with more refinement, will not have any effect on the value of safety factor.

12. The applied element method is a trusty tool for the installing process of diaphragm wall in the earthen dam. The numerical evaluation using FEM analysis was successfully carried out to investigate the effects of installing process on the surrounding soil.

13. The diaphragm wall is analysed by the presented 3D analysis, taking into consideration the influence of pore water pressure variations with the time.

14. Good matching between the measured and numerical results has been obtained using Plaxis.

Jet grouting:

1. The value of the vertical displacement resulting from the weight of the drill is (0.24mm). Also, the horizontal and vertical displacement (jet pile installing) is almost equal to zero, and it matches the real data in the field measurement performed by TBD company (Hodák, 2014).

2. The horizontal displacement in the connection zone (cross section C-C) reaches its height value during decreasing water is (17.9 mm), and during increasing water is (11mm), taking into consideration the influence of pore water pressure variations with the time.

3. The weight of the machine has no effect on the dam state and the displacement resulting from its loading can be ignored.

4. It is clear that in the result of horizontal and vertical displacement with section length E-E at dam crest during constructions pile, almost equal to zero. In other words, could be ignored and no additional risk during jet grouting process.

5. The failure is shallow, flatter with a small radius in both stages (initial state. last state) and the most critical surface in both stages is at the top of the dam. The safety factor even goes a little bit as up as 1.62 for the last state, with the little difference in its shape can be ignored.

6. Regarding the investigation of failure state, the minor principal stress is compressive in all connection zone, so there is no probability of hydraulic fracture occurrence in the connection zone, and the failure of the core does not occur for the connection system.

7. Dynamic analysis was conducted with some simplifications, and the result shows that the influence of the wave motion on the dam crest is within the allowable value so, there is no obvious effect on the dam stability.

8. It is very important to choose the appropriate period for decreasing and increasing water level in the reservoir. In uncontrolled drawdown, water load disappears so, there is no supporting pressure to dam stability. Also, the generated tensile-

downward forces lead to a decrease in shear strength of the upstream slope. On the other hand, the unplanned filling the reservoir creates excess pore pressure which may put the dam at risk in some critical conditions. As for the case studied and depending on some recommendations (ČSN 75 2310) the level of water was decreased by one meter per day.

9. The process of jet grouting in the case study was modelled by using Plaxis 3D analysis, taking into consideration the influence of pore water pressure variations with the time.

10. The measured and numerical results seem to be close.

8 REFERENCES

ABRAMSON, L., LEE, T., SHARMA, S., BOYCE, G. 2002. Slope Stability and Stabilization Methods. John Wiley, New York, ISBN: 978-0-471-38493-9. P 712

AMBIKAIPAHAN, 2011. Failure of an Earth Dam. Master Thesis in Geosciences, University of Oslo, Norway.

APPLICATION, 2001. Application of the Finite Element Method to Slope Stability. Rocscience Inc. Toronto, 2001. [online]

https://www.rocscience.com/assets/resources/learning/papers/Application-of-the-Finite-Element-Method-to-Slope-Stability.pdf

AU, S, K, A., SOGA, K., JAFARI, M, R., BOLTON, M, D., KOMIYA, K. 2003. Factors affecting long-term efficiency of compensation grouting in clays. Journal of geotechnical and geo environmental engineering. ISSN: 1090-0241.

BAYESTEH, H., SAMBERMAHANI, M. 2020. Field Study on Performance of Jet Grouting in Low Water Content Clay. Journal of Engineering Geology. ISSN: 0013-7952.

BEDNÁROVÁ, E., GRAMBLIČKOVÁ, D. 2006. VD Karolinka – těsnící clona. Dokumentace pro vydání stavebního povolení, Hydroconsulting s.r.o. Bratislava.

BENZ, T. 2007. Small strain stiffness of soils and its numerical consequences. PhD thesis. University Stuttgart. Germany.

BHAVIKATI, S.S. 2005. Finite Element Analysis. New Age International Publishers. New Delhi, India. ISBN: 81-224-1589-X.

BOLTON M. D., STEWART D. I., 1994. The effect on propped diaphragm walls of rising groundwater in stiff clay .Journal of Geotechniqu.Vol 44 (1): pp. 111-127.

BRINKGREVE, R. B. J., ENGIN, E., SWOLFS, W. M. 2017. PLAXIS 3D Anniversary edition. [online] https://www.plaxis.com/support/manuals/plaxis-3d- manuals.

BRINKGREVE, R, B, J., ENGIN, E., SWOLFS, W, M. 2014. Plaxis full manual. ISBN 978-90-76016-15-3. [online] http://www.plaxis.nl.

BRITISH DAM SOCIETY. 1994. Reservoir Safety and the Environment. Thomas Telford Ltd. ISBN: 9780727720108.

BRZAKALA, W., GORSKA, K. 2007. On safety of slurry-wall trenches. [Online] https://www.researchgate.net/publication/27610321.

BUCHET, G. 1999. GOSMUS: New methods for compensation grouting. Balkema. Rotterdam. ISBN: 90 58090663.

CHARLES, J. A., TEDD, P., HUGHES, A. K., LOVENBURY, H T. 1996. Investigating embankment dams, a guide to the identification and repair of defects.

CHEN J. J., WANG. H. J., LEI. H. 2014. Numerical analysis of the installation effect of diaphragm walls in saturated soft clay. Journal of Acta Geotechnica. Vol. 9: pp.981-991.

CHEN, Y., ZHANG, S. 1989. Test embankment dam of fracture grouting. American society of civil engineers. Journal of geotechnical engineering. ISSN: 1944-8368.

CHOI, Y.F.R. 2005. Review of the Jet Grouting Method. B. Eng thesis. Queensland University, Australia.

CONTI, R., SANCTIS. D. L., VIGGIANI. B. M. G. 2012. Numerical modelling of installation effects for diaphragm walls in sand. Journal of Acta Geotechnica.Vol. 7: pp.219-237.

CROCE, P., GIUSEPPE, M. 2007. Design of jet-grouting cut-offs, January 2007, Proceedings of the Institution of Civil Engineers Ground Improvement. Vol.11(1): pp. 11-19.

ČERNÝ, V., DROCHYTKA, R., JANDORA, J. 2012. The Usability of fly ash for the construction of embankment dams. Advanced materials research. Switzerland.
ISSN: 1022- 6680.

ČSN 75 2410. 2011. Malé vodní nádrže. Small water reservoirs. Prague

ČSN 75 2310. 2006. Sypané hráze. 2006. Embankment Dam. Prague.

ČSN EN 12716(731072). 2002. Provádění speciálních geotechnických prací - Trysková injektáž. Execution of special geotechnical work - Jet grouting.

DAREBNÍK, Z. 2017. Zatěsňování vodních děl pomocí injektáží. [Online]:
https://www.asb-portal.cz/stavebnictvi/inzenyrske-stavby/geotechnika/zatesnovani-vodnich-del-pomoci-injektazi

DAWSON, E. M., ROTH, W. H., DRESCHER, A. 1999. Slope stability analysis by strength reduction. Geotechnique. Vol. 49(6): pp. 835–840.

DING, Y. C., WANG, J. H. 2008. Numerical Modeling of Ground Response during Diaphragm Wall Construction. Journal of Shanghai Jiaotong University. Vol 13 (4).

DOBES, I. 2002. Study of reconstruction of Bystricka Dam. Technical Report. AQUATIS a.s. Brno, Czech Republic.

DSN grouting. 2017. Bonded Strand Post-Tensioning System. [Online]
https://www.dsiamerica.com/

FANG, S.Y., LIAO, J. J., SZE, C, S. 1994. An empirical strength criterion for jet grouted soilcrete. Engineering Geology. Vol. 37(3): pp. 285-293.

FATHANI, T., LEGONO, D. 2012. Dynamics of Earth Dam Stability caused by Rapid Rising and Drawdown of Water Level. The 3rd International Workshop on Multimodal Sediment Disasters Challenge to Huge Sediment Disaster Mitigation.

FREDLUND, G, D., RAHARDJO, H. 1993. Soil mechanics for unsaturated soils. John Wiley & Sons. New York. ISBN: 047185008X.

FREDLUND, G, D., SCOULAR, E, G, R. 1999. Using limit equilibrium concepts in finite element slope stability analysis. Proceedings of the international symposium on slope stability engineering. Matsuyama, Japan. pp.31-47.

FREDLUND, G, D., SCOULAR, E, G, R., ZAKERZADEH, N. 1999. Using A Finite element stress analysis to compute the factor of safety. Proceedings of the 52nd Canadian Geotechnical Conference, Regina. Saskatchewan. pp. 73-80.

FU, X., GU, C, S., SU, H, Z., QIN, X. 2018. Risk Analysis of Earth-Rock Dam Failures Based on Fuzzy Event Tree Method. International Journal of Environmental Research and Public Health. Vol 15 (5).

FUCHEN, L., XINGQI, C., WEI, Z., AIHUA, S. 2010. Finite element analysis of split grouting on earth-rock dam based on Duncan-Chang model. Electronic journal of geotechnical engineering. ISSN: 1089-3032.

GALAVI, V. 2010. Technical report: groundwater flow, fully coupled flow deformation and undrained analyses in PLAXIS 2D and 3D. Plaxis BV.

GHANBARI, A., RAD, S, S. 2015. Development of an empirical criterion for predicting the hydraulic fracturing in the core of earth dam. Acta Geotechnica. ISSN: 1861-1125.

GOH, A.T.C., ZHANG. F., ZHANG.W., ZHANG.Y., LIU. H. 2017. A simple estimation model for 3D braced excavation wall deflection. Magazine of Computers and Geotechnics. Vol. 83: pp.106-113.

GRAMBLIČKOVÁ, D., ŠKVARKA, J., BEDNÁROVÁ, E. 2016. Leakages Remediation on Hydraulic Structure Karolínka. 16th International Multidisciplinary Scientific Geo Conference. Book 1. Albena, Bulgaria. pp. 163 –170. ISBN 978-619-7105-57-5.

GROTENHUIS, T, R. 2004. Fracture grouting in theory. M.SC. PhD thesis. Amsterdam.

HAIMONI, A, M., WRIGHT, R, H. 1999. Protection of Big Ben using compensation grouting. Ground Engineering. London.

HENN, R, W. 1996. Practical guide to grouting of underground structures. Institution of civil engineers. New York. ISBN: 0784401403.

HODAK, J. 2014. Karolinka Dam-Dam safety supervision during diaphragm1wall construction. In XXXIV. Priehradné dni 2014. Košice, SR: Slovenský vodohospodársky podnik, š. p. Odštepný závod Košice, 2014. ISBN: 978-80-971596.

HOULSBY, I, C. 2008. Cement Grouting: Guide to Grouting in Rock Foundations. Wily. ISBN: 9780470318621.

IOOSS, B., LEMAITRE, P. 2014. A review on global sensitivity analysis methods. Hal archive [On line] https://hal.archives-ouvertes.fr/hal-00975701/document

JANDORA, J., ŘÍHA, J. 2007. The failure of embankment dams due to overtopping. ISBN: 978-80-214-3527-8.

JAREŠ, Z., KREJČÍ, V. 2014. VD Karolina-rekonstrukce hraze. XXXIV. Priehrande dni 2014. Slovakia. ISSN: 971596-6-6-5.

JAREŠ, Z., KREJČÍ, V. 2015. VD Karolinka – rekonstrukce hráze (Karolinka dam and water reservoir - dam reconstruction). Setkání vodohospodářských kateder 2015 (Meeting of water management departments 2015).

JARITNGAM, S. 2003. Design Concept of the Soil Improvement for Road Construction on Soft Clay. Proceedings of Eastern Asia Society for Transportation Studies. ISSN: 00466828.

JANSON, Y, W. 2008. Numerical modelling the behaviour of ground improvement in soft clay. American society of civil engineers.

KELLER.2005. The soilcrete-jet grouting process. [Online] http://www.keller.com.au

KEOGH, S, K. 2005. Properties of cement grouting-based permeation grout used in ground engineering. PhD thesis. University of South Carolina.

KUMMERER, C. 2003. Numerical modelling of displacement grouting and application to case histories. PhD thesis. Graz University, Austria.

KUTZNER, C. 1996. Grouting of rock and soil. Rotterdam, Netherlands.
ISBN: 90-5410634-4.

LABUZ, J. F., ZANG, A. 2012. Mohr–Coulomb Failure Criterion. Rock Mechanics and Rock Engineering. Vol 45(6), pp. 975–979.

LIBRETEXTS. 2018. Comparing Simple Harmonic Motion and Circular Motion [Online] https://status.libretexts.org.

LAGERLUND, J. 2009. Remedial injection grouting of embankment dams with non-hardening grouts. PhD Thesis. Sweden. ISSN:1650-951X.

LITTLEJOHN, S. 2003. The development of practice in permeation grouting and compensation grouting a historical review (1802 – 2002) Part 1 Compensation grouting. American Society of Civil Engineers. ISBN: 978-0-7844-0663-2.

LURA, P .2003. Autogenous Deformation and Internal Curing of Concrete. DUP Science Netherlands. ISBN: 90-407-2404-0.

MASINI, L., RAMPELLO, S., SOGA, K. 2014. An Approach to evaluate the efficiency of compensation grouting. Journal of geotechnical and geo-environmental engineering. American society of civil engineers. ISSN: 1090-0241.

MAZLOOM, M., BROOKS, J, J., MEGAT, M, A. 2000. Effect of admixtures on the setting times of high-strength concrete. Journal of Cement and Concrete Composites. Vol. 22: pp. 293 – 301.

MICHAEL, R., THOMASH, K., AGNEL, G. 2015. Seepage management control for a dam rehabilitation project using deep cut off wall construction and jet grouting. Proceedings of the Annual Conference Mississauga, Canada. [Online] http://www.klohn.com/wpcontent/uploads /2016/01/150808-CDA-2015-Paper-Morriso Dam Submitted-ID1036.

MOORMANN.C. 2004. Analysis of wall and ground movements due to deep excavations in soft soil based on a new worldwide database. Magazine of Soils Found. Vol. 44: pp.87-89.

NASH, D. 1987. Comprehensive Review of Limit Equilibrium Methods of Stability Analysis Journal of Slope Stability. Chapter 2. pp. 11-75. Wiley. New York.

NIKBAKHTAN, B., AGHABABAEI, H., POURRAHIMIAN, Y. 2007. The effects of jet grouting on slope stability at Shahriar dam, Iran. Proceedings of the 1st Canada-US Rock Mechanics Symposium. [Online] https://www.researchgate.net/publication/280293011.

NIKBAKHTAN, B., AHANGARI, K. 2010. Field Study of the Influence of Various Jet Grouting Parameters on Soilcrete Unconfined Compressive Strength and its Diameter. International Journal of Rock Mechanics and Mining Sciences, Vol. 47: pp.685-689.

PAŘÍLKOVÁ, J., ZACHOVAL, Z., PAŘÍLEK, L. 2016. The earth-fill dam of the Karolinka water reservoir monitored by the EIS method. Eureka 2016. 4th Conference and Working Session within the Framework of the International EUREKA, Project No.: E!7614, Lednice, Czech Republic 13–14.10.2016, pp.185–209.

PIU, M, C. 2005. Analysis and modelling of grouting and its Application in civil engineering. PhD thesis. University of Southern Queensland.

POTTS, D. M., LIDIJA, Z. 2001. Finite element analysis in geotechnical engineering application. ICE Publishing. United Kingdom. ISBN: 0727727834.

Povodí Moravy, S. P. 2014. [online]: http://www.pmo.cz/cz/media/tiskove-zpravy/povodi-moravy-zahajuje-opravu-hraze-podhradskeho-rybnika/

RICHARDS, L, A. 1930. Capillary conduction of liquids through porous mediums, American Institute of Physics. ISBN: 318–333.

ŘIHA, J., ŠVANCARA, J. 2006. The failure of the Mostiště embankment dam. Improvements in reservoir construction, operation and maintenance. Thomas Telford. London. 2006. ISBN: 0-7277-3470-9.

ŘIHA, J., KOTAŠKA, S., PETRULA, L. 2020. Dam Break Modelling in a Cascade of Small Earthen Dams: Case Study of the Cižina River in the Czech Republic. Water [online]: http://hdl.handle.net/11012/194870

SCHWEIGER, H., GENS, A., WEI, S. L., CHEUK, J. and CHEANG, W. 2012. PLAXIS Advanced course on computational geotechnics. Hong Kong.

SHU, J., SUN, J., ZHANG, D., Wei, H. 2019. Sequential Measurement and Analysis of Large Underground Retaining Structures by Diaphragm Wall Anchor for the Spring Area. Journal of Advances in Civil Engineering. Vol 2019: pp 1-20.

SIVAPRIYA, S., GANDHI, S., SUNDARAVADIVELU, R. 2018. Effect of Lateral Movement of Soil in Diaphragm wall - A Case Study. 3rd Indian Young Geotechnical Engineers Conference. India.

TAZAWA, E., MIYAZAWA, S. 1997. Influence of constituents and composition on autogenous shrinkage of cementitious materials. Magazine of Concrete Research. Vol 49 (178): pp 15-22.

THIEU, N, T, M., FREDLUND, M, D., FREDLUND, D, G., HUNG, V, R., 2001. Seepage modelling in a saturated/unsaturated Soil System. International Conference on Management of Land and Water Resources (ICWRCOE'15). Vietnam.

TINDALL, A, J., KUNKEL, R, J., ANDERSON, E, D. 1998. Unsaturated zone hydrology for scientists and engineers. Pearson education. London. ISBN: 978-0136607137.

TSING, H, T. 1998. Guidelines for Injection in Underground Construction and Tunnelling. [Online] http://fast10.vsb.cz/science/seminar2002/pics/18

VERFEL J. 1989. Rock grouting and diaphragm wall construction. Elsevier. New York. ISBN: 0444564357.

WANG, F., WANG, J., SHI, M., GUO, C., ZHONG, Y., ZHANG, B., WANG, X. 2011. Directional fracture grouting method with polymer for seepage control of dikes and dams. Patents. US 20110103898 A1. Zhengzhou uretek technology LTD.

WANG, Z.F., SHEN, S.L., YANG, J. 2012. Estimation of the Diameter of Jet-Grouted Column Based on Turbulent Kinematic Flow Theory. Proceeding of the 4t International Conference on Grouting and Deep Mixing, pp. 2044-2051.

WATANABE, H., KANAZAWA, K. 1995. Soil-Diaphragm Wall Interaction in Floating Dam. Third international Conference on Recent Advances in Geotechnical Earthquake Engineering and Soil Dynamics. Volume I, St. Louis, Missouri. [Online] https://scholarsmine.mst.edu/cgi/viewcontent.cgi?article=3103&context=icrageesd

WISSER, C., AUGARDE, C, E., BURD, H, J. 2005. Numerical modelling of compensation grouting above shallow tunnels. International Journal for Numerical and Analytical Methods in Geomechanics. New York. ISSN: 1466-5123.

World & Weather Climate Information. 2016. [Online] https://weather-and-climate.com/

XANTHAKOS, P, P., ABRMSON, L, W., BRUCE, D, A. 1994. Ground control and improvement. Wiley, New York. ISBN: 978-0-471-55231-4.

9 LIST OF SYMBOLS

u	Displacement vector	[-]
D^e	Material stiffness matrix	[-]
ε_e	Elastic strain	[-]
ε_p	Plastic strain	[-]
L^T	Transpose of differential operator	[-]
S_u	Undrained shear strength	[kN/m^2]
q_x , q_y , q_z	Discharge per unit area in direction (x, y, z)	[m/s]
i	Hydraulic gradient	[-]
τ	Shear stress	[kN/m^2]
$\lfloor K \rfloor$	Element stiffness matrix	[-]
$\{\delta\}$	Nodal displacement vector	[-]
$\{F\}$	Nodal force vector	[-]
b	Body force vector	**[-]**
σ_x , σ_y , σ_z	Normal stress in direction (x, y, z)	[kN/m^2]
σ'_1, σ'_3	Major and minor effective principal stress	[kN/m^2]
τ_{xy} , τ_{yz} , τ_{zx}	Shear stress in direction (x, y, z)	[kN/m^2]
τ_f	Failure shear strength	[kN/m^2]
ε_x , ε_y , ε_z	Normal strain direction (x, y, z)	[-]
γ_{xy} , γ_{yz} , γ_{zx}	Shear strain in direction (x, y, z)	[-]
u, v, w	Displacement in direction (x, y, z)	[m]
p_w	Pore water pressure	[kN/m^2]
$H_1(t), H_2(t)$	Piezometric head in boundaries borders	[m]
$h_{p,0}$	Initial piezometric head	[m]
H_0	Specified piezometric head in the reservoir	[m]
σ'_V	Vertical effective stress	[kN/m^2]
σ'_h	Horizontal effective stress	[kN/m^2]
K'_0	Coefficient for lateral earth pressure	[-]
F_x , F_y , F_Z	Body forces per unit volume in direction (x, y, z)	[kN/m^3]

G	Shear modulus	[kN/m^2]
E	Elastic modulus	[kN/m^2]
ν	Poisson ratio	[-]
k_x, k_y, k_z	Coefficient of permeability of soil in direction (x, y, z)	[m/day]
n_i	Normal vector in directions (x, y, z)	[-]
t	Time	[day]
m	Water storage	[m^{-1}]
φ	Friction angle	[°]
c	Cohesion	[kN/m^2]
ψ	Dilation angle	[°]
σ'_N	Effective normal stress	[kN/m^2]
σ'_h	Effective horizontal stress	[kN/m^2]
σ'_v	Effective vertical stress	[kN/m^2]
ϕ'	Effective angle of internal friction	[°]
$\acute{C}$	Effective cohesion	[kN/m^2]
R_{inter}	Interface reduction factor	[-]
M	Mass matrix	[-]
$u, \dot{u}, \ddot{u}$	Relative nodal displacement, velocity, and acceleration	[-]
C	Global damping matrix	[-]
K	Stiffness matrix	[-]
F	Load vector	[-]

10 LIST OF ABBREVIATIONS

2D	Two Dimensional
3D	Three Dimensional
AES	Average Element Size
FEM	Finite Element Method
FDM	Finite Difference Method
FCFD	Fully coupled flow-deformation – calculation type in Plaxis
LE	The Limit Equilibrium
MC	Mohr-Coulomb
MS	Method of Slices
Msf	Safety Factor value in Plaxis
M a.s.l	Metres above mean sea level
OAT	One-At-A-Time Method
RGIT	Radial Ground Improvement Technology
SF	Safety Factor
TBD	Czech Consulting Company for Dam Safety
UCS	Unconfined Compressive Strength
WL	Water Level
W/C	Water ratio to Cement ratio in mixture

11 LIST OF TABLES

12 LIST OF FIGURES

13 LIST OF APPENDICES

13.1 Hand calculations

14.1.1 Diaphragm wall

- ***Machine***

Fig. 13.1 Liebherr specifications (www.liebherr.com)
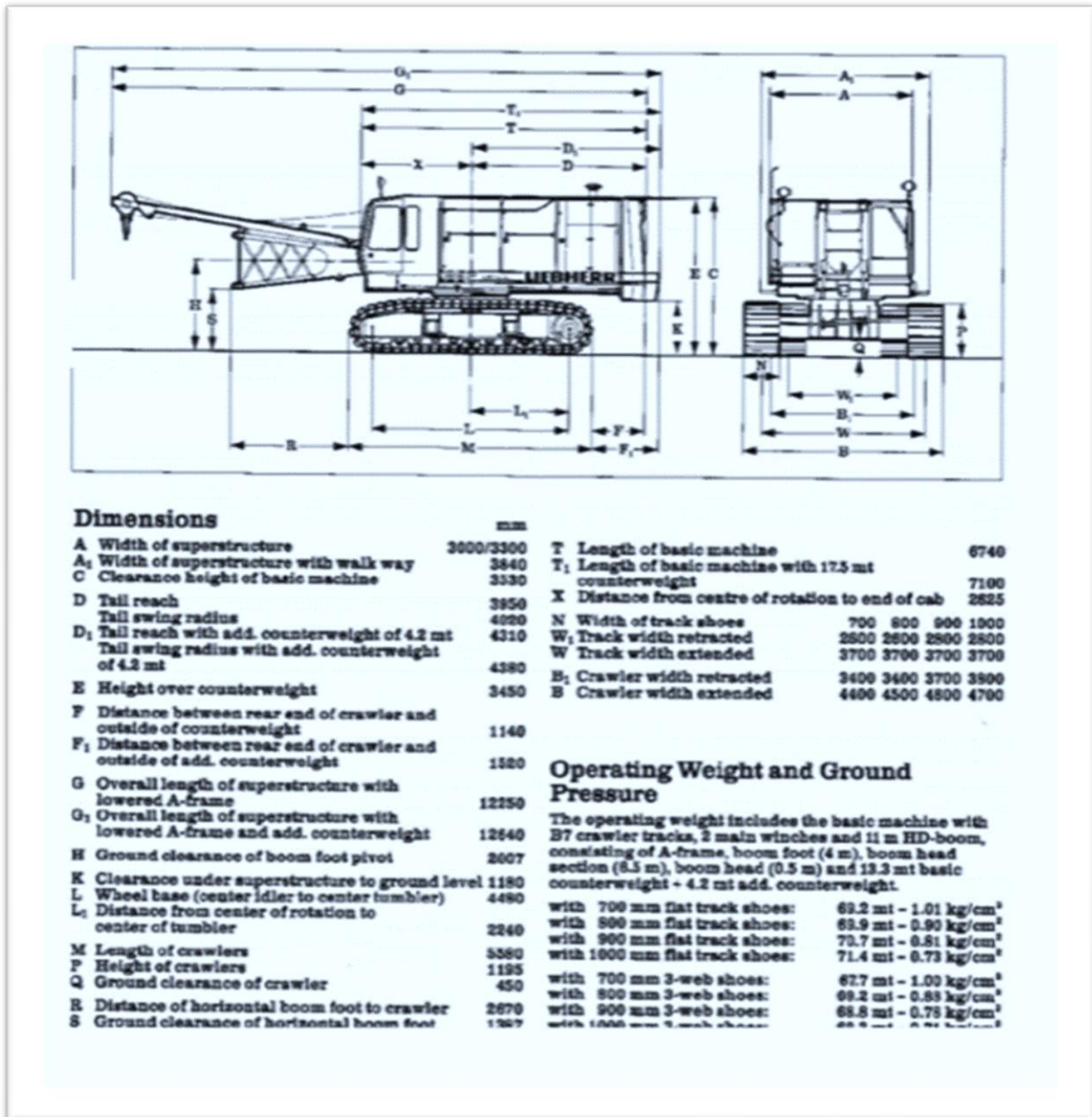
Liebherr HS 852 HD, Weight 83, 6 ton

Pressure of Liebherr
$$P = \frac{Weight*9.8}{Dig\ area\ *10^3}$$

Pressure of Liebherr cutter

$$P1 = \frac{Weight\ cutter * 10^3 * 9.8}{Wall\ area * 10^3}$$

- ***Cement shrinkage:***

The typical mix proportions of the wall diaphragm are as follows:

Cement   350 Kg, Bentonite   35 Kg, Water   870 Kg

The autogenous shrinkage is (Tazawa, 1997):

$$\frac{0.4cm3}{100gr} = (0.4 * 10^{-6})/(0.1 * 10^{-3}) = 0.004\ m^3/ton$$

350+35+870=1255 Kg Mixed

350/1255=0.27   ⟹ 0.28/0.03=9.3 Cement

35/1255= 0.03   ⟹ 0.03/0.03=1 Bentonite

870/1255=0.71   ⟹ 0.71/0.03=23.6 Water

As a result, the ratio of mixed is (9.3: 1: 23.6)

Volume $_{wall}$ = 0.6*3.6*18.6=40.18m^3

The mass of cement wall is:

$40.18 * 2.5 = 102$ tons

 Thus, the mass of cement in the mixture is:

(102*9.3) /33.9 = 27.9 tons

So the shrinkage of cement is:

$0.004\ m^3/ton * 27.9 = 0.11$ m^3

13.1.2 jet grouting

Fig. 13.2 GI-50 CII-JG specifications (https://www.ybm.jp)

- ***Pressure of machine GI-50CII-JG***

$$P(\,kN/m^2) = \frac{\text{Weight} * 9.8}{2 * \text{Area} * 10^3}$$

- ***Angular moment of jet rod M***

$$m = \frac{\gamma * V}{g}$$
$$I = m * r^2$$
$$M = I * W$$

Where:

I   Moment of inertia

W   Angular speed

m, r   Mass and radius of rod

- ***Inertia force F***
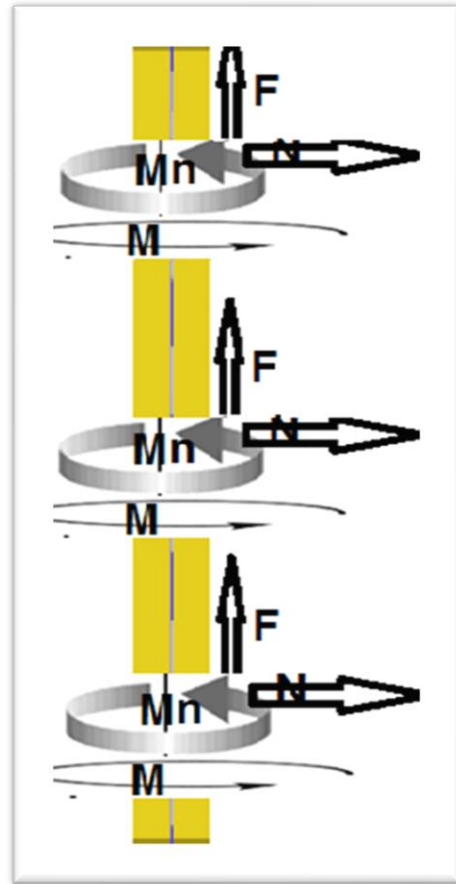
$$F = m * (a + 9.8)$$

a Acceleration

- ***Feed force N***
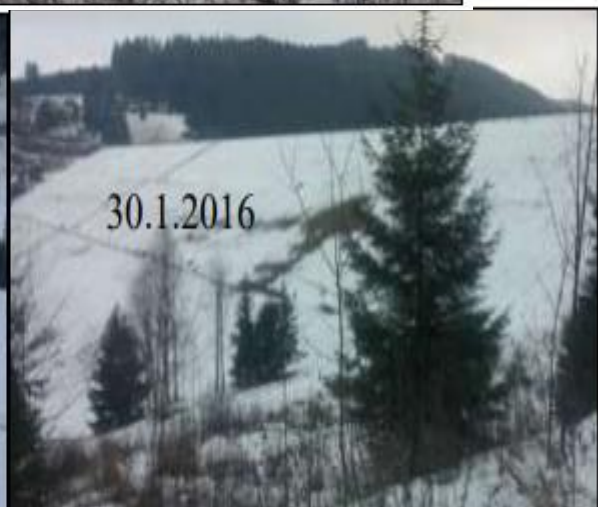
$$N = P * A$$

P Grout pressure

A Area of nozzle

- ***Rotation torque Mn***

Drilling rod

.

13.2 The archival photographs of downstream face seepage (Pařílková et al, 2016)

13.3 Some photographs of the dam reconstruction (Hodak, 2014)

14 PROFESSIONAL WORKS

14.1 Publications

BREDY, S. 2014. Přehrady v Syrii. Časopis Vodní hospodářství. Vol 4: pp. 34-37.

BREDY, S., JANDORA, J. 2019. Three-Dimensions Modelling of a Jet Pile Construction in the Karolinka Dam. Acta Journal. Vol 67(3): pp. 621-636.

BREDY, S., JANDORA, J. 2019. Numerical Modelling of a Diaphragm wall Process in Karolinka Dam. International Journal of Sciences: Basic and Applied Research .Vol 48(7): pp. 93-109.

BREDY, S., JANDORA, J. 2020. Effect of Dam Height on The Stability of Earth Dam (Case Study: Karolinka Dam). Journal of Engineering. Vol 26(3): pp. 117-126.

14.2 Professional activity

Participation in the research work:

• 1.9.2017- 31.1.2019

Contract job with BUT, Project MOST number CZ.02.2.69/0.0/0.0/16_015/0002430. Modern and open study of technology.

• 1.1.2014- 31.12.2015

New progressive rehabilitation tchnologies of dikes and embankment dams. Nové progresivní technologie sanace sypaných hrází. Project MPO number FR—TI4/335.

• 1.1. 2012 - 31. 12. 2012

Research of methods improving water management effectiveness of small reservoirs. Výzkum metod zvyšujících vodohospodářskou účinnost malých vodních nádrží s ohledem na rizika předpokládaných klimatických změn. Project NAZV number QI92A139.

• 1.1.2012 - 31. 12. 2013

Application of numerical analysis in geotechnical structures. Aplikace výpočtových postupů v analýze geotechnických konstrukcí.. Project number FAST-S-11-39